

THESIS FOR THE DEGREE OF DOCTOR OF PHILOSOPHY

Digital shaping

Meshless computational methods for form
generation in architectural design

JENS OLSSON

Department of Architecture and Civil Engineering
Division of Architectural Theory and Methods
Architecture and Engineering Research Group
CHALMERS UNIVERSITY OF TECHNOLOGY

Göteborg, Sweden 2022

Digital shaping
Meshless computational methods for form
generation in architectural design
JENS OLSSON
ISBN 978-91-7905-729-9

© JENS OLSSON, 2022

Thesis for the degree of Doctor of Philosophy
Doktorsavhandlingar vid Chalmers tekniska högskola
Ny serie nr. 5195
ISSN 0346-718X
Department of Architecture and Civil Engineering
Division of Architectural Theory and Methods
Architecture and Engineering Research Group
Chalmers University of Technology
SE-412 96 Göteborg
Sweden
Telephone: +46 (0)31-772 1000

Cover:
Nodal connection approximated with 100.000 randomly scattered particles. Image created
by the author.

Chalmers Reproservice
Göteborg, Sweden 2022

Digital shaping
Meshless computational methods for form
generation in architectural design
Thesis for the degree of Doctor of Philosophy in Architecture
JENS OLSSON
Department of Architecture and Civil Engineering
Division of Architectural Theory and Methods
Architecture and Engineering Research Group
Chalmers University of Technology

ABSTRACT

This thesis explores methods for integration of structural analysis into a digital design, specifically by introducing the family of meshless methods—usually found in physics and mechanical engineering—into the context of a design process and the materials typically used for structures in the built environment. The thesis takes the design process for the Mexico City Airport project as a point of departure. The project is presented as an example of digital shaping and motivates the research to focus on structural nodal connection. Three historical case studies where nodal connections are used in different ways are introduced and followed by the formulation of four research questions. These questions motivate the contextualisation, which is divided into four parts; the use of form representation in digital design, design conditions from materials and production, computational methods for shape finding and numerical methods for structural analysis.

A particular focus in the thesis is dedicated to the development of a meshless method called Force flux peridynamics (FFPD). This method is hypothesised to be suitable in digital design partly because the point cloud discretisation is relatively easy to automate and partly because of the ability to simulate complex phenomena such as brittle fracture. Such capabilities could be especially helpful in supporting the design of lightweight components.

The five papers that are included in the thesis follow a trajectory from large to small. The first paper describes the computational design work with the roof of the new international airport for Mexico City. The second paper addresses one of the challenges faced in that project with material inefficiency for nodal connections. The third paper explores a generative approach for creating lightweight porous structural components inspired by bone growth. The fourth paper presents Force Flux Peridynamics, an extension/modification of the peridynamics theory that allows for variable particle sizes and an irregular particle distribution through the introduction of the force flux density concept. The development is motivated by the limitations of the current theory from a design process point of view. The new formulation enables the simulation of phenomena such as yielding and brittle fracture and is shown to correlate with Griffith's theory of fracture. The final paper then applies FFPD to the simulation of concrete, where fracture plays an essential role in mechanical characteristics.

Keywords: Structural design, Digital design, Simulation, SPH, Peridynamics, Steel structures, Nodal connections, Structural efficiency, Design process, Conceptual design, Design theory, Force flux density.

ACKNOWLEDGEMENTS

I would first of all like to thank Karl-Gunnar Olsson, who has been my examiner, for allowing me to embark on the PhD journey and for the encouragement and guidance throughout the work with the thesis. I am particularly grateful for the help and enthusiastic encouragement while writing and structuring the thesis. It is difficult to see how the thesis would have come together without his support.

I would especially like to thank Chris Williams for the supervision, the encouragement to explore new territory and the many insightful conversations on research, theory development and applications. Our fruitful dialogue during these years has given me many new insights and perspectives. The thesis would not have been possible without his guidance.

Thanks are also due to Mats Ander for co-supervision and support in the process of article writing and encouragement to navigate the theoretical territory of the topic. Mats have also been an inspiring teacher, and I have very much enjoyed and learnt from the supervision of master thesis students under his guidance.

I also want to thank Morten Lund and Maja Kovacs for the opportunity to learn and grow in the role of a teacher in the Matter Space Structure studio. Thanks are also due to Daniel Norell, Naima Callenberg, Peter Christensson and Jonas Carlson for the much appreciated and inspiring collaboration in that teaching context.

Special thanks are also due to Erica Hörteborn, Alexander Sehlström and Emil Adiels for many valuable discussions and for the opportunity to share the winding path of the PhD endeavour with the three of you.

I would furthermore like to thank Martha Tsigkari, Francis Aish, Sam Joyce, Henrik Malm, Adam Davis, Stamatios Psarras and the rest of the Applied research and development team at Foster and Partners. Thanks are also due to Al Fisher for his guidance when I came to Buro Happold as an intern and to Shrikant Sharma for giving me that opportunity.

Additional thanks are directed to Paul Shepherd for the much-appreciated feedback at my licentiate seminar and to Fredrik Larsson for the thorough comments and questions at my 90% seminar, which motivated me in the final weeks of writing. Thanks are also directed to Eduard Hryha and William Hearn for the collaborative work on metal-based additive manufacturing.

Finally, many thanks to Fondazione Renzo Piano, Milo Keller and Acetual for generously allowing me to use their photographs in the thesis.

THESIS

This thesis consists of an extended summary and the following appended papers:

- Paper A** M. Tsigkari et al. “The computational challenges of a mega space frame”. *ACADIA Conferance proceedings*. Association for Computer Aided Design in Architecture (ACADIA). 2017
- Paper B** F. Aish et al. “Form Finding Nodal Connections in Grid Structures”. *Conference proceedings: IASS Boston 2018*. 2018
- Paper C** J. Olsson, M. Ander, and C. J. K. Williams. “Adaptive bone re-modelling for optimization of porous structural components”. *Conference processdings: IASS Beijing 2022*. 2022
- Paper D** J. Olsson, M. Ander, and C. J. K. Williams. The Use of Peridynamic Virtual Fibres to Simulate Yielding and Brittle Fracture. *Journal of Peridynamics and Nonlocal Modeling* **3.4** (Apr. 2021), 348–382
- Paper E** J. Olsson, M. Ander, and C. J. K. Williams. The numerical simulation of standard concrete tests and steel reinforcement using force flux peridynamics. *Structural Concrete* (Aug. 2022)

Publications and Master thesis projects supervised by the author and related to the thesis topic:

1. J. Hilmersson et al. “Isogeometric analysis and form finding for thin elastic shells”. *Conference processdings: IASS Barcelona 2019*. 2019
2. G. Edefors and D. Jonsson. “Interactive Design Using Peridynamics”. MSc thesis. Chalmers university of technology, 2021
3. K. Thorsager and M. Udén. “3D Strut-and-Tie Modelling - Interactive Design Using Peridynamics”. MSc thesis. Chalmers university of technology, 2022

CONTENTS

Abstract	2
Abstract	i
Acknowledgements	ii
Thesis	iii
Contents	v
1 Introduction	1
1.1 Mexico City Airport	1
1.2 Nodal connections	5
1.3 Defining the scope	7
1.4 Research questions and limitations	11
2 Conditions for digital shaping	17
2.1 Digital shape representation	23
2.1.1 Computer aided design	23
2.1.2 Dealing with point clouds	26
2.2 Materials and production	32
2.2.1 Steel	35
2.2.2 Concrete	42
2.2.3 Wood	48
2.3 Numerical analysis	54
2.3.1 Meshless methods	57
2.3.2 Solver and discretisation	61
2.4 Shape finding	64
2.4.1 Form finding	64
2.4.2 Topology optimisation	66
2.4.3 Emergence	66
3 Methodology	70
3.1 Methods	70
3.2 Research methodology	71
4 Summary of papers	75
4.1 Paper A	75
4.2 Paper B	75
4.3 Paper C	76
4.4 Paper D	76
4.5 Paper E	77

5	Conclusions and discussion	78
5.1	Research questions and achieved results	78
5.2	Conclusions	83
6	Future work	85
	Figure credits	87
	References	89
7	Appended papers A–E	102

1 Introduction

The real world is complex, far beyond our comprehension. Material objects consist of an almost infinite amount of information, while our digital representations are finite and, in comparison, very coarse. Avogadro’s constant is a proportionality factor that relates, for example, the number of molecules to the amount of that specific substance and serves well to exemplify this discrepancy. In 1 ml of water corresponding to 1 cm³ of volume, the number of molecules calculated from Avogadro’s constant is approximately $3.3e22$. The combined world consumption of data in 2021 was estimated by *Statista* to be 79 zettabytes ($7.9e22$ bytes and $1e22$ double precision numbers) which is not even enough to store the position of these molecules of the small water cube [175].

Methods in computer-aided design, whether in drawing or analysis, therefore start with interpolation. In drawing, that is exemplified with the use of splines and in analysis with the Finite Element Method (FEM). The vast material complexity requires approximate methods and, thus, sound engineering judgement in the execution phase.

In this thesis, an extension to a meshless method called peridynamics is presented and discussed in relation to the possibility it may provide in an architectural/engineering design context. Meshless methods can be considered to be a special case of FEM in which the elements overlap instead of having distinct boundaries, and the methods are therefore classified as non-local. The design work behind the roof for the new international Mexico City Airport is my own experience of working with digital tools in a complex design process and has had an important influence on the thesis. It has brought my attention to the importance of nodal connections for structural design and motivated the choice to study nodal connections to investigate material-informed digital shaping. The exploration of numerical concepts for material mechanics led me to look closer at the family of meshless methods, both for the simulation of mechanical behaviour and to serve as a representation that aid the explorative digital shaping. The aim and the limitation of this study is summarised in four research questions. These questions take the reader into the contextualisation, which is organised as an expose on the related notions of digital shape representation, materials and production, numerical analysis and shape finding methods.

1.1 Mexico City Airport

In September 2014, British architects Foster + Partners, in collaboration with the Mexican firm FREE Architects, were announced winners of the competition for the new international airport in Mexico City. The initial master plan for the project suggested a plan layout with two terminal buildings connected with an underground train link, as was typical for airports of such a scale and proposed by the competition brief. During the initial stages of design work, the split terminal idea was scrutinised, and the team came to question the master plan strategy. Due to the complicated soil conditions at the site, it was concluded that a single terminal building would be more efficient in terms of people flow, logistics and even cost. The final proposal handed to the competition jury was a single terminal building, with a continuous roof embracing the whole building as



Figure 1.1: *Render showing the exterior of the roof for the proposal of the new Mexico City Airport, shown from a bird's-eye view. See attribution in the figure credits list.*

a gesture of the unifying strategy. The roof also functions to unify the often spatially fragmented organisation of an airport with the structural member of the space frame system as the repeated and recognisable element. The choice to work with a lightweight roof structure was partly a response to the complicated soil condition at the site and partly a strategy to design for flexibility, where the enclosed space is uninterrupted, except for the 21 protruding columns. The roof covers a space of approximately 0.5 million square meters with a footprint stretching 1.6 x 0.5 kilometre, creating a continuous space with spans between structural supports exceeding 100 meter. The shape of the roof is derived based on structural and spatial concerns, enclosing the interior like a tightly wrapped skin, acting as walls, daylight intake and environmental shield for the building. With high aspirations in terms of sustainability, material efficiency, flexibility and concerns about loading the continuously settling soil, the aim was to create a lightweight roof. Hence, form-finding was adopted as the primary strategy for shaping the roof. Due to heavy seismic activity in the area, the idea of a single-layer grid shell was found unsuitable in favour of a double-layer space frame with a tetrahedral configuration that provided shear and bending capacity. From a longer-term perspective, the airport project is part of the iterative design development of the airport as a building typology, the eighth project in that category for Foster + Partners. This process is described in the keynote lecture by Norman Foster, and Francis Aish at the conference *Advances of Architectural Geometry* in 2016 [94]. The 1981 Stansted Airport was the first airport designed by the office, reinventing the typology by reversing the typical airport organisational diagram. Technical and mechanical systems were placed underground to facilitate the technical needs from below, enabling a lightweight roof that functions more as a daylight filter.

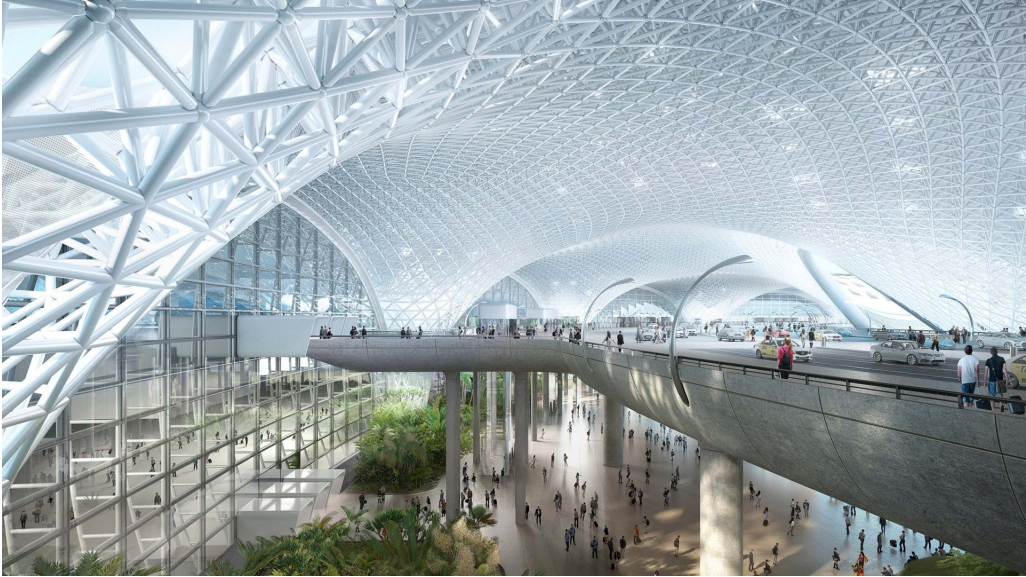


Figure 1.2: *Render of the Mexico City Airport proposal showing the roof over the drop of area which has been shaped using digital tools and conditioned by the Mero space frame system in steel. See attribution in the figure credits list.*

The main space of the building was thus re-envisioned through this strategy into a space of light and drama. The 1998 Chek Lap Kok Airport continued the development of the same principle while increasing the spans to suit a significantly larger airport. The 2008 Beijing Capital International Airport became the third iteration of a similar scheme, but this time in the form of an even larger structure. It was adorned with symbolic features such as the dragon skin-like cladding and the particular colouring scheme. The airport rationale was woven together with elements of local folklore [94]. The ambitions of structural lightness put the Mexico City Airport project in yet another context. The development of lightweight gravity structures owes gratitude to several people, including Gaudi, Gustavino, Otto, Fuller, Isler, Nervi and many others. However, there is one project in particular that influenced the design objectives and the project workflow more than the rest. That is the British museum great court roof, shown in figure 2.39, for which the computational design was carried out by Chris J.K. Williams, as described in [195]. This paper became a major inspiration for approaching the design of such a complex, undulating, lightweight roof structure.

During the design development from the competition until production drawings, a couple of dozen versions of the roof geometry were drawn using various computational design techniques. Due to the multi-functional nature of the roof, how it connects to other architectural elements, and the ambitious sustainability goals, the initial phase of design development was much about understanding the constraints and how they were interlinked. As a strategy for natural daylighting, a consistent pattern of scattered triangular skylights was distributed over the roof, constraining the roof geometry by the

manufacturing limits of these glass panels.

The same triangle size also drives the depth of the space frame due to concerns of structural efficiency. An equilateral tetrahedral configuration with 60 degree angles between the bars provides the most lightweight solution because it ensures the smallest possible nodes. The ambition to get as close to equilateral as possible links the triangle size on the roof surface, with the triangles on the innermost layer but also the triangles in the depth direction. To furthermore create a continuous roof all the way down to the ground, the choice of triangle size needed to consider interfaces such as doors and other apertures that penetrate the roof surface. All in all, the strict geometric control requirements meant that the roof needed to be designed starting from the outside and the inside layer of the structure was created through a shifted offset. Additional adjustments were made to ensure that the inner layer of nodes in the space frame would align with slab edges, the glass facade at the entrance and other internal walls. For a free-form undulating surface, see figure 1.2, it is difficult to define the tetrahedral geometry using only geometrical primitives or rational shapes. The variation in surface curvature that comes from patching together parts of geometrical primitives with a partial form found structure, driven by load cases, spatial consideration and geometrical constraints results in a geometry that does not follow simple mathematical logic. Therefore the design strategies needed to be flexible enough to allow for compromises with the many design drivers.

The nodes in a Mero-like space frame system are milled out of solid steel spheres and, therefore, the heaviest component of the structure. Thus reducing the node size was identified as the most efficient way to reduce the structure's weight. The angles between bars in the space frame and the bar diameters are the two primary drivers for the node size. By maximising the bar angle and minimising the bar diameter, the right conditions are obtained to achieve the smallest possible node. Smaller nodes meant a reduction in the weight of the structure and, therefore a reduction in the bar diameters, enabling further node size reduction. Even though the Mexico airport project was designed for a Mero-type ball node space frame which utilises material relatively efficiently, there were still problem areas with large nodes due to structurally disadvantageous compromises.

After the completion of the project in terms of design work, the question was then raised what would be the next step in the development of such a structure? The obvious answer was dealing with the reduction of materials used for some large and heavy nodes. Could they have been 3D printed? How would one go about shaping such a large number of connections to reduce the weight?

The airport project exemplifies a *digital shaping* process of iterative character, driven by ambitions of lightness, smoothness, efficiency and flexibility but also a range of external constraints such as site conditions, regulations, and cost, among other things. The process was also driven by material and production conditions and structural principles. From that point of view, the concept *digital shaping* can be defined as

An iterative process based on value judgement and external constraints where a digital shape is defined while attending to material properties and production specific conditions by the use of computational means.

1.2 Nodal connections

In the study of nodal connections for structures in architecture and engineering, three commonly known but somewhat different buildings have been studied and are presented in brief in this section. That includes George Centre Pompidou with its cast steel gerberettes, the concrete structure for the Trans World Airline (TWA) terminal and the glulam structure for the Tamedia office. These projects are chosen because they exemplify a conscious fusion of architectural vision, material, production and structural function which are relevant aspects to consider, also in digital shaping.

Centre Pompidou gerberette

In 1968 the head engineer at Arup’s structures group 3 in London, Ted Happold, approached Richard Rogers and Renzo Piano with a proposal to collaborate in the competition for the Beaubourg, a new centre of contemporary art in Paris. It took some convincing, but the team eventually signed up for the competition. In an interview with the AA files in 2015, Rogers describes their vision to create a democratic building, “a place for all people, all ages and creeds, and both rich and poor”, combined with a vision of structural lightness based on material ‘truth’, spatial transparency and organisational flexibility.

After the competition was won, among 681 proposals, the team developed the design through many iterations with the Arup engineer Peter Rice. The space frame at Expo 70 in Osaka by Kenzo Tange inspired the use of cast steel for the nodes, which eventually developed into the cantilever beams, shown in figure 1.3 [74]. Peter Rice describes in [157] how the choice to work with cast steel was driven by the will to deconstruct his own ‘fear’ of high culture. He wanted to make the building feel accessible and familiar to ordinary people. The familiarity of the formal language of the victorian cast steel component, which is recognisable from bridges, aqueducts, warehouses and railway stations in public spaces, seemed to be just right to create an “approachable and sympathetic building” according to Rice [157].

The shaping was also inspired by the sculptural pieces of forged steel of the masts at Frei Otto’s Munich Olympic Stadium [74] and primarily derived based on structural logic. The gerberettes profile follows the bending moment diagram, and the cross-section transitions from a box section to an I-section. The shape became an almost bone-like element with soft curves and rounded corners, as shown in figure 1.4. After being drawn, redrawn and redrawn again, with manufacturing constraints and structural function in mind, the gerberettes became “an essay of how it worked” according to [157]. The structural integrity of the gerberettes got examined with the Finite element method by Arup engineer Alister Day. French and British experts in casting were also inspecting the production process. However, cast steel was poorly understood as a structural material, and the production methods were mainly crafts based, which had not developed much since the end of the 19th century. The development of steel jackets for nuclear reactors had pushed the understanding of fracture mechanics and the study of imperfections and flaws in cast steel. The goal was, therefore, to take these – at the time – new insights onboard to the casting of the gerberettes.

The merge of the new theory with crafts-based manufacturing and the additional language barrier with the German steel company resulted in misunderstandings. The first and the second gerberette split in half at initial testing with just half the testing load. The misunderstandings were eventually sorted out with the help of professor Kussmaul at Stuttgart University. The 45 gerberettes and additional beam nodes that had been produced could be rescued using heat treatment [157]. Figure 1.5 show the gerberettes on the factory floor in Germany.

TWA terminal columns

The 1962 Trans World Airline (TWA) terminal shell structure by Eero Saarinen shown in figure 1.7 exemplify an ability to handle complex building geometry with analogue methods. However, the project started in some ways a few years earlier with the concrete shell of the Kresge Auditorium at the Massachusetts Institute of Technology. The design team fronted by Saarinen proposed a shape for the auditorium shell based that was not defined by structural logic nor with the construction process in mind. The building was finished in 1955, resulting in a sagging and cracking roof. In an interview after the project was finished, Saarinen expressed that “one cannot rely on geometry for the sake of geometry” [192]. From the experience of a complicated construction process with the single shell auditorium at MIT, the TWA terminal was instead split into parts that could be independently cast, see figure 1.8. The split also simplified the structural logic and became a strategy to let daylight into the main space. The geometry of the columns and other interior elements were derived based on ruled surfaces as shown in figure 1.9, which mimics a formwork for casting built with straight planks. Saarinen’s vision is captured in a quote from [161]: “the shapes of these vaults were deliberately chosen in order to emphasise an upward-soaring quality of the line rather than the downward gravitational one common to many domed structures. We wanted to counter act the earthbound feeling and the heaviness that prevails too much in the M.I.T auditorium.”

The resulting structure is not necessarily lightweight compared to the shells of Félix Candela or Heinz Ilser. However, the strictly geometrical approach with ruled surfaces for model making enabled the shaping of expressive details as shown with the columns in figure 2.24 and the interior of the building in figure 1.8.

Tamedia office building

The 2013 headquarters in Zurich for the media company Tamedia by Shigeru Ban is said to take inspiration from the Japanese carpentry traditions, Miyadaiku, and Sukiya-daiku [120]. The influence is seen in the use of metal-free solid wood connections that are carefully crafted and express the modular structural approach. The Japanese Miyadaiku carpenters are known for making elaborate wooden details for temple buildings, and the Sukiya-daiku carpenters for building tea-houses and residential buildings [31]. The structure of the Tamedia office fuses these traditional influences with high-precision production using CNC machines. The glulam spruce members are prefabricated and joined together with connectors in beech plywood. The oval shape of the beams that protrude through the nodes lock the connections for rotations, effectively making the building a frame structure [165].

The exposed wooden structure had to be put through extensive testing to meet the demands of the Swiss fire regulations. Therefore, the structural members were dimensioned for extra fireproofing, giving the structure an oversized look and a unique character. The exposure of the wood also gives the office space a feeling of warmth and the scent of nature.

Blumer-Lehmann engineer Martin Antemann describes in an interview with *naturally:wood* how the structure functions as a skeleton [129]. Antemann explains that the skeleton approach means some elements protrude throughout several floors instead of the more conventional story-based building techniques. The columns are up to 22 meters long, and the primary beams reach spans up to 18 meters. The long elements can be produced with glulam, which removes the size constraints that natural logs put on timber structures. Antemann describes further how the relative softness of the spruce is suitable for milling and sculpting the structural elements into their appropriate shapes.

1.3 Defining the scope

The focus on nodal connections to explore digital shaping is based on the following reasoning. Nodal connections are often complex in terms of geometry, structural performance, and loading conditions. They are often manufactured relatively inefficiently with poor attention to detail. A wide variety of shape-finding techniques has been developed and applied to the global form of structures, justified as promising strategies for material savings. However, only a few projects are built with such budgets and ambition, so these techniques remain a niche and are applied in small numbers. Structural joints, however, are needed in all structures, and there is potential for applying new strategies to make material savings while attending to the importance of the detail in architecture.

Sustainability

Sustainability has saturated the contemporary discourse in architecture in academia and practice over the last decades. The sustainability challenge can be approached from many different perspectives. According to the *UN Environment Global Status Report 2017* the building sector stands for 36-39 % of the world's CO₂ emissions. A large part is consumed by operational usage, but a significant portion is also due to embodied carbon. Catherine De Wolf presents a detailed review on possible gains with structural efficiency as a prioritised driver in architecture to reduce embodied carbon in her PhD thesis [196]. Wolf contributes with a method for evaluating embodied carbon coefficients (ECC). The results for a particular project will be tied to the resources of a particular region making comparative studies difficult. However, the typical buildings range is 200 - 550 kgCO_{2e}/m², and the results from one of the extreme low carbon project that is mentioned in the thesis show a reduction to 30 kgCO_{2e}/m² [196]. Such reasoning motivates the ambition in the thesis to explore the design of lightweight components.

Nodal connections in engineering

Nodal connections in a typical may not be the centre of attention, but the mechanics of the node often lay the foundation for the conceptual workings of a structure. That can be exemplified by comparing the pin joint and a moment connection and the effect the two joining strategies have on the stability and dimensions of a structure. The node acts to distribute the forces and the moments, which is crucial to consider in pursuing lightweight design. The nodal connection also becomes a point of assembly for the erection of a structure, dictating the building process and the possibility of repair, reuse and disassembly. Design for disassembly has become a movement in architecture and engineering, emphasising the possibilities of circular use of building components to reduce consumption, waste and pollution [13].

The development of nodal connections in engineering history owes gratitude to an extensive range of inventors. At least 250 different types of systems have been developed only in the context of spatial structures [84]. Alexander Graham Bell experimented with space frame structures in the early 20th century, and Buckminster Fuller explored spatial structures with geodesic domes such as the Montreal Biosphère. Cedric Price explored tensegrity structures with the Aviary at London Zoo, Shoji Yoh worked with timber space frames with the Oguni Dome in Kyushu, and Kenzo Tange created the space frame for Plaza Osaka at Expo 70 using cast steel nodes. Hwang presents a comprehensive overview of nodal connections for spatial structures in his PhD thesis [84]. He discusses the importance of nodal connections for the geometry and stability of spatial structures. His research focuses on the effects of bolt spacing in nodal connections. Peter Rice furthermore articulates the fundamentals of engineering in *An Engineer Imagines* where he states “An engineer must not be wrong, because human life and human safety are dependant on the engineer’s work being right. That is bottom line.”

Architectural details

Like other details in architecture, the bodily scope of the node is essential for the overall architectural expression. The maxim that *God lies in the detail* has been attributed to Mies van der Rohe in architecture, to the German art historian Aby Warburg in the context of art history research and Gustave Flaubert in the context of literary production [57]. In the essay *The tell-the-tail detail*, Marco Frascari unfolds the significance of the detail and the inherent link between the design process and construction by examining the work of Carlo Scarpa [19]. The role of the detail, according to Frascari is to communicate meaning; “the detail expresses the process of signification; that is, the attaching of meanings to man-produced objects”.

Frascari then defines two concepts; *Construction* and *Construing* that he uses in the discussion of details. *Construction* is related to the operative and manual process of assembling building elements, *construing*, on the other hand, relates to the creation of meaning through narrative. Frascari argues that both of these dimensions must be present in the creation of meaningful architecture. We cannot have architecture without the physical elements, and neither can architecture be reduced to the purely physical without the narrative layer. According to Frascari, Carlo Scarpa’s Scarpa’s work exemplifies the union of these two dimensions where each detail tells us the story of its making, placement,

and dimensions. His selection of details is driven by practical function while responding to contextual layers of historical, social and cultural character.

The three examples in the previous section exemplify the complexity of nodal connections and potentially also Frascari's two dimensions. In designing the gerberettes for the George Centre Pompidou, the team considered the complexity of cast steel productions and structural performance while remaining sensitive to a vision based on societal and cultural conditions. The concrete columns for the TWA terminal exemplify the importance for designers to understand construction and materials properties to enable the sculptural potential which is used in the project to manifest a vision of space and drama. The nodes in the glulam structure for the Tamedia office fuse a traditional building technique with new production techniques while attending to the new conditions of the modern office building typology.

Frascari also points to the importance of details in relation to the development of architecture as a field when he says: "In the details are the possibilities of innovation and invention, and it is through these that architects can give harmony to the most uncommon and difficult or disorderly environment generated by culture." [57]

Digital design

Digitalisation in architecture started with the introduction of computer-aided design (CAD) tools in the '90s. CAD became a liberating force in terms of production efficiency and shape expression but simultaneously made the shaping of objects a rather abstract activity [141]. Object shapes no longer relate by necessity to their materials or the process of their making. For example, the maquette used in a sculptural endeavour by a car designer was partially replaced by a digital counterpart. The representation of materials in a computer-based design context has primarily focused on surface appearance based on textures, bump maps, refraction and reflection of light. Ray-tracing-based rendering programs recreate the appearance of physical objects through a simulation that mimics the physics of light. The objects are represented as surfaces, and their shapes are defined with the available tools in the modelling environment. The response to material conditions has to be indirectly managed by the designer. Since the famous desk lamp animation *Loxo Jr.* by John Lasseter for Pixar in 1986, computational power has increased by a factor of more than one million. Together with the additional improvements in algorithms for ray-tracing, rendering has almost become a real-time activity.

The shaping of objects in a digital context can be explored entirely agnostic of the conditions that materials and production present for the designer. Graphic design and digital art may exemplify such liberation from the production of artefacts. Architecture could be argued to reach beyond material constraints in idea-based and visionary projects (for example, in the work of Le Corbusier, Etienne-Louis Boullée and more recently, OMA, MVRDV and Diller Scofidio+Renfro). However, the ambition of this project is to explore digital shaping within the constraints of material conditions. The shaping of the nodes in the previous three examples was largely conditioned by material and production constraints and exemplified the importance thereof. Motivated by Frascari's reasoning captured in the quote about innovation, with a design process character and the power of modern computation in mind, one may therefore ask:

Could the computational environment support an introduction of materials into the digital shaping of objects?

The ambition would not be to replace physical prototypes or to automate the design process (which seems to presume unreasonable predictability) but to support the decisions that drive a structural engineering/architectural endeavour.

Numerical methods

To introduce structural material properties in a digital model, a numerical concept must be formulated and linked to a form representation, which could be a polygon mesh, a non-uniform rational b-spline (NURBS) surface or a point cloud. The ambitions to better integrate computer modelling analysis have motivated the development of automated meshing techniques for FEM [64], integration of NURBS and FEM with Isogeometric analysis (IGA) [88], and more recently, meshless Monte Carlo-based approaches [162]. These strategies aim to reduce the engineers' time converting design models to mesh models suitable for analysis. Automated meshing is powerful for many cases but requires rather complicated algorithms and long processing times for complex domains. IGA, which seems very elegant at first glance, also becomes rather complicated for models containing multiple trimmed bidirectional NURBS patches often needed for modelling a complex part. Meshless Monte Carlo seems interesting but is a relatively new concept and has not been studied in depth.

While the thesis does exemplify the use of mesh-based approaches for the shaping of nodal connections, the main efforts are concentrated on meshless methods based on the following reasoning; meshless methods are rather simple to implement while enabling the modelling of rather complex phenomena, such as brittle fracture. Meshless methods generally move the spatial derivatives to a kernel function which means a relaxed requirement on discretisation quality. It is, therefore, easier to automate the setup of the analysis model, making design iterations more efficient. The non-local nature of meshless methods also means that they are generally better suited to approximate stress concentrations than local methods, which become increasingly important with design for lightness and material efficiency.

Ever since the inception of meshless methods with Smooth Particle Hydrodynamics (SPH) in 1977 [66], a large variety of methods have been developed [38]. The contextualisation in section 2.3 is limited to the exploration of SPH, since it is the original meshless formulation, but also includes Peridynamics, a new concept since 1999 [166] and frequently studied in research related to fracture mechanics.

The thesis is limited to the application of materials such as steel and concrete. Application to wood is also discussed but mainly included to point out a direction for future work.

1.4 Research questions and limitations

The following research questions have been formulated based on the reasoning in the introduction and motivate the contextualisation in the next chapter.

- i. How can form finding as a strategy usually applied to shape the global geometry of structures be applied in the shaping of structural components, and what may be the pros and cons of such an approach compared to topology optimisation?
- ii. How can meshless methods be used to generate lightweight structural components with an internal porous structure?
- iii. The ability to vary particle density is essential to vary precision in the analysis of structural components where yielding and fracture may occur. How can the peridynamic formulation be modified to enable variable particle density and irregular particle distribution?
- iv. Force flux peridynamics enables modelling of brittle materials. What is an appropriate strategy to tune such a meshless method for analysis of materials in general and concrete specifically?

While the research questions focus on the study of seemingly detailed subjects, they are addressed with the overall complexity of a design process context in mind. Therefore, the characteristics of the design process and its tools mark the introduction to the contextualisation chapter but are not subjects of study in their own right. Rather, the design process characteristics are outlined to relate to the possibilities that meshless method may provide in future work. The first research question is contextualised in section 2.4 and touched upon in paper A where strategies for digital shaping are applied to the global geometry of a roof structure which is conditioned by the constraints of a steel space frame. The question is more directly addressed in paper B, where the form-finding process is readapted to the scale of a nodal connection and compared with a topology optimisation approach under the conditions of metal 3D printing. The second research question is contextualised in sections 2.1.1, 2.4 and 2.3 and addressed in paper C. The third research question is contextualised in section 2.3 with the definition of meshless methods and the introduction to smooth particle hydrodynamics and peridynamics. An attempt to answer the research question is presented in paper D. The fourth research question is contextualised in section 2.2 where a broad introduction to three common types of building material is presented. Each material is presented with a brief historical account, an introduction to mechanical properties and related production techniques. The role of production is included because of its fundamental role in shaping of objects, as discussed in section 1.2. An effort to answer the fourth research question is presented in paper E.



Figure 1.3: The western facade of the George Centre Pompidou under construction, from October 1975. Photo by courtesy of Fondazione Renzo Piano, for details see the figure credits list.

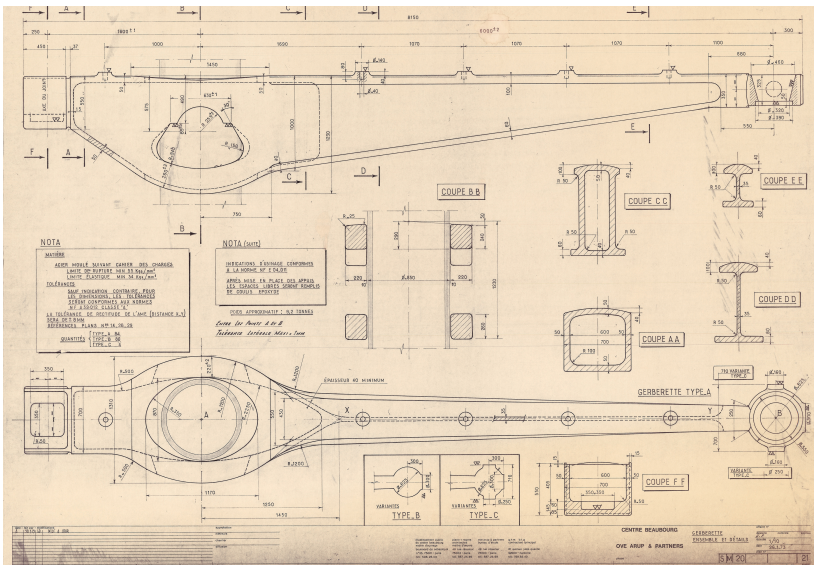


Figure 1.4: Drawing of the cast steel gerbrettes for the Centre Georges Pompidou Paris, France. Photo by courtesy of Fondazione Renzo Piano, for details see the figure credits list.



Figure 1.5: *The production of the gerberettes in the Pohligh Heckel Bleichert factory, Krupp Group, in Rohrbach, Germany. Photo by courtesy of Fondazione Renzo Piano, for details see the figure credits list.*

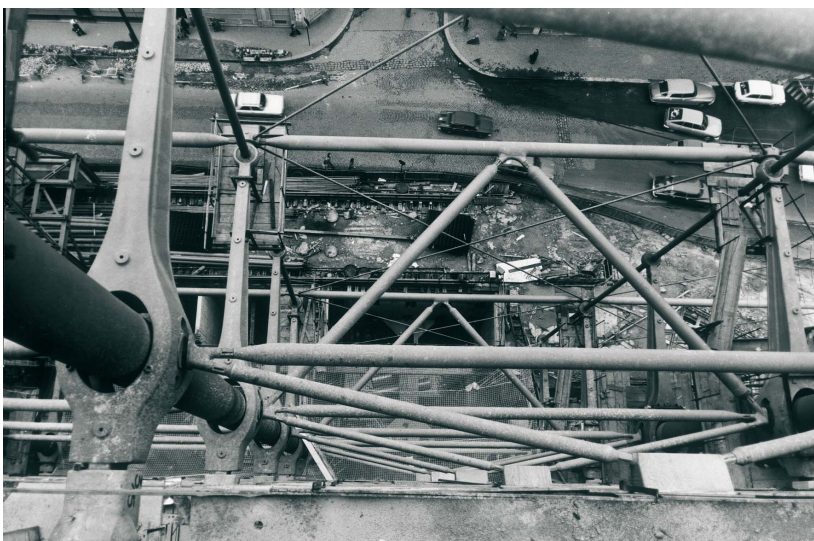


Figure 1.6: *Photo from the Centre Pompidou construction showing a view of the bracing from the upper levels of the eastern façade. Photo by courtesy of Fondazione Renzo Piano, for details see the figure credits list.*

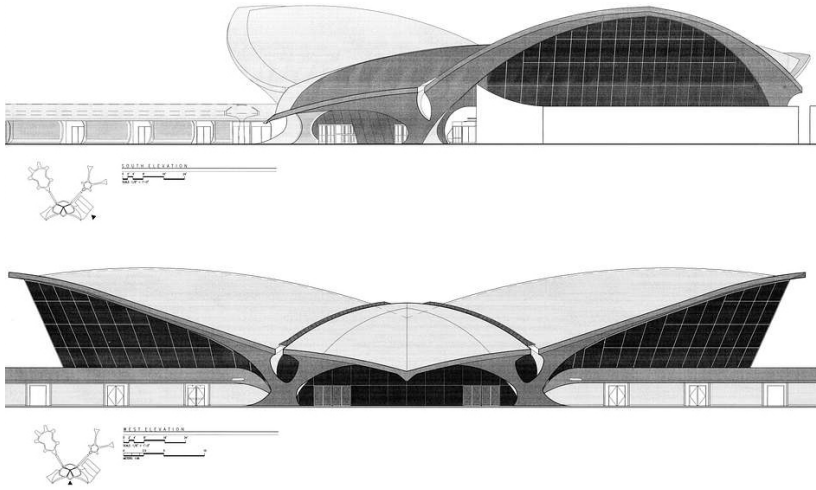


Figure 1.7: *Two of the elevation drawings for the TWA terminal building used to recreate a simplified column geometry. Other drawings seem to suggest that the columns are solid concrete. See attribution in the figure credits list.*



Figure 1.8: *Interior of the John F. Kennedy TWA terminal building in New York City in the early 1960s. Photos taken by Balthazar Korab, for details see the figure credits list.*



Figure 1.9: *Scale model for one of the columns of the TWA terminal created by ruled surfaces using paper which mimics the form work of real concrete casting. Photos taken by Balthazar Korab, for details see the figure credits list.*

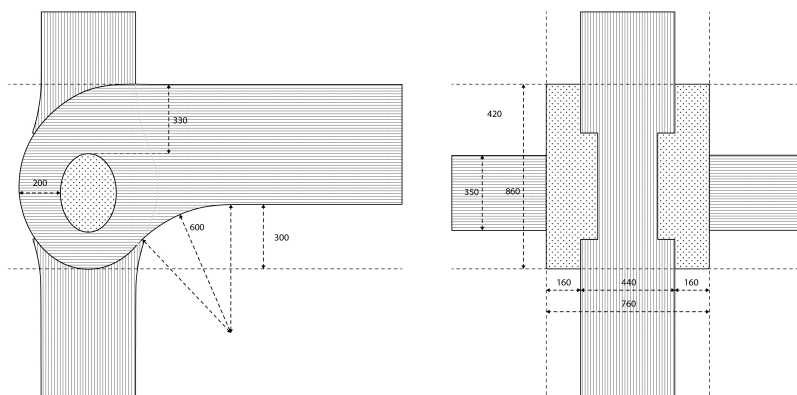


Figure 1.10: *Drawing for the structural connection with lines that illustrate the fibre direction of the wood.*



Figure 1.11: *Construction of the Tamedia office building by Shigeru Ban Architects. The columns can be seen to run continuously across the floor levels of the building as a strategy to reduce connection complexity. See attribution in the figure credits list.*

2 Conditions for digital shaping

This section starts with a general reflection on the design process, which is the context in which digital shaping takes place. That includes the changing roles of architects and engineers, a brief mention of design theory and a note on the designer-computer relationship. The role of tools and representations is then elaborated in the second half of the introduction.

The rest of the chapter focuses on four topics identified as important for the design and structural details. These are furthermore highlighted in blue in figure 2.1. That includes digital shape representation, the conditions that material and production place on digital shaping when the intention is to create physical objects, the numerical representation of materials with meshless methods and digital shape finding strategies that can be useful in design of light weight structural components. Figure 2.1a shows a diagram of the design processes based on the author's experience. The coloured circles represent conditions, methods and perspectives which can be used in design work. The overall circular structure of the diagram alludes to the iterative cyclic nature of the design. The outermost and innermost layers of circles represent external and internal project drivers. However, it should be noted that such a distinction is probably not as clear-cut. Sustainability could, for example, be a value-based driver carried by the design team but could also be introduced through external rules and regulations.

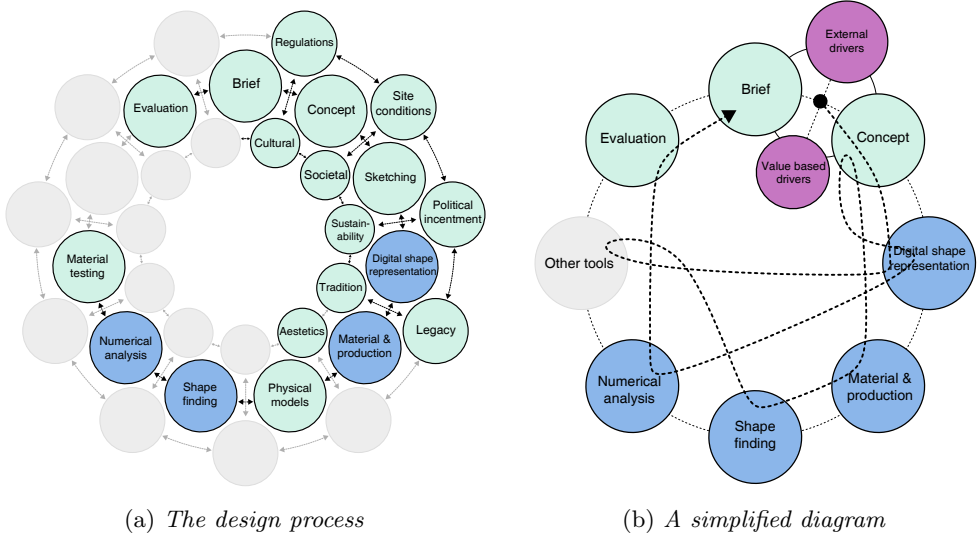


Figure 2.1: The diagram to the left illustrates the design process and its constraints, methods and drivers based on the author's experience. The circular shape alludes to the iterative cycles in design, and the blue circles represent topics that are addressed in the thesis. The dependencies illustrated by the arrows are better represented in the simplified diagram to the right showing a hypothetical non-linear design process.

The simplified diagram to the right in figure 2.1b concentrates on the topics addressed in the thesis, where the blue circles represent the section in this chapter. The irregular dashed curve represents a hypothetical design iteration. The starting point is grounded in the intersection of external and internal divers/constraints, which are formulated in a brief and translated into a concept. The design iteration ends back at the start with an opportunity to reformulate the approach.

Roles

The organisation of design work in architecture inevitable builds on teamwork where different actors have different roles and responsibilities. These roles have historically gone through various phases as a response to different factors, some of which are societal, technological and political. The relationship between theory and practice is another crucial aspect that has shaped the architect's role. Tendencies are furthermore regional, cultural and historical. However, the long trajectory follows the rest of knowledge development within society with increasing specialisation, virtually exploding with the enlightenment and the industrialisation [86].

The pre-industrial architects were knowledgeable of most steps in the building process, acting also as engineers and project leaders in the role of the master builder. Project time frames and the hands-on approach to architecture were essential for building such a generalist type of knowledge. These were also times when mathematics and geometry were most highly regarded and natural know-how of the architect. During the Renaissance, the architect's role was to materialise the holistic unity of all things with a mathematical foundation, often with an undertone of platonic thinking. The architect was expected to be knowledgeable in music, art, philosophy, astronomy and linguistics.

During the industrial era, the role of the master builders got split into architect, engineer and builder due to specialisation. Civil engineering also developed as a discipline in the 18th century. Unlike the role of the scientist, whose aim is to know, the engineer's role is focused on doing. Whereas scientists tend to study phenomena out of pure knowledge pursuit, engineers tend to work with problems as they arise in a practical situation. Usually, in a way where multiple conflicting criteria are compromised through the application of predominantly two types of natural resources, material and energy. [172]. The architect got furthermore distanced from the act of making, resulting in a more abstract type of work. The drawings were expected to be delivered in a type ready to build fashion, to meet the needs of the increasingly industrialised construction process [98].

The roles of architects and engineers in the digital era continuously adapt to new conditions, partly affected by the tools for drawing and the possibilities enabled by new means of production. The digitalisation of the production process may enable a new type of bespoke mass production, and the shared digital workflow seems to blur the borders between professions that have for a while been drifting apart. The emphasis on computer modelling makes the expertise in mathematics once more relevant know-how in the architect's toolbox.

Design theory

Design theory aims to make sense of what constitutes a successful design process and tries to understand how it should be organised. Initial attempts to understand and systematise the design process through a scientific inquiry sprang from the structuralist and functionalist thinking from the '60s and '70s [98]. The goal was to rationalise design activity and remove its somewhat mystical connotation. The design process was split into discrete stages such as analysis, synthesis and evaluation and structured more or less linearly. However, the model was soon rejected as insufficient. Other attempts were made to understand this process, starting from the perspective of the designer or artist, who was asked to document their process. However, the focus on documentation interrupted the process, effectively invalidating the subject of study itself. Later studies attempted to place architects and designers in 'objectively' controlled environments such as a laboratory where the subject's behaviour could be observed systematically. Other studies focused on observing the designer in a more natural studio environment. However, neither of these strategies could successfully reveal what was going on in the head of the designer [98]. The identifiable stages of the design process were organised in various schemes, with inbuilt iterative loops, but the same linear assumption characterised these attempts. During the second generation of design theory research in the '70s, the linear model was replaced with a structure of a dialectic character. A criteria-based solution focus replaced the assumptions of an analytical point of departure. Nevertheless, the results were deemed problematic. The attempts to capture the objective core of the design process up until then appeared more focused on creating theoretical systems of logic than looking at what the studies actually indicated [98].

The third generation of design theory rejected the assumptions of design as a rational problem-solving process, notably exemplified and explained in *How Designers Think - The Design Process Demystified* by Bryan Lawson [100]. The design process was understood as intuition driven in the process of analysis and synthesis. Design was understood as a particular way of thinking, including indirect, implied and contextual knowledge. Analysis in this context is the exploration of patterns and relations, the sorting and classification of information. Synthesis is the move towards a solution to a problem, the creation of a solution. The simultaneous process of analysis through synthesis is a key concept in Lawson's approach to the challenge of complex design situations.

Designer and computer

Conceptual design has been understood to play the most significant role in the design process of new products [82]. The capabilities of computers to represent form and simulate material in an "immaterial" way makes it an attractive tool for such a pursuit. According to Imre Horváth in [82], the conceptual design work varies to some extent between different fields such as architecture, product design and mechanical design. Architects often work with bespoke solutions for unique situations, whereas product developers often design for mass production. Horváth outlines some common denominators [82] and points out how the process is characterised by "abstraction, incompleteness and uncertainty". He describes the process as an iterative search where the designer gathers, transforms, generates, manipulates, and communicates information and knowledge related to the

external constraints of the task. He describes the process as characterised by inherent abstraction, which is a challenging prerequisite for a binary machine like the computer.

Bryan Lawson describes how computers can support the design process [101] by defining three conceptual modes, the oracle, the draughtsman and the agent. The oracle can be understood as the super rationaliser of automatic design, which Lawson describes as merely wishful thinking, as he refers to early design automation ambitions from the '60s and '70s. The computer as draughtsman refers to the use of computer-based geometric drawing/modelling, including the mesmerising and almost seductive potential these tools bring to the table, according to Lawson, often without actual gains in terms of architectural quality. It is furthermore described as a mode in which design is approached as a problem-solving process based on procedural knowledge. The computer as an agent is the final and somewhat speculative mode where Lawson describes the computer as an assistant to the thinking designer. A valuable type of agent, according to Lawson, is one that supports the designer having "a conversation with the drawing", to cite Donald Schön from his book *The reflective practitioner* [164]. This type of interaction does not rely on a procedural structure but instead on a reflective practice that builds on episodic knowledge.

Representations

The output of the architectural design process is often some form of representation (drawing, images or digital model), and one could argue that this is the primary communicative device in the architect's repertoire. Lawson [100] divides representations into three categories; *instructive drawings* for the builder, *communicative drawing* aimed at the client, and the *design drawing* which is the process drawing used in the act of making and integral to the thinking process itself.

Heidegger and Wittgenstein questioned the structures and connotations of language and its instrumental function in communication during the mid-19th century. For them, we are not in charge of language. Rather language provides a framework for expression. Several theorists and philosophers took this thinking to heart and applied the same reasoning to other fields. Drawings standards, for example, can be understood as another non-neutral instrument for expression. CAD systems and software tools present other vocabularies that condition expression in architectural design. The same can be said for the choice of a particular material for making physical models or for the choice of a drafting tool, for example, the style and thickness of a pen. The tools that are used to create a representation are thus naturally closely linked to the outcome. The choice of a tool is in itself a choice that can be understood as an indirect design decision. How the tools are developed can make the design process more or less efficient and allow for more or fewer perspectives on the subject matter.

David Hockney takes on a particular discussion about the overseen influence of tools within the arts by the European painters during the middle ages in his book *Secret Knowledge* [81]. He builds a case for the usage of tools such as optical lenses, mirrors and technology such as the camera obscura for many of the celebrated master painters that were active hundreds of years before the invention of the camera. These tools, according to Hockney, allowed the artists to capture the texture of cloth, patterned

garments in complex folds, glare and reflections in metal armour and complex shapes with almost camera-like precision. Hockney's argument is a disputed matter [116], but it raises interesting questions regarding the role of tools and technology in the creative process.

Due to the size of buildings, architectural representations are typically made in a scale different from reality. Various drawing techniques and scales have been used to bridge the gap between the representations and real objects. Just like in the arts, more than measurements of distance and size can be conveyed in an architectural representation, notably of importance for the *communicative drawing*. Materiality, mass, void, light, atmosphere, and even the sound of a space or other sensory impressions may be communicated in a drawn format. As the architect becomes more distant from the building process, the communicative capacity of the drawing has become more significant [100].

Digital drawing

Descriptive drawing was introduced as a fundamental core subject at the Ecole Polytechnique in Paris and enabled the systematic reduction of a 3D object onto a 2D drawing with precise measurements. It was a key invention and an enabler for the industrial revolution for which production required both control and precision [148]. The pre-industrial speculations of the transcendental in geometry, which was common in discussions of philosophy and theology, became a marginal perspective and geometry was treated as a pragmatic representation of empirical reality. Descriptive geometry became the foundation of many modern endeavours ranging from the artistic drawings with the particular style of the Ecole des Beaux-Arts to the functionalism of the Bauhaus [148]. The computer-based representation of modern CAD systems builds on the same geometric principles but with a higher degree of sophistication. The objects in a computer can be rotated much like in the real world, and the new perspectives are calculated and projected onto the screen fast enough to enable a virtual real-time interaction.

With computers as a primary design tool in contemporary practice, the exchange of information between collaborative parties is often shared directly as digital representations. Typically in a format that will reduce the information to parameters that can be converted to a binary form (distance, colour, names, areas etc.). Other forms of representation are thus indirectly contained or omitted by the "infrastructure" of the process. The drawing as it is represented in terms of the binary data and the abstract act of drawing with computer programs is discussed by Austin and Perin in *Drawing the Glitch* in [189]. They describe the two dominating computer graphics techniques, vector and raster graphics, and their numerical representations. Whereas the handmade drawing only exists in its physical form, the digital version is also represented as a matrix of numbers, allowing for different possibilities for sharing and manipulation.

Whereas the precise nature of vector-based computer representation comes with clear benefits in terms of precision, the same precision requires the drafter to give precise instructions. For raster graphics, on the other hand, the manipulation of precise positions of points and vectors is replaced by manipulations of pixel fields without clear borders and edges. It is a technique that is gaining traction with the development of photo editing and sketching pads, enabling a form of digital sketching. Whereas CAD modelling builds on the logic of vector graphics, image manipulation is more likely to be associated with

raster graphics. There are methods for transitioning between the two formats (with more or less loss of information). After all, what is shown on the computer screen is always a rasterised image. [189].

Computer-based CAD software initially replaced hand drawing of plans, sections and details. Additional features such as the possibility to copy and array objects and increased precision resulted in higher production efficiency of drawings. As 3D modelling matured, new design conditions appeared, and an era with experimental architectural form followed. The possibilities with texture mapping and ray-tracing allowed the creation of photo-realistic images of unfinished visions. The emergence of Building Information Modelling (BIM) tools enabled a central repository to synchronise 3D modelling information from different collaborating disciplines. These tools automatically generate 2D drawings as section cuts in a 3D model. Geometric entities (such as surfaces, lines, and curves) are replaced with building elements with properties of the corresponding physical elements and their interfaces. The elements are grouped in families with parameters that dictate the possibility of variation related to their construction logic. Compared to a typical 3D modelling environment, the BIM tool conditions the available expression in a more limited way. The efficiency of production is prioritised at the sacrifice of intuitive flexibility [35]. Design entities that cannot be quantified within the categories of the given system logic, i.e. unconventional design solutions, tend to become problematic disruptions of otherwise well-oiled machinery for production.

The development of software and technology for laser scanners, photogrammetry, and parametric and algorithm-driven design has changed the meaning and functions of drawings and representations. The possibilities to capture and relate to existing environments with high precision have become accessible in new ways with photogrammetry, and algorithms that simulate natural growth have spurred thinking where design is the creation of processes rather than an object [141]. Some speculate that the new format for this type of representation should be understood as algorithmically based [35], yet others think of it as based on simulation. The agency of simulations in this context can be explored with objectives to quantify and measure or to explore order, form and organisation qualitatively. Norell highlights how the physics simulations from game engines and through modelling software have found their way into design and architecture, enabling further creations of hybrids between digital and physical worlds, between representation and reality [132].

2.1 Digital shape representation

Geometry is fundamental in making physical objects and representing those objects in a digital context. Various digital representation techniques have been developed for which the most important in digital modelling are discussed in this section. The geometric representation also has a foundational role for numerical concepts in engineering and in production of real structures of physical materials. This section is focused on the fundamentals of geometric description for computer modelling. It also contains an additional section with hands-on strategies that are dedicated to the handling of point clouds.

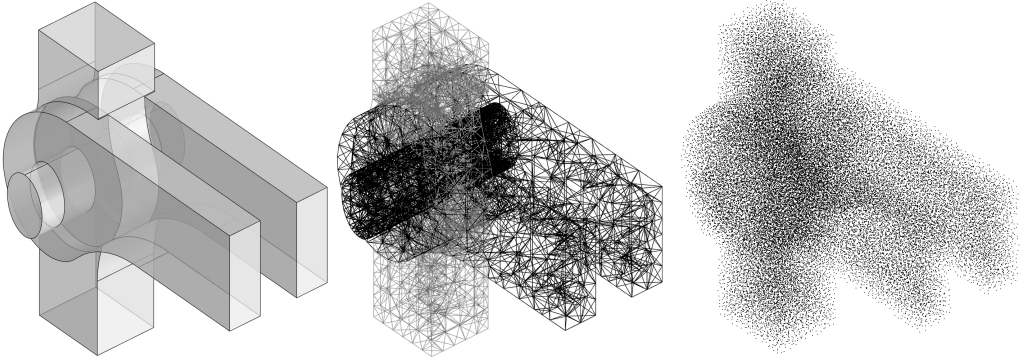


Figure 2.2: *The glulam node of the Tamedia office structure shown in figure 2.30 and 1.10 represented as a 3D model using NURBS, volume mesh and a point cloud.*

2.1.1 Computer aided design

The engineers in the automobile industry during the late 1950s wanted to expand the repertoire of classical geometric shapes (such as the circle, the ellipse, parabola etc.) for descriptive purposes, with a curve that could take any shape and form. Bezier and Casteljau made breakthroughs in what came to be known as spline geometry, which was later refined to Non-Uniform Rational B-Splines (NURBS). However, their inventions required large amounts of calculation and were impractical until computers were available. The introduction of Computer Aided Design (CAD) became a design enabler in many ways. Various software packages have been developed to design cars, ships, and aeroplanes and to create animations. Frank Gehry is one of the first architects to use such tools in building design, notably with the golden fish sculpture in Barcelona [33]. In order to deal with geometry in a computational environment, a suitable geometric representation must be chosen. Such a representation also needs to fulfil various requirements in terms of user interactivity, capabilities to model certain forms and allow for the required precision.

Surface modelling

Surface modelling was developed with the ambition to represent 3D geometry in a precise way, and the main contributors come from the vehicle and machine industry, where the challenge has been to represent geometry for car bodies, aeroplane frames and boat hulls with high precision. The general idea is to model surface geometry by interpolating a bi-directional net of points. The most commonly used technique is Non-Uniform Rational B-Splines, which will be briefly described.

The basic equation behind the shape functions used for NURBS modelling reads,

$$N_{i,p}(\xi) = \frac{\xi - \xi_i}{\xi_{i+p} - \xi_i} N_{i,p-1}(\xi) + \frac{\xi_{i+p+1} - \xi}{\xi_{i+p+1} - \xi_{i+1}} N_{i+1,p-1}(\xi), \quad (2.1)$$

where $N_{i,p}$ is the B-spline basis function at the i^{th} control point for degree p , ξ is the parameter position along the basis function and ξ_i is the knot with index i . The equation is solved using a recursive algorithm, such as Cox-De Boor [149].

For the application on 2D surfaces, these shape functions are applied in the two parameter directions and associated with a control point to provide user interaction. The description for the surface S is obtained through the multiplication of the two shape functions such that,

$$S(\xi_1, \xi_2) = \sum_{i=1}^n \sum_{j=1}^m N_{i,p}(\xi_1) M_{j,q}(\xi_2) P_{i,j}, \quad (2.2)$$

where n, m are the number of control points in direction 1 and 2, N, M are the shape functions in the two directions and $P_{i,j}$ is the bidirectional control point net [149].

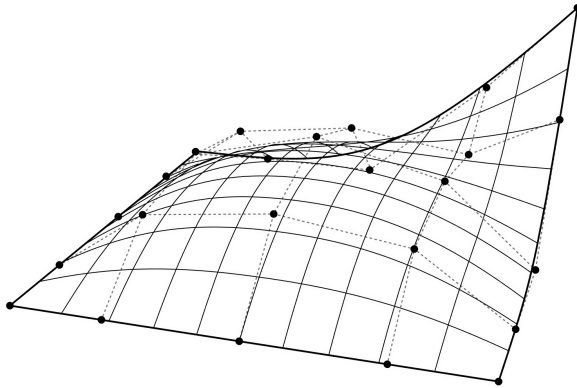


Figure 2.3: A bi-directional grid of points and the resulting NURBS surface. Each point on the surface is calculated as a weighted average from the control points using Eq.2.2.

Figure 2.3 illustrate an example of a surface and its corresponding control point net. Since the basic form of a NURBS surface has a bi-directional structure, it is not very well suited to represent triangular shapes. However, the possibility of creating sub-domains on

a surface allows for trimming and cutting to alleviate these shortcomings. A set of surface patches can be grouped to form a poly-surface, and the matching of the control points over the edge to a neighbouring surface will dictate the continuity across an edge. G0 refers to position continuity, G1 to tangential continuity, G2 to continuity of curvature etc. The structured grid of points on a NURBS surface makes it easy to convert to a mesh or point representation. The visualisation of the surface on a screen is typically a mesh, so efficient translations are core functionality for most 3D modelling software.

Polygon modelling

The polygon mesh is commonly used to represent free forms in a digital environment and was developed as a modelling technique by the film industry. For modelling, the emphasis leans towards artistic freedom rather than high precision. In essence, a mesh is a collection of vertices with topological information that describes the connectivity with other vertices to create edges, triangles, quads, or ngons. Each vertex is given three coordinates which are all stored in a matrix.

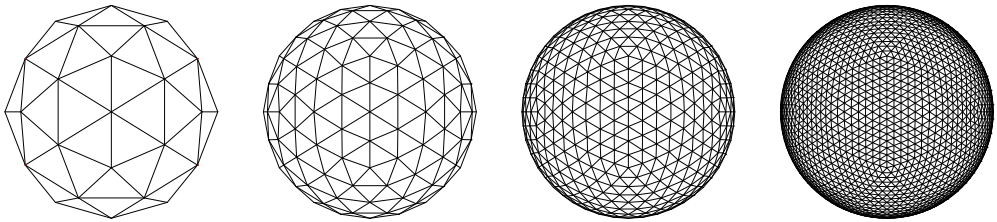


Figure 2.4: *Illustrating how to create smooth shapes with increasing subdivision of a polygon mesh approximation of a sphere. Smoothness comes at the cost of data storage since higher levels of subdivisions require many vertices.*

The edge and face matrices are then just a collection of vertex indices; thus, the mesh becomes relatively lightweight and straightforward. However, a high mesh density may be required to approximate curved shapes well, and a recursive subdivision algorithm may be applied. In contrast to NURBS surfaces, the organisation of a mesh is unrestricted in terms of holes and disjoint parts. Therefore, it is a free, simple and flexible representation. The application of subdivision, as shown in figure 2.4 adds smoothness but also results in shapes that are complicated to control and produce. A mesh can be divided into points to create a point cloud, but it is challenging to recreate a surface from an arbitrary mesh. The polygon mesh representation can also be extended to a volume mesh where tetrahedral elements replace the triangles. Figure 2.9 show a digital recreation of a column from the TWA terminal roof as described in section 1.2, modelled as a volume mesh. The volume mesh can be used to perform point inclusion calculations to generate a representation, as shown in figure 2.9.

Point clouds

The third way geometry tends to be represented in a digital environment is through point clouds, as shown in figure 2.5. Just like it sounds, it is essentially a collection of points that represent the geometry of an object and is not typically recognised as a modelling technique. It is a rather rough form representation and is often converted to a mesh for further data processing. Point clouds are particularly relevant for 3D scanners and other devices used for measurement that record data in discrete points, that includes, for example, laser-based LIDAR sensors. Algorithms that generate 3D models from photographs, such as photogrammetry, also generate point cloud representations. The point cloud as a form representation typically requires handling large quantities of data.

It is a much more primitive representation technique than NURBS or polygon mesh representation. It is only useful when it is combined with the vast computational power of modern computers. Algorithms such as Delaunay triangulation, marching cubes or alpha shapes can then be applied to convert point clouds to mesh data with reasonable accuracy.

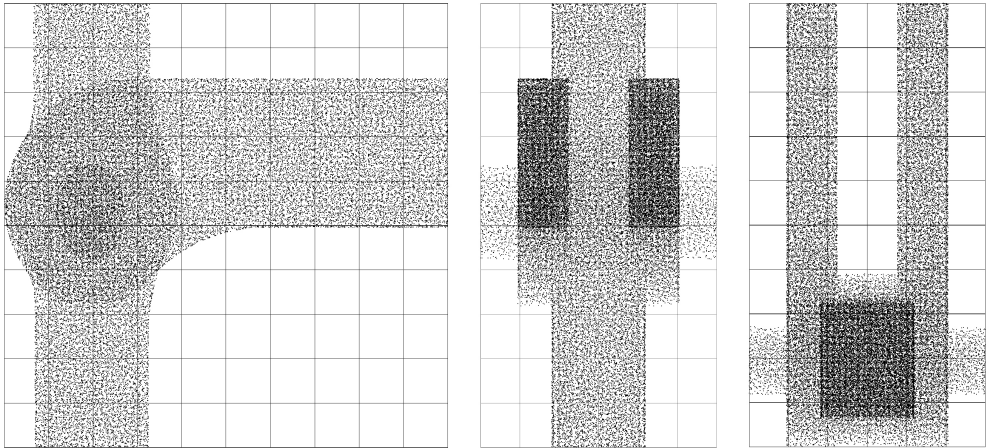


Figure 2.5: *Point cloud representation for a node in the Tamedia office structure. Darker fields indicate more particles based on the node geometry and view direction.*

2.1.2 Dealing with point clouds

Each of the digital form representation techniques presented thus far is applied in the appended papers of this thesis. However, a particular focus is concentrated on meshless methods; therefore, some mathematical techniques supporting the management of point clouds are mentioned in short. That includes barycentric coordinates for point inclusion calculations, a Monte Carlo method for introducing noise in the particle distribution and structuring points using zones.

Barycentric coordinates

Barycentric calculus is an approach to treating points in geometry as centres of gravity in relation to other points to which weights are ascribed. It can be used to evaluate triangle and tetrahedral centres and point inclusion. A Barycentric coordinate system is furthermore a type of coordinate system where the location of a point is specified in relation to a simplex, which is a triangle in 2D and tetrahedron in 3D, see figure 2.6. For example, if a point p is evaluated in relation to the Barycentric coordinate system of a triangle ABC or a tetrahedron $ABCD$ and all the coordinates of p are positive in each respective case, then p lies inside the triangle or the tetrahedron.

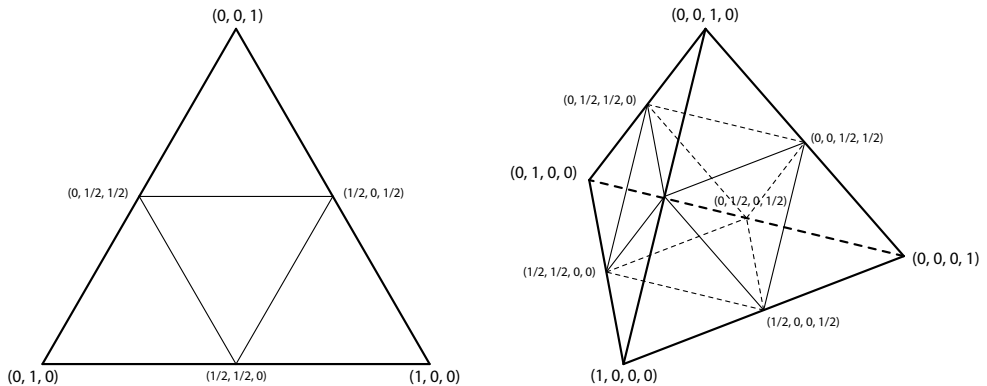


Figure 2.6: *Barycentric coordinates for the 2D and 3D. The coordinate system in each case is defined by the corners of the simplex.*

Monte Carlo Methods

Monte Carlo methods used random samples to approximate a probability distribution. The typical use case is when many calculations are required to solve a task. Such an example can be found in computer rendering, where light calculations are done by tracing a large number of rays bouncing around in the scene. A vast amount of rays would be needed to represent photons in natural light, which becomes unfeasible. The problem can be solved by using a random sample or rays with a Monte Carlo simulation. The more rays that are used, the more realistic the light appears, and the simulation converges on the right solution [91]. A Monte Carlo simulation can also be used to distribute particles in a known random configuration. An initial grid of regularly spaced particles is first generated. Each particle is then moved along a random vector. The new position for the particle is accepted if the overlap with the neighbouring particles is less than a given limit value. The results converge on the same probability for each position which becomes a good starting point for the setup of a problem where irregular material conditions are desirable. This approach is used in papers [138] and [137].

Zones

Zoning is a fundamental concept in the setting up of a meshless model or a particle model. Searching through all particles n for all other particles n only works for really small models, and a strategy to limit the search domain is needed. A model with 10k particles would require 1e8 searches, including distance computations with square roots, if zoning is not used. Creating an arm for a particle a in a 2D model using zones requires a search through 9 zones in the worst case. For a 3D model, the worst case is a search through 27 zones. Typically, the zones are constructed based on the bounding box for the object that should be populated with particles, as shown in figures 2.7 and 2.8.

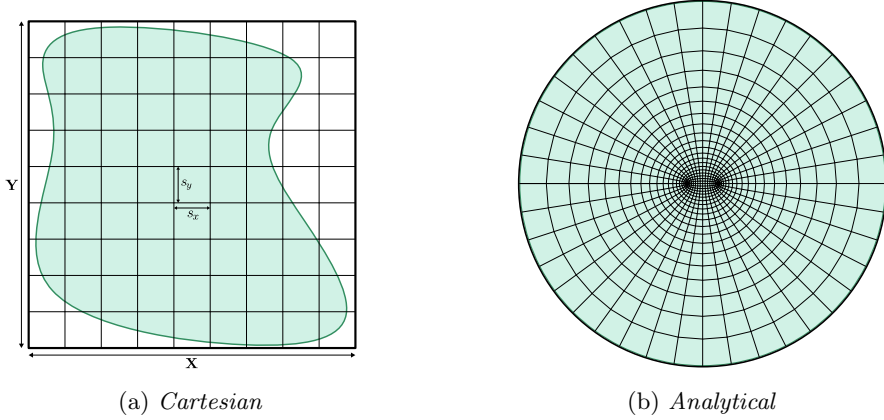


Figure 2.7: Showing two different strategies to create zones in 2D. Left: The zones are aligned with the Cartesian coordinate system. Right: The zones are aligned with the parametrisation of the surface, which also defines the object.

In a Cartesian coordinate system the axis aligned bounding box (AABB) can be defined as a set such that

$$\mathbf{AABB} = \{\mathbf{X}, \mathbf{Y}, \mathbf{Z}\}, \quad (2.3)$$

where $\mathbf{X}, \mathbf{Y}, \mathbf{Z}$ are ranges such that

$$\mathbf{X} = \{x_{\min}, x_{\max}\}, \quad (2.4)$$

$$\mathbf{Y} = \{y_{\min}, y_{\max}\}, \quad (2.5)$$

$$\mathbf{Z} = \{z_{\min}, z_{\max}\}. \quad (2.6)$$

The domain \mathbf{AABB} is then divided into zones based on a zone size \mathbf{S} which is defined for each dimension such as

$$\mathbf{S} = \{s_x, s_y, s_z\}, \quad (2.7)$$

with the condition that $\min(\mathbf{S}) > \max(h_a)$ meaning that the smallest zone dimension is larger than the largest particle horizon. The number of zone divisions \mathbf{N} can then be

calculated from

$$n_x = \lfloor (x_{\max} - x_{\min})/s_x \rfloor, \quad (2.8)$$

$$n_y = \lfloor (y_{\max} - y_{\min})/s_y \rfloor, \quad (2.9)$$

$$n_z = \lfloor (z_{\max} - z_{\min})/s_z \rfloor. \quad (2.10)$$

If the zones are defined and created through incremental steps in the $\mathbf{X}, \mathbf{Y}, \mathbf{Z}$ ranges following precisely that order, the zone index a_{zi} for a particle $\mathbf{a} = \{x, y, z\}$ where $\mathbf{a} \in \mathbf{AABB}$ can be calculated from

$$a_{zi} = \frac{x + (x_{\max} - x_{\min})}{2s_x} + \frac{y + (y_{\max} - y_{\min})}{2s_y}n_x + \frac{z + (z_{\max} - z_{\min})}{2s_z}n_xn_y. \quad (2.11)$$

The zoning strategy for a particular problem can also be defined using another coordinate system. This is exemplified in Figure 2.7b with elliptical coordinates and also used for the numerical experiments in paper D. Eq. 2.11 is, however, only valid in the Cartesian case, and the present form is written for the 3D case, but the equivalent equation for another coordinate system could be derived based on the same principles.

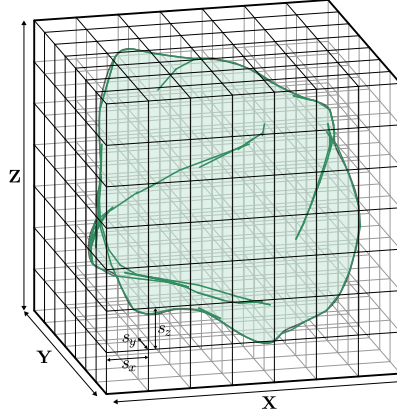


Figure 2.8: *Zones in 3D defined from the bounding box around some object for which each point $p \in \mathbf{AABB}$. Image create by the author.*

Particle representation of the Gerberetter and the TWA terminal column from section 1.2 can be seen in figures 2.9 and 2.10 respectively. In each case, the object's shape is defined with NURBS surfaces converted to a mesh. The mesh is then converted to a volume mesh and filled with a regular grid of particles. The particle noise can then be introduced using said Mote Carlo strategy, should that be deemed appropriate for the simulation at hand.

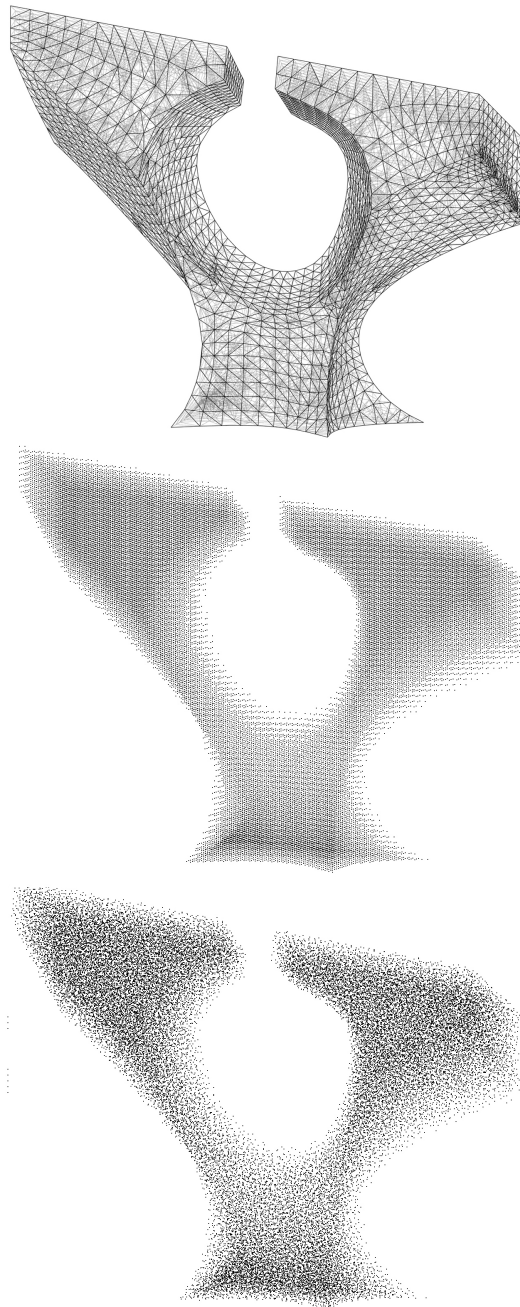


Figure 2.9: *Tetrahedral volume mesh and two types of particle distribution for the geometry of the TWA terminal column.*

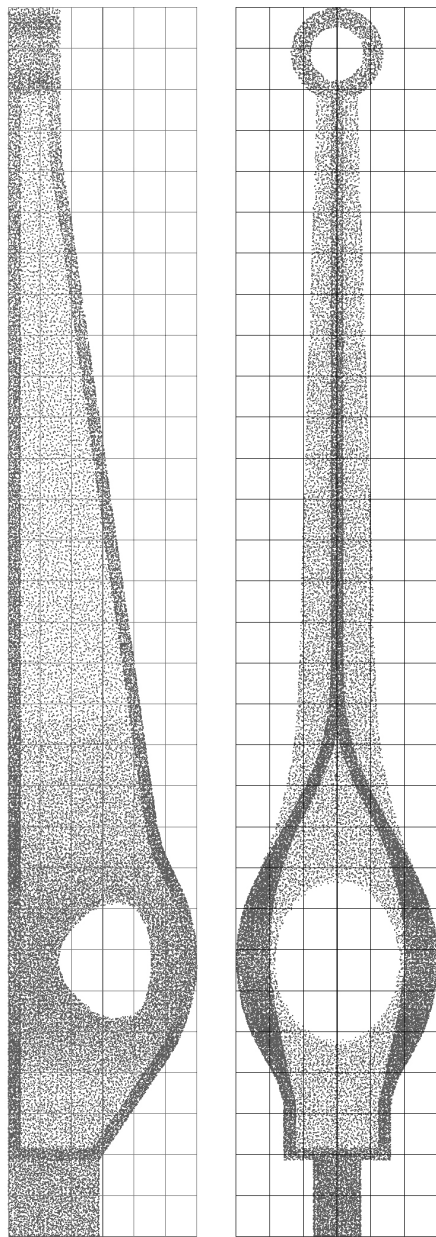


Figure 2.10: *The gerberette for the Centre Pompidou modelled with randomly distributed particles.*

2.2 Materials and production

This section touches upon some physical material conditions paramount to the digital shaping of structural details. That includes material properties and techniques for manufacturing. The section is sorted based on the three classical building materials, steel, concrete and wood. This choice is made partly because of the wide use of these materials in construction but also due to the characteristic differences between the three. Steel is an isotropic, ductile and high-strength material, concrete has high strength but is brittle and, therefore, most often used as a composite with steel, and timber is an orthotropic and organic material. The characteristics of these three materials in terms of toughness (the ability to absorb energy without fracture) and strength (the ability to withstand load without plastic deformation) is shown in figure 2.11a.

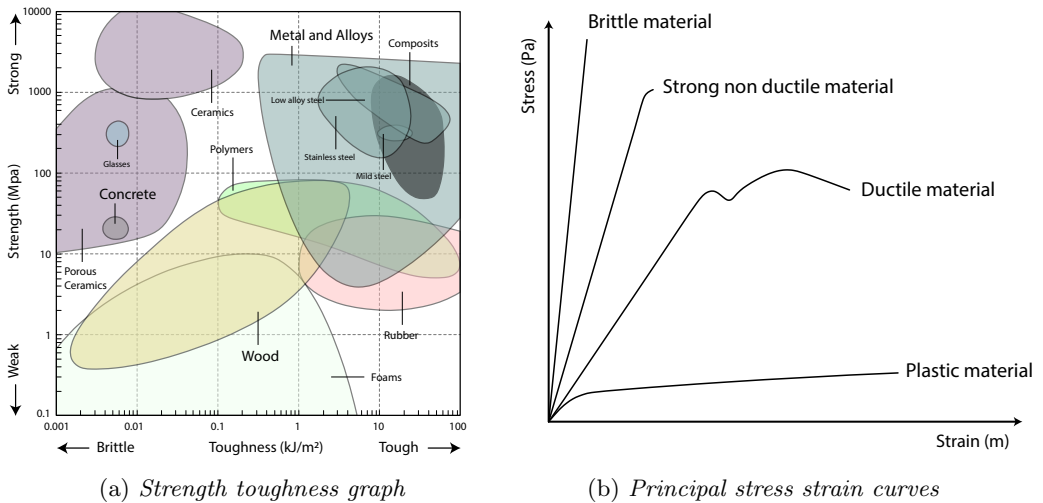


Figure 2.11: *Left: A variety of materials described in terms of strength and toughness. Right: Stress and strain graph for a set of different types of materials. See attribution in the figure credits list.*

The study of materials can be approached from different perspectives, for example, through experiments and empirical work, the crafts tradition in manufacturing and the study in science. Each of these contributes essential perspectives for understanding how materials function. The study of materials is often divided into scales such as the microscopic, mesoscopic and macroscopic scales. While the microscopic scale determines the behaviour in the macroscopic scale, most applications require significant simplifications for practical reasons.

Materials are also typically classified as solids and fluids. Whereas fluids tend to flow under the influence of a force, a solid remains seemingly unchanged, and the difference in behaviour can be seen in the atomic bonding forces. It is not easy to draw a shape line

between these two states, which motivates another class of materials called viscoelastic, whose behaviour is partly solid and partly fluid. In order to discuss the structural properties of solids, a set of definitions will help. Considering a solid with a cross-section area A and length L exerted to some external force F which extends or compresses the material. The stress σ is then defined as

$$\sigma = F/A. \quad (2.12)$$

Stress is similar to pressure, with the difference that stress can be both tensile and compressive, whereas pressure is always compressive. The length change dL of the material compared to its original length L can be used to compute the strain ϵ such that,

$$\epsilon = \frac{dL}{L}. \quad (2.13)$$

The stress and strain can then be linked via Hook's law which states that

$$\sigma = E\epsilon, \quad (2.14)$$

where E represents the slope in the stress-strain diagram and is typically referred to as the material's stiffness. Similar relationships can be postulated for other types of deformation and stress. The shear stress τ is linked to the shear strain γ via the shear modulus G such that,

$$\tau = G\gamma. \quad (2.15)$$

Under hydro-static pressure p the volume change in the material can be expressed as,

$$p = -K \frac{dv}{V} \quad (2.16)$$

where K is the bulk modulus, dv is the change in volume and V is the initial volume.

The inter-atomic forces in the microscopic scale of materials can be illustrated using the Condon-Morse curve as shown in figure 2.12. The figure shows the bonding force between two atoms as a function of their intermediate distance. Although it can be difficult to draw direct conclusions about macro-scale behaviour from atomic models, a few interesting observations from the Condon-Morse curve are made in [85] and the most relevant observations for this context are presented below in short:

1. When a material is extended or compressed, the stress-strain relationship follows an initially linear path, as postulated in Hook's law.
2. Since the total force curve in figure 2.12 is initially symmetric about the equilibrium position. The stiffness is the same in compression and tension.
3. At large strains, the linear relationship between stress and strain, according to Hooke's law, no longer holds.
4. There is a limit to the tensile strength of the material.
5. There should be no possible failure in compression since repulsive forces between atoms increase *ad infinitum*.

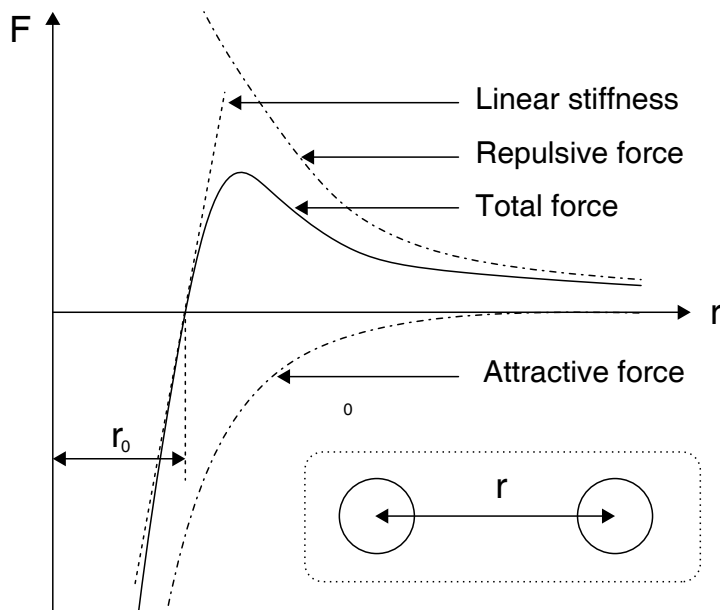


Figure 2.12: *Cordon-Morse curve showing the forces between two atoms as a function of their intermediate distance. It shows that it is easier to pull atoms apart then to push them together which motivates why materials fail in tension. See attribution in the figure credits list.*

Many materials display a plastic behaviour when the load is increased beyond the elastic zone, as indicated schematically in figure 2.11. Plastic deformation results in a permanent shape change after unloading, and it may be a valuable property, for example, in manipulating certain materials. Plastic deformation may eventually lead to fracture when a material is loaded further. Fracture requires the creation of new surfaces in a body, which is caused by a supply of energy of some form. In this context, such energy supply is limited to only strain energy.

The theoretical strength of a material can be estimated by adding up the strength of its inter-atomic bonds. However, the strength registered in physical experiments has been to be much lower. Griffith addressed this discrepancy in 1923 based on experimental work with glasses. He suggested that the discrepancy could be explained by initial imperfections weakening the material. Griffith then balanced the strain energy of deformation with the notion of surface energy and postulated that,

$$\sigma_{failure} = \sqrt{\frac{2E\gamma}{\pi a}}, \quad (2.17)$$

where $\sigma_{failure}$ is the failure stress, E is the young's modulus for the material, γ is the surface energy and $2a$ is the initial crack length.

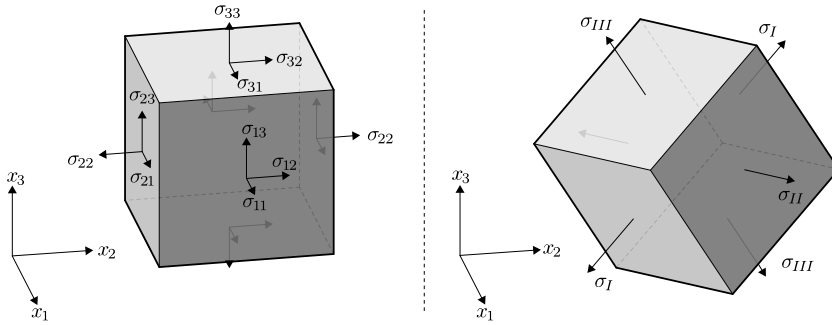


Figure 2.13: Material point and the components of the stress tensor σ to the left and the principle stress directions to the right.

2.2.1 Steel

The development of steel as a structural material has played an essential role in the growth of the modern industrialised world. It was used to build machines that enabled factory-based mass production, but it also enabled a whole new typology of infrastructure with railway tracks and bridges. It was used to build the first skyscrapers but was also a key material in the invention of reinforced concrete.

Cast iron was initially used to replace wood in everyday items such as ploughs, sewing machines and pots for cooking. Steel was at the time a known material but was regarded as a premium product. It was expensive to produce and was used for small items such as watches, springs, knives and swords. Train tracks were developed as an infrastructure to assist the expanding industries in Great Britain in the middle of the 18th. They were initially built of timber but were later on reinforced with a layer of cast iron to enable the transport of heavier loads. However, the brittle character of cast iron meant that the tracks often cracked. Wrought iron was invented in 1820, and the production process was improved over the following decade, making production more efficient and, therefore, more economical [15].

At the inception of iron as a structural material, the structures were designed based on techniques used for wooden carpentry, so naturally, this new building material was first applied using similar joining techniques. The wooden carpentry details in cast iron with the 1781 Iron bridge can be seen in figure 2.16, where mortise, tendon and blind dovetail connections are used for joining the precast structural elements [163].

The development of steel production with the Bessemer method in the mid-18th century made steel production more efficient. Further improvements based on Thomas Sydney's method to remove phosphorous from steel resulted in better consistency and higher quality production results. The great Chicago fire of 1871, which destroyed thousands of timber buildings in the city, led to more strict regulations on non-flammable building materials and the lightness of steel compared to stone and masonry made it an attractive choice [110].

Industrialised construction fascinated Mies van der Rohe, and steel as a new building material offered opportunities with high precision prefabrication, strength, durability and

slenderness. Mies believed that the specific properties of each material should be reflected in its proper use, and therefore steel should be used for the load-bearing structure. His architecture was known for the use of extravagant materials and fine detailing, and he favoured the clarity of the orthogonal grid and the right-angle aesthetics, which also seemed to fit with the rational ideal of industrialisation and mass production. Therefore, many of his steel structures are assembled from steel beams, and columns with standard H, I, T and U sections [19].

Mechanical properties

Steel is an important material for the construction industry today. It has the advantage of being strong, predictable and ductile with rather isotropic properties. The specific

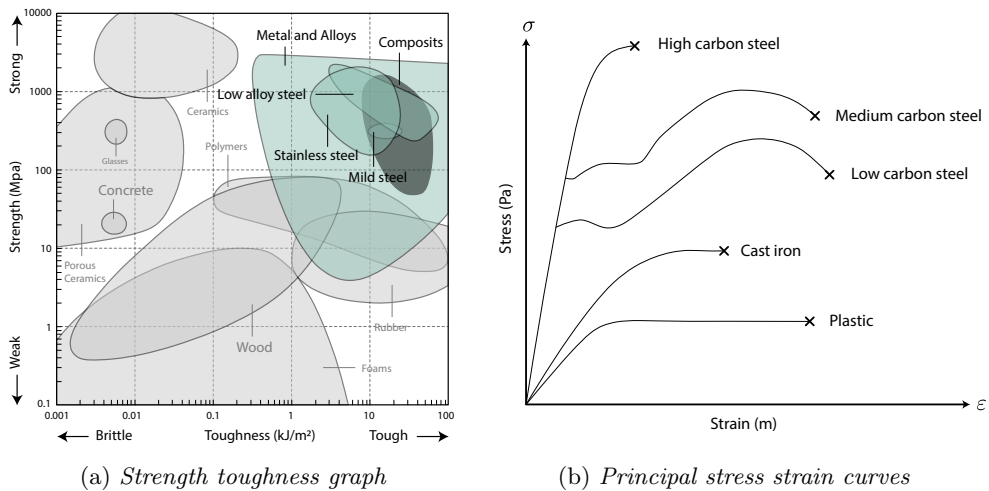


Figure 2.14: Left: A collection of metallic materials in terms of strength and toughness [184]. Right: Illustration of typical stress-strain graph for various metal qualities to give a rough overview of similarities and differences. See attribution in the figure credits list.

properties can also be altered in the refinement process when raw iron is converted to steel. Increasing the carbon content in the iron gives a high strength but more brittle material, whereas a lesser carbon content results in a more ductile and soft material. Typical construction steel has a carbon content of between 0.15 and 0.3 %, making it relatively ductile and appropriate for welding. The crystalline microstructure of the material can be altered through various techniques such as heat treatments and cold working. By rapidly cooling the steel, it will become stronger but more brittle, whereas a slowly cooling specimen will become more ductile. Using cold treatment techniques, such as compression and twisting beyond the yield limit, the grain size will be reduced, increasing the strength of the steel.

From a structural designer's point of view, steel properties, such as yield strength and fracture strength, are essential to understand. The typical stress-strain curve from a

basic tension test is illustrated in figure 2.14 b, and illustrates the initially linear elastic behaviour, yielding, hardening and fracture of the test piece. Yielding is caused by dislocations in the metal's atomic structure and leads to a sudden increase in deformations without significant strength gains. The deformations after yielding are referred to as plastic deformations and do not go back where the structure is unloaded.

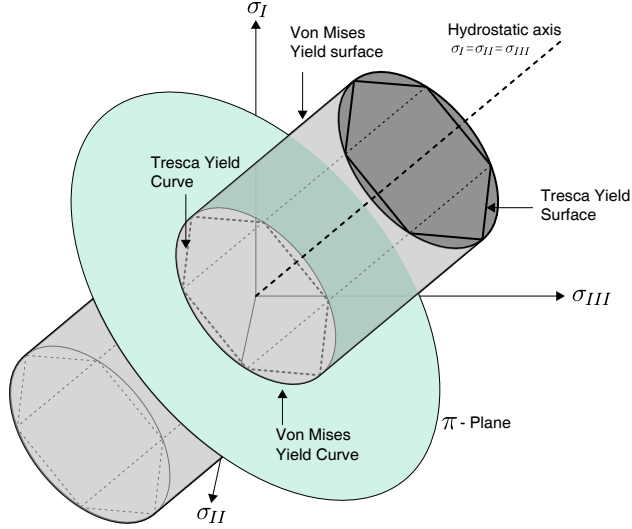


Figure 2.15: The yield surface according to von Mises and Tresca which are often used for metals and alloys. See attribution in the figure credits list.

For a continuum element the yielding of metals can be approximated with von Mises and Trescas yield criterion, see figure 2.15. The yield stress according to von Mises can be calculate based on the stress components from figure 2.13 such that

$$\sigma_v = \frac{1}{2}[(\sigma_{11} - \sigma_{22})^2 + (\sigma_{22} - \sigma_{33})^2 + (\sigma_{33} - \sigma_{11})^2 + 6(\sigma_{23}^2 + \sigma_{31}^2 + \sigma_{12}^2)], \quad (2.18)$$

where von Mises stress σ_v is chosen to be equal to the yield strength σ_y . The yield surface according to Tresca based on the pricple stress directions as shown in figure 2.13,

$$\sigma_v = \max(|\sigma_I - \sigma_{II}|, |\sigma_{II} - \sigma_{III}|, |\sigma_{III} - \sigma_I|), \quad (2.19)$$

where σ_v is chosen to be equal to the yield strength σ_y and $\sigma_I, \sigma_{II}, \sigma_{III}$ represents the three principle stresses.

As the material deforms beyond the yield point, some metals will undergo a phase called strain hardening which can be seen in figure 2.14b for medium and low carbon steel curves. The material then gets harder for a while until a neck forms in the tensile test specimen, and the cross-section area drops such that the stress-strain curve drops until it eventually breaks. The total elongation of the specimen and the change in cross-section area at necking is used as measures for ductility for a metal.

Established production techniques

Riveting is an early joining technique for steel structures that became popular in the 19th century during industrialisation. Rivets are typically applied when assembling layered sheets of steel, even though it is not a necessary restriction intrinsic to the joining technique. Structures made of rivets are nevertheless often based on the geometric logic of flat sheets, which can be altered into the surface shape of developable surfaces. The elastic properties of steel make riveting possible since it involves the plastic deformation of an initially cylindrical pin.

The use of high-strength bolts in steel structures for buildings was first introduced by Batho and Bateman in 1934 [56]. Bolts are mechanically similar to rivets but with the beneficial property of enabling disassembly—a quality which could result in an upsurge of bolted construction due to ambitions of circularity. Unlike rivets, bolts are often used to assemble more elaborate structural members, such as hot-rolled beams and columns.

Welding is the process of joining pieces of metal through fusion, and the technique can be traced back to the bronze age. During industrialisation, arc welding was first used by the automobile industry, and the first all-welded building structure was in 1924. The new technology effectively replaced the previous techniques such as riveting and bolting, especially in the machine industry, where welding resulted in cost savings, increased production speed and more refined products. Like other steel-based techniques, it is often applied as a technique to stitch together plates of steel that are formed prior to assembly. Due to the logic of the method, it is also better at joining plates than solid chunks of steel. The British museum great court roof, shown in figure 2.39 exemplifies the use of site welding in architecture where thick flame-cut star-shaped steel plate nodes are welded to the tapered rectangular steel beams as shown in figure 2.19.

Steel casting is a rather unusual approach in the production of building components. It comes with relatively few formal restrictions, which are mainly due to the mould material choice of mould removal strategy. Both depend on whether or not the mould should be used for multiple casts. One of the first building projects to use steel casting was the Centre George Pompidou, as described in section 1.2. They used cast steel for the gerberettes (shown in figures 1.5 1.4 1.6) which connect the trusses carrying the floor slabs with the lateral support system in the facade. The technique allowed the design team to make a multi-functional structural component carefully crafted into an almost bone-like structure through a meticulous process using different tools and techniques, including models made of insulation polyester [74]. More details about the project, the motivations and challenges with casting are outlined in 1.2.

The nodes in the Mero space frame (referred to in section 1) are created using a subtractive manufacturing technique called milling. It is a technique where a drill removes material from an initial body of material, with the top or the side of the drill, which means that the shaping logic of milling follows the principle of a ruling line. The nodes in the Mero system are initially solid casts from which material is removed with the milling process. The connecting bars consists of hollow extruded steel tube onto which conical castings are welded. The bar is finally attached to the node with a bolt inside the cone. In that way, the Mero system combines a range of standard steel manufacturing techniques. A similar system with a hollow node is shown in figure 2.17.



Figure 2.16: *The first bridge build with iron is located in Shropshire in England and is called the Iron Bridge. The transition from wood craft to iron casting can be seen in the details which replicate the joining techniques from traditional timber structures. See attribution in the figure credits list.*

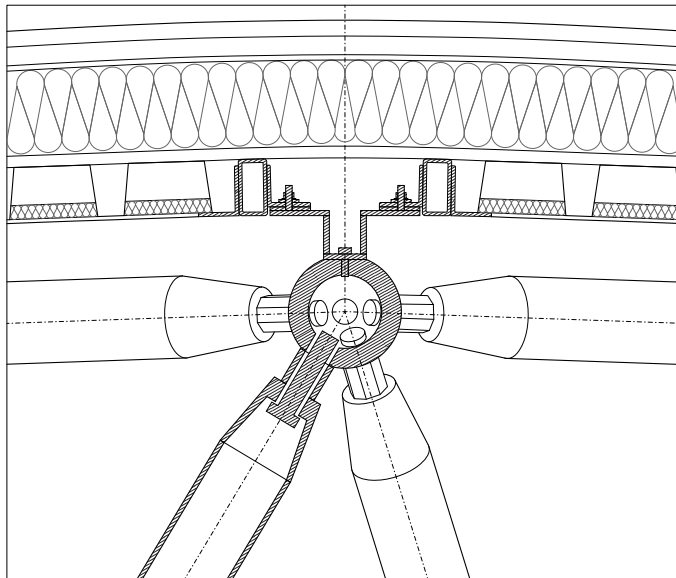


Figure 2.17: *Nodal connection for a space frame with hollow spherical nodes. The drawing is recreated from one of the details from the Mexico City airport project.*



Figure 2.18: *Worker attaching one of many bolts at the Empire state building during construction in 1930. The Chrysler building can be seen in the background. See attribution in the figure credits list.*



Figure 2.19: *Flame cut star-shaped node of the Great Court roof for the British Museum in London. The nodes were attached to the rectangular members using welding on site. See attribution in the figure credits list.*

New production techniques

Some consider additive manufacturing (AM) to be one of the key drivers in the current industrial revolution. It has been applied to metals using techniques such as Laser Powder Bed Fusion. AM provides greater design freedom than most other manufacturing strategies and comes with benefits such as increased production flexibility, product customisation, reduced lead-time, efficient material utilisation, and reduced weight [61]. For the architecture and construction industry which is widely relying on construction steel, AM has the potential to remove many limitations posed by other production techniques related to geometrical complexity with the potential to enable a new approach to the design of modern structures. However, until now, there are only a few examples of AM applications by architects and engineers. One example is the MX3D bridge created with an AM technique called Wire and Arc Additive Manufacturing (WAAM) [128]. WAAM is not restricted by a 3D printer bounding box which is the case for LPBF. There are, however, some challenges when working with metal printing. Large amounts of heat need to be dissipated to avoid overheating, which is shape-dependent to some extent. When the metal cools, it shrinks, and internal stresses build up inside the object and can cause severe deformation if not accounted for correctly. The process of support removal using a mill may also restrict the design space, and production needs to scale up to reduce the current high cost.



Figure 2.20: *Physical prototype of a 3D printed nodal connection in steel created with laser powder bed fusion printing. The shape of the node is found through a topology optimisation process as described in paper B.*

2.2.2 Concrete

Concrete is another essential building material, and it is often found combined with steel as reinforcement. In its earlier forms, the ancient Romans used a material closely related to modern concrete for buildings like the Colosseum and the Pantheon. The fact that some of these buildings stand to this day is a testimony to the material's robustness. Joseph Aspdine of England was credited with the invention of the portland concrete in 1824, and the real breakthrough for concrete happened with the invention of steel reinforcement. W. B. Wilkinson got the first patents for reinforced concrete slabs in 1854 to improve building fire resistance. However, french horticulturalists Lambot and Monier developed similar systems and got patents in the same decade [26]. The development of this new construction technique continued to spread around the world. Design codes were developed to bridge from practice to theory, notably by Matthias Koenen and Edmond Coignet. Unlike wood, steel and stone, concrete results from innovation rather than discovery. It can be considered a composite material where the different constituents are placed purposefully to perform specific structural tasks. Initially, the introduction of steel re-bars was primarily thought of as a safety precaution, but the focus shifted towards seeing it as a load-carrying design strategy.

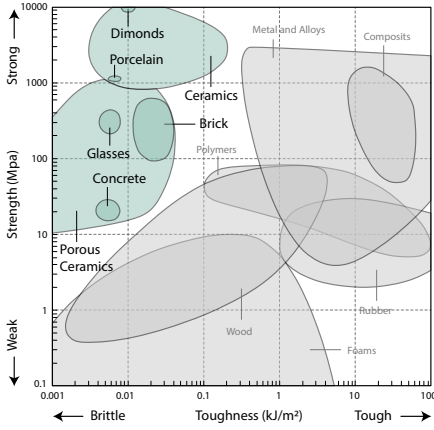
The German civil engineer Emil Mörsch was an important contributor to the field of theoretical discussion of reinforced concrete with an exposition in Wayss and Freytag's publication "Reinforced concrete construction, its application and theory". The French engineer Max Du Bois assisted Mörsch in his work and translated his pioneering publications into French in 1909 in a book called *Le Béton Armé* [19]. Le Corbusier got introduced to reinforced concrete through his acquaintance with Du Bois and became one of the leading proponents of this new building material. He was fascinated with the efficiency of construction enabled by concrete casting and speculated on how casting a building could be similar to filling a bottle of water. While repetition, standardisation and industrialisation were vital for Le Corbusier's architectural vision, he simultaneously explored the formal possibilities with concrete casting in many of his buildings.

Figure 2.23 show a reinforcement drawing for the Pont du Naou-Hounts in France designed by Alexandre Sarrasin in 1931. The drawing illustrates the vital importance of steel reinforcement in the areas where the stress is predominantly tensile.

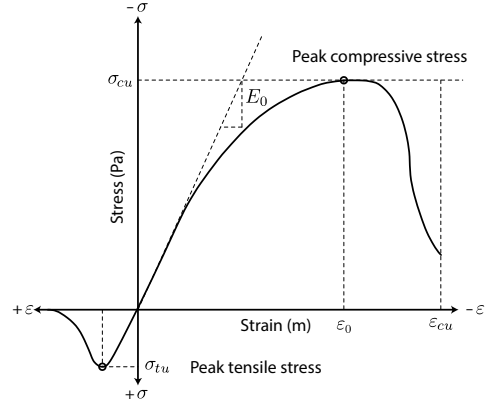
Material mechanics

Concrete was originally a mix of three ingredients: water, cement and aggregate. The cement reacts with water through hydration and acts as a binder between the hard rock aggregates, creating a strong and durable material. In modern concrete, the mix is complemented with admixtures and other additives to tailor the properties and performance of the wet mix and the final product. Concrete is a mineral-based brittle-elastic material with high compressive strength but only a fraction of that capacity under tensile load, illustrated in figure 2.21b. Therefore, the tension forces introduced in a concrete structure are taken care of using steel reinforcement [146].

Cement is a crucial ingredient in concrete and is typically produced from lime and silica, found in limestone and shale. The production process is relatively simple but involves high temperatures. The limestone and the clay are ground into a fine powder and heated



(a) Strength Toughness Ceramics



(b) Typical stress strain for concrete

Figure 2.21: Left: Showing the properties of the family of ceramic materials, including concrete [184]. Right: Showing a typical stress-strain curve for concrete. See attribution in the figure credits list.

in a rotating kiln where calcium silicates, calcium aluminates, and other compounds are formed into clinker. The clinker is cooled, ground and mixed with a few percentages of gypsum, slowing down the hardening phase so that the concrete mix remains workable during construction. The aggregate in the concrete mix stands for around 70-80 % of the bulk volume. However, the cement paste which binds together the mix controls the strength. The ratio between cement and water determines the porosity of the hardened concrete, which plays an essential role in the strength properties. The importance of the water-cement ratio was first recognised by Abrams in 1918 and compiled in a formula sometimes referred to as Abrams law. It states that the concrete strength f_c can be calculated from

$$f_c = \frac{k_1}{k_2^{w/c}}, \quad (2.20)$$

where w/c is the water-cement ratio and k_1, k_2 are empirical constants based on type of cement, age, curing regime etc [85]. Water cement ratios rarely exceed 1.0, making the concrete mix too fluid and rarely below 0.3 since the concrete becomes difficult to compact, and the heat released in the hydration process may cause problems.

The final concrete mix typically consists of fine and coarse aggregates, water, cement and chemicals, usually referred to as admixtures. The purpose of the admixtures can be to alter the properties of the wet mix, the early hardening phase or the final hardened concrete. A range of different admixtures can be used, including accelerators (speeding up hydration), plasticisers (improving workability of the mix), retarders (delaying the hydration process), air entering agents (to entrain air bubbles to reduce freeze-related damage) etc. The choice of admixtures makes it possible to tailor the concrete for a specific use case. As the curing starts, the strength of concrete develops gradually over

time and has reached most of its capacity after 28 days, which is also the curing time for cylinders and cubs used for strength tests.

The non-linear stress-strain behaviour of concrete in compression, see figure 2.21b is due to the appearance of micro cracks, which increase in number and length as the load increases. Glucklich divides the non-linear stress-strain curve into four stages and discusses the characteristics of each stage in [67]. The first stage is, according to Glucklich, characterised by cracks in the transition zone between aggregate and cement past. In the fourth stage, the cracks have spread to a network of relatively large cracks causing large strains and eventually failure.

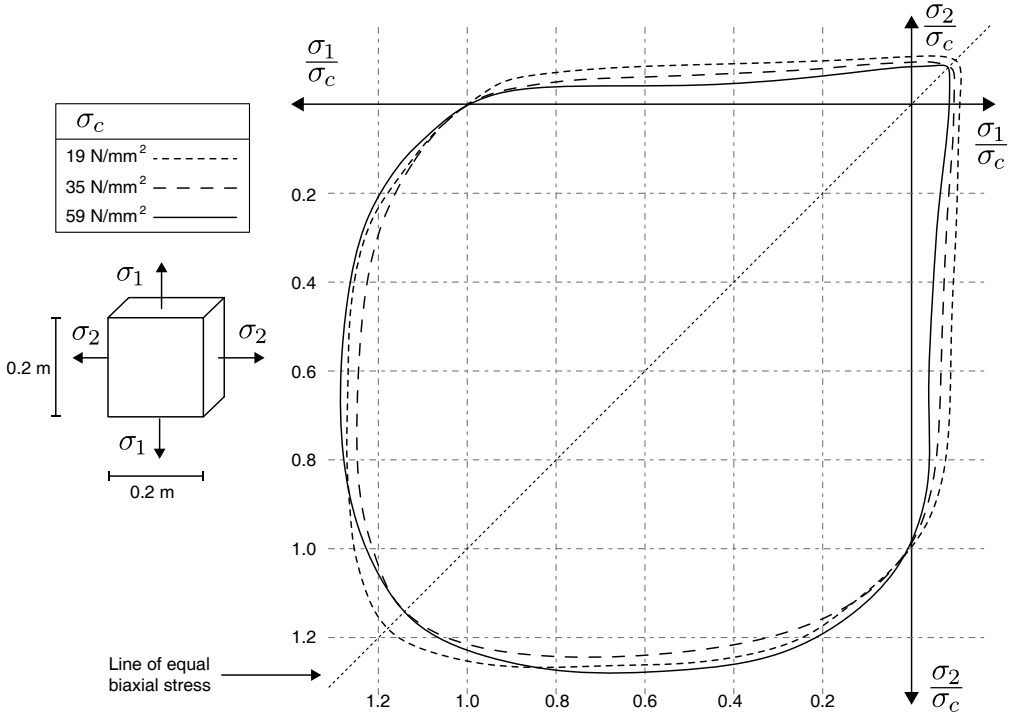


Figure 2.22: Biaxial strength of concrete based on experimental data by Kupfer et al from 1969. The original diagram can be found in figure 6 in paper [99].

Griffith's fracture theory was first applied to concrete by Kaplan and Glucklich as described by Soroka in [174]. According to Griffith, the energy required for a crack to form is determined by the initial crack's length and the material's specific surface energy. However, according to the findings by Glucklich, fracture in concrete is characterised by a great number of microcracks which develop in many highly stressed zones simultaneously. Thus more than just the surface area of the critical crack should be considered in calculations of required energy. Cracks in concrete do not typically propagate in straight lines but rather follow irregular paths around cement grains and aggregate particles.

In a real structure, especially in complex loading situations, the concrete will likely be subject to a multi-axial stress state. Such conditions may lead to a rather abrupt change in performance and failure stress. A 2D version of a failure envelope based on Kupfer in [99] is shown in figure 2.22. The graph illustrates how the proportions of stress σ_1/σ_c and σ_2/σ_c vary in a biaxial loading scenario, where σ_c represents the uni-axial failure stress. The three different types of curves represent three different concrete mixes, which are shown to behave similarly in relative terms. The figure also illustrates the low strength of concrete in tension and the rapid loss of capacity as either one of σ_1 or σ_2 is in tension. For concrete failure in a triaxial stress state, the Drucker-Prager yield surface introduced in [50] can be used.

Established production techniques

Casting is the primary construction technique for concrete structures. It can be performed onsite, so-called in-situ casting or in a factory environment, often referred to as pre-casting. Whereas in-situ castings are not limited in size due to transport, the onsite conditions may be challenging in terms of climate control and precision. Pre-casting, on the other hand, can be done with high accuracy, but sizes are limited due to transport and the process of erection. The particular characteristic of concrete connections produced from in-situ casting construction is the seamless integration with adjacent elements, shown clearly in the photographs from the construction of the JFK terminal building. There is no definite distinction between the column, the node and the roof structure, which are all integrated into one continuous structural system.

The geometrical possibilities with cast concrete structures are quite literally a mirrored reflection of the material used for the mould. For moulds based on timber planks and plywood sheets, the geometry effectively belongs to the class of ruled surfaces (thus can be constructed with straight plank lines), of which some are developable (can be constructed by bending sheet material such as plywood). However, there are other casting techniques, such as fabric casting, for which the structure's shape can obtain the characteristics of a minimal surface, again based on the mould material properties [186]. An example of fabric casting is the *KnitCandela* shell by the Block research group, described in [152].

New production techniques

Another construction technique that is getting attention in concrete research is additive extrusion-based 3D printing. Either as an in-situ based extrusion where the printer is brought to the site and a wheel-base is used to increase the immediate reach of the printer. Or in terms of pre-printing in a factory environment where the printed object needs to fit within the printer range. One early example of such manufacturing is the *Radiolaria Pavilion* as described in [28]. It is made using a concrete-like material based on sand and with a cement-like binder.

Two main challenges to this technique need to be overcome for application on a large scale. The first one is about creating a mix that hardens fast enough not to require a supporting mould while still retaining as much of the high strength as possible that can be achieved with traditional casting. Since the concrete mix needs to be distributed through a nozzle, the opening size will dictate the maximum size of aggregate that can be used.

The second challenge is to introduce reinforcement to improve the tensile strength and to do that with good bonding between the concrete and the reinforcing material[145] [131]. Various attempts have been made in that regard and are described in [73]. Some of these include; the placement of reinforcement material horizontally in between printed layers, metal cables placement along with the concrete extrusion, and the use of concrete mixed with short fibres (of carbon or glass). Another strategy is to print the formwork, where reinforcement is placed, and concrete is poured, like in conventional casting.

The application of 3D printing with concrete structural components will likely rely on the success of the reinforcement strategy. It is unlikely that the inherent tensile capacity of the concrete is enough for the range of load cases a complex structural node may be exerted too. That would render the design space for such components too limited.

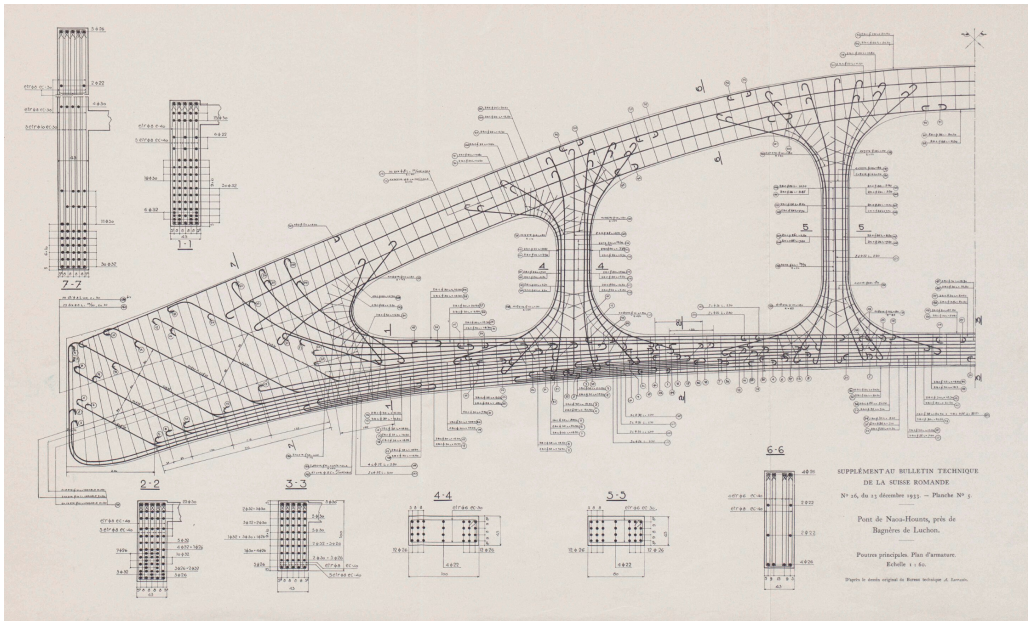


Figure 2.23: Reinforcement drawing for the vierendeel concrete bridge Pont du Naou-Hount in France from 1931 by Alexandre Sarrasin. See attribution in the figure credits list.



Figure 2.24: *A photo from the construction of the TWA terminal in New York City in the early 1960s. The in-situ concrete joint is characterised by the seem less blending of roof and column. See attribution in the figure credits list.*

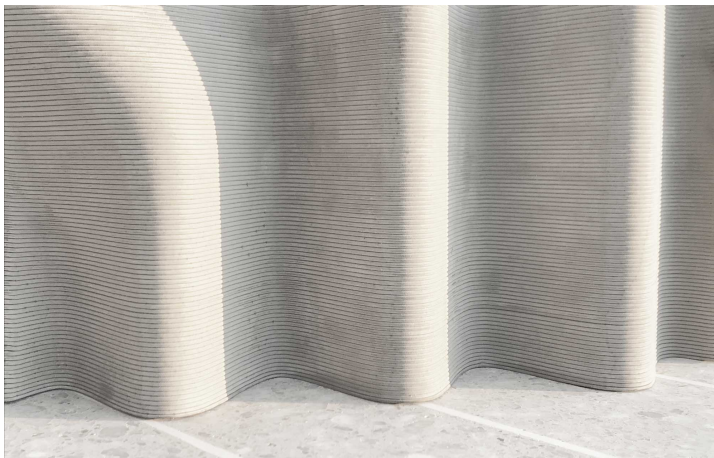


Figure 2.25: *3D printed concrete wall by Aectual. A Dutch company that develops platforms for circular, tailor-made interior objects from 3D printed recycled materials. See attribution in the figure credits list.*

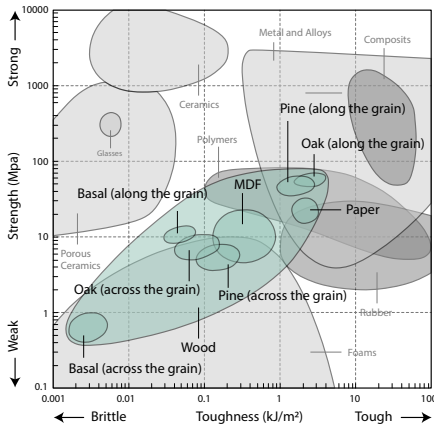
2.2.3 Wood

Wood has been an essential material for the construction of buildings in many cultures and regions, and a wide variety of construction techniques have been invented to tame the grain-based material. Sometimes the skills have travelled between continents along trade routes or due to wars and take over of land. However, as Elias Cornell points out in [40], the travel of technology is sometimes overemphasised, and it is likely that similar building techniques also developed independently of each other. After all, the techniques are developed from the material properties point of view. Even though timber qualities vary with climate (even within the same species), the main characteristics of the timber will be the same independent of place.

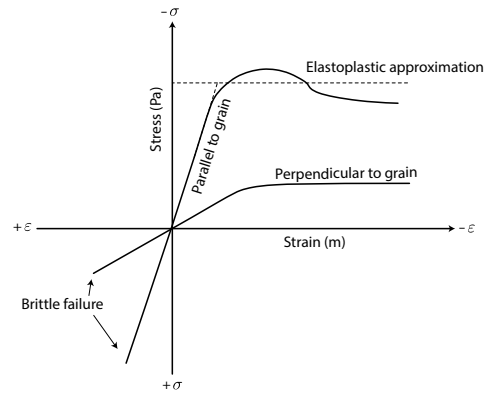
The development of construction technology and timber-based products has led to an up-surge in the use of timber structures worldwide [183]. The use of timber is argued to reduce the environmental impact of a building based on the following reasoning: wood is a renewable construction material, it requires comparatively little energy for processing, wood store carbon, and timber products are reusable and recyclable [183].

Material mechanics

Wood is typically described as an orthotropic material, meaning the mechanical properties vary with the direction of a specimen. Due to the cylindrical nature of the log, these directions are usually referred as the longitudinal direction (parallel to the grain), the transversal direction (along with the rings in the cross-section) and the radial direction (perpendicular to the surface of the cylindrical shape).



(a) Strength and toughness for wood



(b) Typical stress strain for timber

Figure 2.26: Left: Showing the strength and toughness properties for the family of wood based products [184]. Right: Showing a typical stress-strain curve for wood [191]. See attribution in the figure credits list.

Many variables influence the stiffness and strength of wood, including growth rate

(which determines the density), moisture content and imperfections such as knots and cracks. However, due to the anisotropy of wood, one of the most crucial strength parameters is the relationship between grain direction and loading angle. Compression strength depends on moisture content tension strength less sensitive to such variations. However, the tensile strength is more sensitive to loading angle than compressive strength, as shown in figure 2.27. At loading angles of about 60 ° relative to the grain angle, the tension strength has dropped to about 10 % of its maximum, and the compressive strength at roughly 15 %.

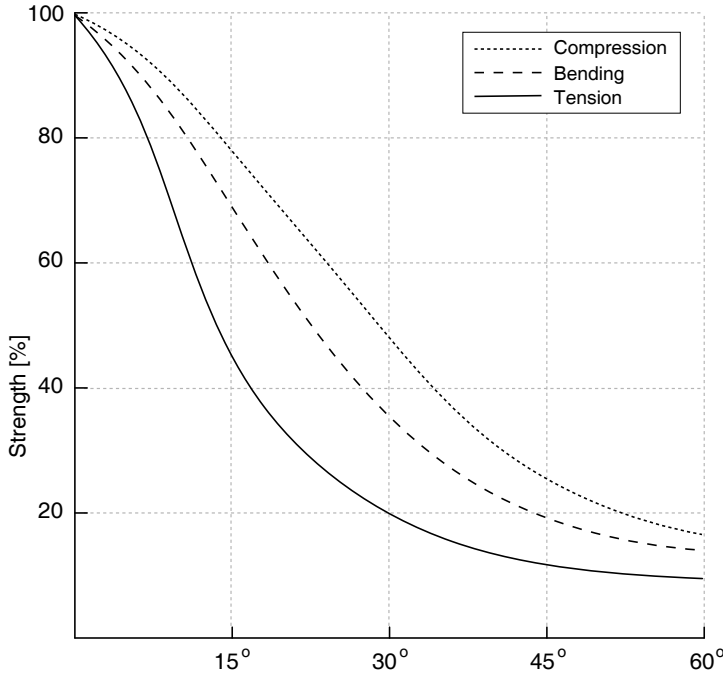


Figure 2.27: The strength of wood in compression, tension and bending based on the angle between grain direction and load direction. Graph redrawn based on figure 39.1 in [85] originally from [18].

The strength of wood for a given load to grain angle can be approximate using Hakinsons formula which states that the strength σ_θ at angle θ relative to the grain direction can be calculate from,

$$\sigma_\theta = \frac{\sigma_p \sigma_q}{\sigma_p \sin^n \theta + \sigma_q \cos^n \theta}, \quad (2.21)$$

where σ_p is strength parallel to the grain, σ_q is the strength perpendicular to the grain and n is a numerically determined constant. In tension n is typically in the range 1.5 – 2.0 and in compression 2 – 2.5.

Established production techniques

The log house is traditionally built by stacking horizontal logs that are connected at the corners through notching, and it has been an important building technique for the Nordic countries. Peter Sjömar gives a detailed description of how the construction and design of such buildings progressed in Sweden with case studies of log houses from the 13th and 14th century. The illustrations in his PhD thesis exemplify the carefully detailed connections that were possible to make only through skilled carpentry. Even so, the detailing requires both time and effort [170].

The rise in popularity of steel and concrete as building materials in the early 19th and 20th centuries, discussed in the previous sections, also meant a decline in the popularity of timber. The emphasis for refined wood-based products shifted from structural elements toward components such as floor slabs, doors and windows, leaving the forest and timber industry deeply depressed [178]. Quite surprisingly, the opposite happened in the aeroplane industry with de Havilland Aircraft as designers assisted by furniture industry expertise for production. They introduced the Mosquito flight bomber in 1940, shown in figure 2.28, built on a wooden structural frame.

An upsurge for timber construction came a few years later with the technological advancements in plywood production and the invention of a urea-formaldehyde resin called Redux. The inventor, Norman de Bruyne, was a researcher in the de Havilland propeller division and made important contributions to various types of glue for structural use. Properties such as strength, water and heat resistance meant that the new glue could be used to laminate wooden planks to make beams, columns and other more complicated shapes. Effectively removing the girth as a restricting parameter for a wooden structure and opening a new world of possibilities.

Apart from the new possibilities with glulam elements, the issue of connecting elements remained. The attention shifted to explore the strength of screwed/nailed joints and bolted connections with shear plates and splint-rings right, which significantly increased the strength [178]. The type of handcraft detailing in joinery that Sjömar portrays was deemed obsolete due to increased pressure of standardisation, higher production rates and reduced cost. Skilfully crafted timber detailing, which required the shaping of complicated three-dimensional forms, was replaced by standardised off-the-shelf products.

The first code of practice for structural timber was published in 1952, and the first international structural engineering conference was held in Southampton in 1961. The wave of interest in concrete shell structures in the UK then led to a surge of hyperbolic shell structures in timber built until the interest suddenly dropped in the late 70s.

In parallel with the development of timber shells in the UK, french architect Jean Prouvé experimented with timber construction in combination with other materials [23]. With a background as a metal worker, Prouvé's work translated technology from industry to architecture, industrial and furniture design. With a mindset to use "the right material in the right place," he broke old traditions in carpentry and paved the way for industrial production in the architectural context. Exemplified by his use of large plywood panels that were bent into shape over a steel structure with the Evian pump room and also the Youth club in Ermont Paris.



Figure 2.28: *The Mosquito aeroplane designed by de Havilland Aircraft with a frame structure in wood. See attribution in the figure credits list.*



Figure 2.29: *Youth club in Ermentau outside of Paris from 1967 by Jean Prouvé. The roof is made by sheets of bent plywood. See attribution in the figure credits list.*

New production techniques

The first digitally controlled machine for the refinement of timber elements was invented in the 1980s and was initially used to improve accuracy in production. Five-axis CNC machines with automatic tool switching were introduced to the market in the '90s and enabled the manufacturing of complex three-dimensional elements which could be used for joinery. The new possibilities with computer-controlled machines inspired a tendency to look back at the traditional handcraft. Aspiring to rejuvenate the detailing of a skilled craftsman but with the aid of computational technology and the efficiency of industrial mass production.

Japanese architect Shigure Ban has become re-known for his innovative work with inexpensive and unusual materials such as cardboard and paper has also broken ground with some complex timber structures. The new headquarters in Zurich for the media company Tamedia as shown in Figure 1.11 and introduced in section 1.2 exemplifies the use of glulam and CNC production technology.

In academic research Prof. Christopher Robeller has explored the possibilities with CNC control refinement of timber elements with a set of experimental buildings, described in depth in his PhD [158]. The temporary extension to Chapel de Loup shown in figure 2.31 exemplifies the use of cross-laminated timber elements, refined using CNC machinery as described in [158]. The remarkable precision in production can be seen with joints of the sharp folds, which also give the structure depth and thus increase bending stiffness.

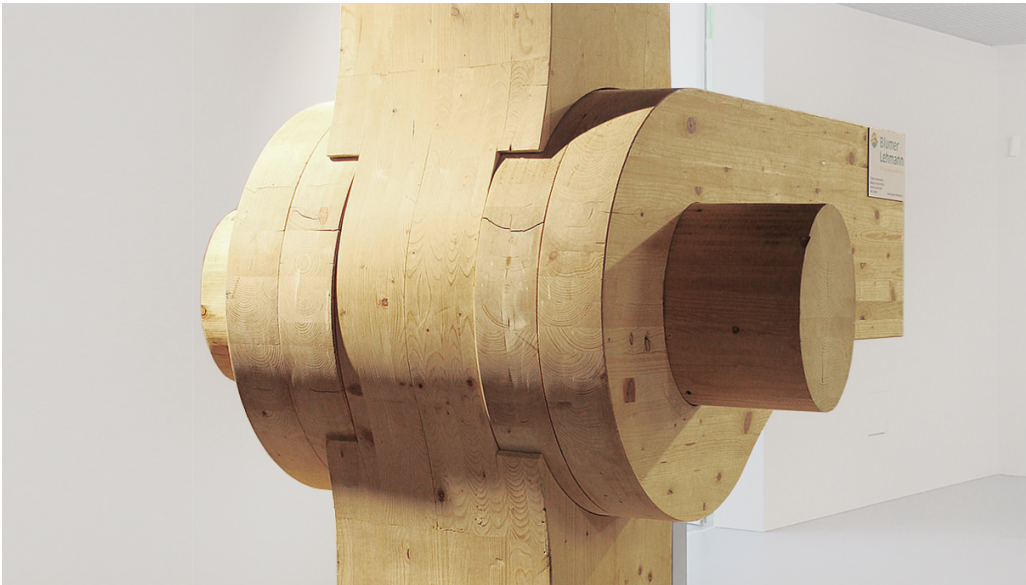


Figure 2.30: Metal free nodal connections for the structure of the Tamedia office building by Shigeru Ban Architects. See attribution in the figure credits list.



Figure 2.31: *Folded plate structure for the Deaconesses of St-Loup in Switzerland by Localarchitecture in collaboration with Prof. Christoffer Robeller. The precision in the joints is achieved with CNC production. Photo by courtesy of Milo Keller, more details in the figure credits list.*



Figure 2.32: *Exterior view of the folded plate structure for the Deaconesses of St-Loup in Switzerland by Localarchitecture in collaboration with Prof. Christoffer Robeller. Photo by courtesy of Milo Keller, more details in the figure credits list.*

2.3 Numerical analysis

Numerical analysis methods can be applied differently depending on the objectives at hand. On the one hand, there is the study of the phenomena of material behaviour under various loading conditions where mathematical models are developed to mimic natural behaviour. On the other hand, there is the development of design codes that assist the engineer in the daily work where safety is the highest priority. That involves the calibration of safety coefficients as a response to theoretical limitations and natural variation of material properties that create uncertainty in performance. The third way analysis can play an important role in structural design is to guide the designer in the design process. That could be for comparative studies of options where the model is evaluated based on stress distribution or deformation. Or for comparison with material strength data from material testing.

When introducing material properties in digital design, a mathematical material model is used to link stress and strain by the constitutive relation. The constitutive models aim to approximate a particular microscopic phenomenon using mathematical relationships retrieved from empirical testing. Some of these relationships are common across many material types, and others are unique for a specific material class, such as fibre delamination in wood. However, independent of the particular material class, the microscopic structures down to the atomic level will determine the macroscopic behaviour as discussed in 2.2. Models used for structural analysis will smear the atomic behaviour over huge areas compared to the atomic scale. Material behaviour varies not only between material classes (should it be crystalline, amorphous or polycrystalline etc.) but also temperature, sometimes moisture content, and loading rate will impact the mechanical properties [159]. Loading cycles, radiation and decay are other factors that may impact the material performance, some of which are difficult to predict. One such (at the time) unpredictable material phenomenon is exemplified by the structural failure of the S.S. Schenectady that broke in half just as she had returned from her sea trial, see figure 2.34. The standard explanation for the incident became known as defective welding. However, later investigations concluded that the butt welded joints were fine, and the failure was more likely due to brittle fracture. The steel used for the hull structure contained high levels of Sulfur and low levels of Manganese, effectively weakening the material and making it more brittle at lower temperatures such as in cold weather [127].

The linear momentum equation which is based on Newton's second law describes that the rate of change of the total linear momentum is balanced by the sum of forces acting on a material body, see Figure 2.33. The external forces can be the gravity force, external load but could also include electromagnetic forces etc. All internal forces within the body are assumed to cancel out according to Newton's third law of equal and opposite forces. The formulation of the linear balance equation thus concerns external forces and can be written as

$$\frac{D}{Dt} \int_V \rho \mathbf{v} dV = \int_V \rho \mathbf{g} dV + \int_A \mathbf{t} dA, \quad (2.22)$$

where D/Dt is the material derivative, V is the volume, ρ is the density, \mathbf{v} is the velocity, \mathbf{g} is the gravitational force, \mathbf{t} is the stress vector acting on the surface A of volume V .

Most solid mechanics simulations start from the assumption that Newton's second

law of motion holds true for every infinitesimal differential volume (i.e. particle) within the analysis domain. Based on the assumption of infinitesimal elements, the use of the Gauss theorem, the Reynolds transport theorem and Navier's formulation of stress, the differential form of Eq. 2.22 can be written as

$$\rho(\mathbf{x})\ddot{\mathbf{u}}(\mathbf{x}, t) = \nabla \cdot \boldsymbol{\sigma} + \mathbf{b}(\mathbf{x}, t), \quad (2.23)$$

where $\rho(x)$ is the mass density at position \mathbf{x} , $\ddot{\mathbf{u}}(\mathbf{x}, t)$ is the acceleration, $\nabla \cdot \boldsymbol{\sigma}$ is the divergence of the stress tensor and $\mathbf{b}(\mathbf{x}, t)$ is the body load.

There are different ways to classify the numerical methods that can be used to approximate the solution to Eq. 2.23, and an overview becomes too large of a scope for this context. However, a few distinctions can be made to discuss the pros and cons of different classes of methods. Eq. 2.23 can be approximated in its strong form, which is typically the case in SPH and peridynamics. Alternatively, it can be approximated after a reformulation into a weak form which is typically the case with the Finite element method (FEM) as explained in [160]. The approach to tackle the approximation can also be done using a local method such as FEM or a non-local method such as peridynamics. The stress state in a material point with a local method is given by the points of the immediate vicinity, which is preferable when dealing with free surface boundaries. However, a local method may be problematic when approximating point loads or sharp corners, where stress concentrations may occur such that the stress does not converge when the mesh is refined. Non-local methods approximate the stress state of a material point a using all neighbours within a certain distance h_a and tend to predict stress concentrations more accurately see figure 2.35. However, this class of methods typically suffers in defining free surfaces compared to local methods.

The partial differential equation can also be formulated using the Eulerian or Lagrangian specification. In the Eulerian specification, the point of observation is fixed, such that the value of function f is dependent on the position x and the time t . This type of specification is often applied in the context of fluid mechanics, where for example, it may be of interest to study how the pressure at a fixed position varies over time. In the Lagrangian specification, on the other hand, individual particles are followed through time, and the particle carries quantities of interest. The position X is dependent on the initial position x and the time t such that the evaluation of a function f becomes $f(X(x, t), t)$. The Lagrangian specification is typically applied in solid mechanics where deformations are small, but it can also be applied in fluid simulations to capture splashing and multi-phase mixing of fluids since mass conservation is guaranteed.

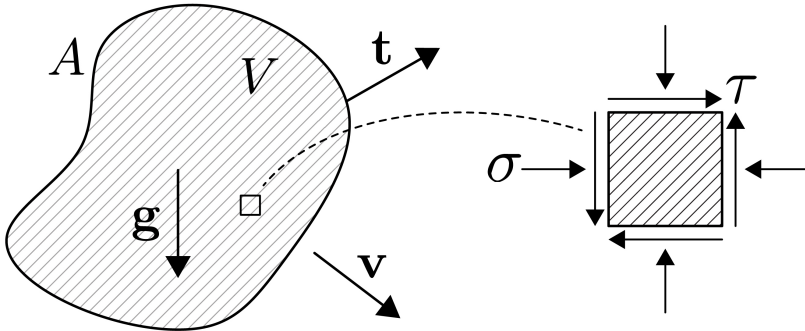


Figure 2.33: An arbitrary material body with volume V and surface area A moving with a velocity \mathbf{v} while exerted to a surface force \mathbf{t} and a gravity force \mathbf{g} to the left. To the right an illustration of an infinitesimal material point with the normal stress and shear stress components from the stress tensor in equation 2.23.

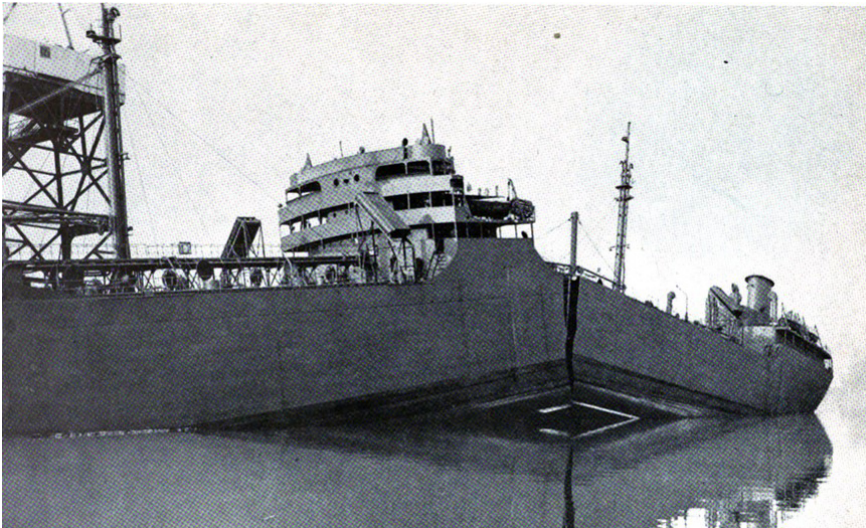


Figure 2.34: View of S.S. Schenectady after splitting in two at her outfitting dock. Brittle fracture of the steel hull due to temperature changes in the water is understood to have caused the failure. See attribution in figure credits list.

2.3.1 Meshless methods

Meshless methods are a class of methods used for solving Partial differential equations where the unknown quantity is approximated based on a field of scattered points without mesh connectivity [38]. The invention was to establish how to take the derivative of a function without using a mesh. For other techniques, such as the Finite Element Method (FEM), a mesh is used to interpolate the quantity of interest between the nodes using shape functions.

When the approximation of the derivative is separated from the configuration of the mesh, the strong tie between mesh quality and the quality of the approximation can be relaxed. Furthermore, the simplicity of implementation without requirements for numerical integration while simultaneously reaching capabilities of solving highly complex problems has made this class of methods attractive.

The methods in the meshless family are sometimes referred to as particle methods which may not necessarily be a good description. The meshless method approximates a continuum domain using a set of material points usually referred to as particles, where each particle a reaches other particles b with a distance h_a from its position, and the approximation is carried out over this area. Particle methods such as the Discrete element method (DEM) approximate the behaviour of a system based on contact laws with some surface forces. Only the immediate neighbours of a particle a have an influence on the overall system behaviour. Based on that distinction, SPH and Peridynamics are meshless methods but are not strictly particle methods.

While meshless methods are typically more computationally demanding than mesh-based approaches, the absence of a mesh enables other types of simulations. That includes, for example, a simulation where the material may fracture or disintegrate, situations where the geometry may move out of alignment, and highly nonlinear material behaviour and stress concentrations or singularities.

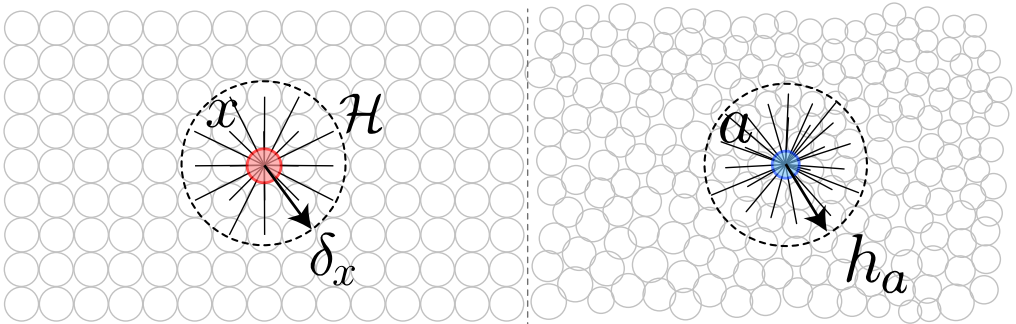


Figure 2.35: Rectangular sub region of a continuum with a varying sized material points/particles. The material point to the left is annotated with the notation used in peridynamics and the particle to the right is annotated according to the SPH standard. All the bonds/arms are drawn for material point \mathbf{x} and particle \mathbf{a} within the horizon which is defined by the radii δ_x or h_a , respectively.

Smoothed particle hydrodynamics

Smooth particle hydrodynamics (SPH) is often referred to as the first meshless method, and it was introduced in 1977 by R.A. Gingold, and J.J. Monaghan [66]. The method was developed for simulations of astrophysics-related problems but has frequently been applied to simulate other phenomena, such as fluid dynamics. It offers several advantages over grid-based methods for fluid simulations, such as automatic mass preservation (since it is a Lagrangian method), but also the possibility to simulate more complex phenomena, including two-phase materials and solid-fluid interaction. The grid-free nature of SPH makes it suitable for modelling of fracture and large deformations, for example, in the context of rock mechanics and geoengineering. The method has also proven helpful in simulations of manufacturing-related processes involving large deformation of solids, for example, extrusion and forging metals.

The drawback with many particle methods, including SPH, is computational cost since large numbers of particles are required for accurate simulations. Like other non-local methods, SPH also faces difficulties in representing free surfaces since the particles on a surface have fewer neighbours compared to non-surface particles and thus become less stiff. Several techniques have been proposed to resolve this issue, such as the ghost particles [187], reproducing kernel SPH etc. Like other particle methods, SPH lends itself well to parallelisation and computation on the graphics card to circumvent the issue of computational cost.

Since the introduction of SPH, tensile instability has been discovered and "marques" SPH with a severe detriment in the context of large deformation solid mechanics. Several additions and corrections have been explored to tackle the issue [125]. Tensile instability was first studied in detail in [179], where it was shown that it leads to non-physical clustering of particles in tension. It is caused when particles lose contact due to large deformations since the radius of the kernel remains constant while the distance between particles increases. Several techniques have been proposed to address the issue, including the Corrected SPH (CSPH), Stress point SPH, principle stress modifications of the classical SPH formulation, and the use of higher order kernels and stability filters, most of which are problematic or unpractical. Monaghan then modified the classical formulation of SPH to tackle the tensile instability by introducing an artificial pressure term R [125]. The formulation was later improved in [68] and related to the sign of the principal stress. This approach, referred to as principal stress correction, does not require significant extra computational effort.

However, the tensile instability problem occurs predominantly in cases of extensive deformations, for example, in the simulation of production processes where the neighbours of particles are updated while the simulation progresses (which is also done with fluids). If the neighbour's connectivity remains constant, the issue seems to diminish. Thus, it is a problem only for very general use of SPH and less of a problem in analysing solid structures even as they disintegrate and fracture. For the implementation of force flux peridynamics in [138] and the application in [137] the issue of tensile instability are not encountered.

The basic principle of SPH can be expressed by the identity in Eq.(2.24) where any

spatial function $A(\mathbf{r})$ can be exactly written as

$$A(\mathbf{r}) = \int^V A(\mathbf{r}') \delta(\mathbf{r} - \mathbf{r}') dV_{r'}, \quad (2.24)$$

where $A(\mathbf{r}')$ is the value of A evaluated at $\mathbf{r} = \mathbf{r}'$ and $\delta(\mathbf{r} - \mathbf{r}')$ is the Dirac delta function. The integral is for a 2D area or a 3D volume depending on the dimensionality of the problem. An approximation is then introduced where the integral is replaced by a summation of values A_b over a region with discrete particles b where the elemental volume $dV_{r'}$ is given by $\frac{m_b}{\rho_b}$. The Dirac delta function in Eq. 2.24 is not differentiable and can therefore not represent any approximated distribution of a continuous field, and is replaced with a weighting function W (also referred to as a kernel function). The SPH approximation of Eq. 2.24 becomes

$$A(\mathbf{r}) = \sum_b m_b \frac{A_b}{\rho_b} W(\mathbf{r} - \mathbf{r}_b, h), \quad (2.25)$$

where m_b and ρ_b are mass and density of a particle b , A_b is the value of A at $\mathbf{r} = \mathbf{r}_b$. The weighting function $W(\mathbf{r}, h)$ typically approximates the Gaussian function, with a compact support and a radius that is $2h$. The weighting function furthermore need to full fill two conditions,

$$\int W(r) dr = 1, \quad (2.26)$$

where the integration is taken over the whole 2D or 3D domain for a particle a . The second condition states that

$$\lim_{h \rightarrow \infty} W(\mathbf{r} - \mathbf{r}', h) = \delta(\mathbf{r} - \mathbf{r}'), \quad (2.27)$$

where, according to Monaghan in [124] the limit is to be interpreted as the limit of the corresponding integral interpolants. The gradient of $A(r)$ is furthermore expressed as

$$\nabla A(\mathbf{r}) = \sum_b m_b \frac{A_b}{\rho_b} \nabla W(\mathbf{r} - \mathbf{r}_b, h), \quad (2.28)$$

and the base equations for approximating a PDE with SPH is thus established. Recalling Eq. 2.23 for the deformation of an elastic body, written with the SPH nomenclature from [124], it reads,

$$\frac{d\mathbf{v}_a}{dt} = -\frac{1}{\rho} \nabla \sigma + \mathbf{g}. \quad (2.29)$$

Applying the SPH approxiamtion from Eq.(2.28) to Eq.(2.29) gives,

$$\frac{d\mathbf{v}_a}{dt} = \sum_b m_b \left(\frac{\sigma_a}{\rho_a^2} + \frac{\sigma_b}{\rho_b^2} \right) \nabla W(\mathbf{r}_a - \mathbf{r}_b, h_a) + \mathbf{g}, \quad (2.30)$$

were $d\mathbf{v}_a/dt$ is the acceleration of a particle a and σ_a, σ_b are the stress at particles a and b .

Peridynamics

Peridynamics is another meshless method which has gained popularity in recent years. Stewart Silling introduced it in 1999 to improve the modelling of spontaneously forming cracks in fracture mechanics. The continuum domain is discretised by a set of material points connected to their neighbours through a set of bonds spanning a distance called the horizon, as shown in figure 2.35. Since the bonds reach further than their immediate neighbours, the method is referred to as non-local and is, therefore, just like SPH, not strictly a particle method. A dense network of bonds makes up the domain of interest for the analysis. Unlike classical continuum mechanics, which relies on the evaluation of partial derivatives, peridynamics works by replacing the differentiation with integration which remains valid also in the presence of discontinuities. The force in a bond is related to the bond deformation and the choice of the constitutive model.

Recalling the linear momentum balance equation for a material point Eq. (2.23) which states that,

$$\rho(\mathbf{x})\ddot{\mathbf{u}}(\mathbf{x}, t) = \nabla \cdot \boldsymbol{\sigma} + \mathbf{b}(\mathbf{x}, t), \quad (2.31)$$

in which the divergence of the stress tensor $\nabla \cdot \boldsymbol{\sigma}$ is replaced in the peridynamic formulation with an integration of force density over the horizon \mathcal{H}_x ,

$$\rho(\mathbf{x})\ddot{\mathbf{u}}(\mathbf{x}, t) = \int_{\mathcal{H}_x} \mathbf{f}(\mathbf{x}, \mathbf{x}', t) dV_{x'} + \mathbf{b}(\mathbf{x}, t), \quad (2.32)$$

which does not rely on spatial continuity assumptions, thus enabling the simulation of phenomena such as fracture. Here ρ is the material density, $\ddot{\mathbf{u}}(\mathbf{x}, t)$ is the acceleration of a material point at position \mathbf{x} at time t , \mathbf{f} is a bond force density acting between two particles at positions \mathbf{x} and \mathbf{x}' , $dV_{x'}$ is the volume associated with particle \mathbf{x}' and \mathbf{b} is the external loading. The calculation of the force density \mathbf{f} varies with the different peridynamic formulations, which are typically classified as bond-based, ordinary state-based and non-ordinary state-based theories as described in [90]. Silling introduced the bond-based theory in [166], and following the notation in [90], where \mathbf{x} and \mathbf{y} represent initial and displaced position of a material point, the bond force is calculated from,

$$\mathbf{f}(\mathbf{x}, \mathbf{x}', t)^{\text{BB}} = cs \frac{\mathbf{y}' - \mathbf{y}}{|\mathbf{y}' - \mathbf{y}|}, \quad (2.33)$$

where \mathbf{y}' is the displaced position of a particle with initial position \mathbf{x}' . The constitutive model is introduced with the micro modulus c , which is calculated from,

$$c = \frac{12E}{\pi\delta^4}, \quad (2.34)$$

where E is the Young's modulus, δ is the radius of the horizon \mathcal{H}_x . The bond stretch s in Eq. (2.33) is calculated from,

$$s = \frac{|\mathbf{y}' - \mathbf{y}| - |\mathbf{x}' - \mathbf{x}|}{|\mathbf{x}' - \mathbf{x}|}. \quad (2.35)$$

Ordinary state-based peridynamics (OSB-PD) was introduced by Silling et. al in 2007 [168] and can be understood as a generalisation of the bond-based theory where the

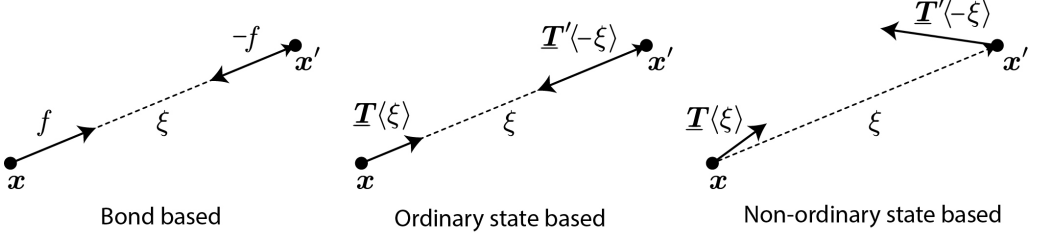


Figure 2.36: Illustration of the 3 types of peridynamics theory, where \mathbf{x} and \mathbf{x}' are two particles, \mathbf{f} is the bond force, $\underline{\mathbf{T}}\langle\xi\rangle$, and $\underline{\mathbf{T}}'\langle-\xi\rangle$ represent the state at each particle.

limitation of a fixed Poisson's ratio is overcome. The OSB-PD builds on the concept of a state which can be described as a mapping. For the application in solid mechanics, the deformation state and the force state are the most central concepts for which definitions and derivation are given in [168]. The equivalent expression for the force density in Eq. (2.31) as outlined for bond-based theory in Eq. (2.33) but instead for the OSB-PD theory is according to [168] given as,

$$\mathbf{f}(\mathbf{x}, \mathbf{x}', t)^{\text{OSB}} = \underline{\mathbf{T}}[\mathbf{x}, t]\langle\mathbf{x}' - \mathbf{x}\rangle - \underline{\mathbf{T}}[\mathbf{x}', t]\langle\mathbf{x} - \mathbf{x}'\rangle, \quad (2.36)$$

where $\underline{\mathbf{T}}\langle\rangle$ is the force state acting on the vector $\mathbf{x}' - \mathbf{x}$ within the angle brackets. For a linear elastic isotropic material the force state is given by,

$$\underline{\mathbf{T}}[\mathbf{x}, t]\langle\mathbf{x}' - \mathbf{x}\rangle = \left(\frac{2ad\delta}{|\mathbf{x}' - \mathbf{x}|} \theta(\mathbf{x}, t) + bs \right) \frac{\mathbf{y}' - \mathbf{y}}{|\mathbf{y}' - \mathbf{y}|}, \quad (2.37)$$

where a , b and d are peridynamic parameters and $\theta(\mathbf{x}, t)$ is the dilatation term [90].

2.3.2 Solver and discretisation

In order to approximate Eq. (2.23) numerically a the temporal and spatial discretisation need to be chosen. An approach to arranging the system of equations also needs to be chosen. For certain types of problems, matrix methods are fast, stable and reliable. However, there are also drawbacks. Matrix methods in computational mechanics typically rely on the inversion of large sparse matrices to solve the equilibrium equation $\mathbf{f} = \mathbf{K}\mathbf{a}$, where, \mathbf{f} , \mathbf{K} , \mathbf{a} are the force vector, the stiffness matrix and the displacement vector. The inverse of \mathbf{K} require quite involved programming or access to certain matrix libraries. This class of methods also run into issues with singular matrices if a local member in a structure fails, causing numerical failure for the rest of the analysis. It is also computationally costly to change a large stiffness matrix during run-time.

On the other hand, the node-wise iterative approach may be slower at run time in many cases but does not run into issues with matrix singularity. If one particle becomes unstable or one arm loses its stiffness (by breaking, for example), that does not affect the continuation of the simulation.

Spatial discretisation

The spatial dimension is discretised with a set of material points or particles with meshless methods. The distribution of particles may vary, but since the principles behind meshless methods do not rely on contact forces between neighbours, the precise packing of particles is less of a concern. However, two different types of strategies are worth mentioning because of how they affect the results: regular and irregular particle discretisation.

The regular particle distribution results in a regular distribution of material properties such as density and stiffness and will also produce symmetric results for a case of symmetric boundary conditions, as, e.g. seen in Figure 2.37a. In that way, the regular distribution is easier to control but represents an idealised case where the material does not have irregularities or imperfections.

The irregular particle distribution, on the other hand, results in an uneven scattering of material properties, which is reflected in results as can be seen for the case of fracture in Figure 2.37b. The scale of the imperfections is dependent on the scale of the noise in the particle distribution. Concrete has, for example, considerable variation in the irregularities based on the scale of its constituents. The scale of imperfections in steel, on the other hand, is much smaller and a regular particle distribution may be a more suitable choice, depending on the scale of the problem domain [137].

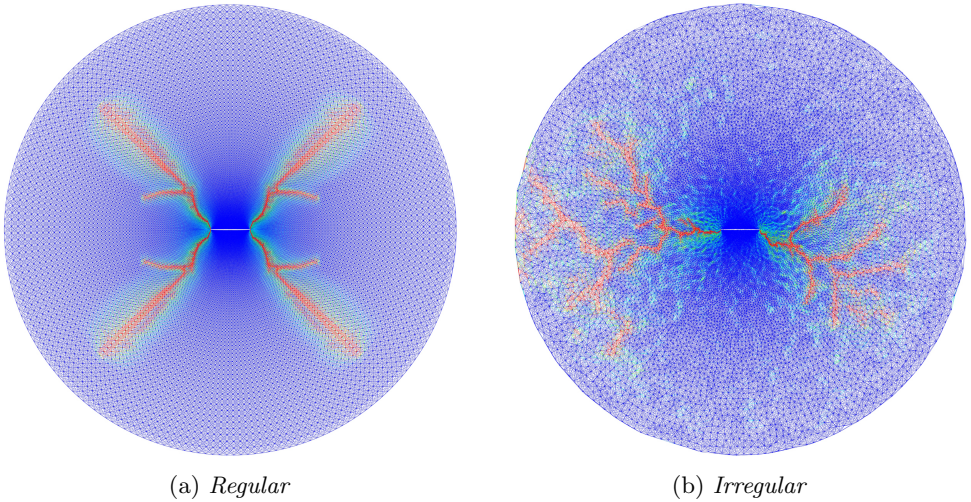


Figure 2.37: *Fracture pattern for the disc in paper D with regular particle distribution to the left and irregular particle distribution to the right. The arms are coloured according to the plastic elongation limit where red represent broken arms and blue arms are intact. For the complete context see paper D.*

Time integration scheme

The differential equation also needs to be discretised in the temporal dimension, and various approaches can be used for that purpose. Time integration techniques can be broadly classified into two categories: implicit and explicit methods [39]. Explicit methods are relatively slow but very robust and thus practical when simulating large deformations, material failure or transient problems. Explicit methods are based solely on the model's current state, which makes them simple to implement. However, explicit methods are only conditionally stable, so relatively small time steps may be needed [108]. Implicit time integration, on the other hand, is unconditionally stable, which means much larger time steps can be used compared to the explicit methods. They rely on the solution of a set of equations involving both the model's current and future states, making them more challenging to implement than the explicit method. Implicit methods are typically more computationally demanding per simulation cycle, but much fewer cycles are needed to reach convergence since the time step can be significantly larger. Whether or not an explicit or implicit approach is used, the equations can then be solved by iterating over the nodes or by compiling and solving a system of equations using matrices. The more non-linear the problem, the more the preference seems to lean toward using explicit methods.

2.4 Shape finding

While all structures are geometrical, only some are designed to work actively with the geometrical principles to serve a structural purpose. In this section, some examples of structural design strategies that integrate geometry and structural function are presented. The common goal for each of these strategies is to reduce material consumption and present elegant and lightweight solutions. Examples of such projects are found in the work of Frei Otto [188], Chris Williams [195] and Philippe Block [24] among others. For lack of a better term, *shape finding* is used in this thesis to gather this group of methods with a common name. The word 'finding' seems appropriate since each of these methods involve a computational process where the shape is 'found' as a result of external conditions such as material properties, support conditions and loading. Some of these methods are typically used to shape entire structures, while others are commonly applied to shape components such as nodal connections.

With the emphasis on the relationship between form and structure, a distinction can be made between two types of shape-finding techniques. There are methods that leave the object's topology unchanged while deforming the object through stretching, twisting and bending. Other methods change the topology of the object by removing material.

Form-finding methods that are used to find minimal surface geometry and size optimisation techniques typically leave the topology intact while changing the form and volume of an object. Topology optimisation, on the other hand, changes the mathematical topology by creating holes and removing material.

2.4.1 Form finding

The term *form finding* in architecture and engineering is used in this context to refer to the process by which the geometrical form is derived based on structural principles. That could include working with soap film, hanging chains and weights, and numerical strategies to derive minimal surfaces or otherwise structurally sound forms. Veenendaal and Block compare different form-finding methods and a range of definitions in [43]. One of the broader definitions states that form finding is the process of,

Finding a shape of equilibrium of forces in a given boundary with respect to a certain stress state. [43]

During the last few decades, various numerical form-finding strategies have been developed. According to [43] these can be classified in the following three categories; the *Stiffness matrix method*, the *Geometric stiffness method* and the *Dynamic equilibrium method*. The last two will be addressed below.

Minimal surface

From a mathematical point of view, the minimal surface can be understood as a surface that locally minimises the area. It is also a surface where the mean curvature is zero everywhere [155]. The principle of minimal surfaces has been applied in architecture for various structural applications. It was an area of significant innovation in the mid-20th

century with Otto, and his research group at the institute of lightweight structures in Stuttgart [188]. The minimal surface structure can be found in nature in various phenomena such as bubbles and spider webs (perhaps more analogous to cable nets). It is also subject to studies in other fields, such as molecular engineering, material science, and general relativity. The shapes have also inspired artists like Robert Engman, Robert Longhurst and Charles O. Perry. Tension structures are shaped as minimal surfaces, and the shape is achieved in a procedure where a pretension force is applied along the boundary of a membrane which is stretched into shape. The reason minimal surfaces are used from membrane structures is to avoid wrinkling of the fabric. A minimal surface has equal stress at each point and is an appropriate form for these types of structures. [6].

In a numerical context, the minimal surface can be approximated using a *Geometric stiffness method* where material stiffness is neglected, and only geometric stiffness is considered. After the shape of the surface has been found with this approach, stiffness and external loading is applied to evaluate the stresses and material thickness needed.

Compression structure

The compression structure is another case of form-active structures where the geometry is vital for efficient performance. It has a long history of exploration, starting with the early stone vaults, progressing with the cathedral domes in the middle ages and continuously driving innovation in the field of large-span structures today. The list is long of important contributors to the development of the structural theories within this field, some of which are Candela, Isler, Shukhov, Nervi, Gustavino, Troja, and more recently Williams and Block [180].

The shape of a compression structure is driven predominately by an external load case and the support conditions, making the precise geometry more challenging to define than a tension structure. There is no elegant mathematical formulation, and the shape is better understood as an equilibrium state where geometry is found through a simulation process driven by boundary conditions and a specific load case like the self-weight. For lighter materials such as steel and timber, the self-weight is often not the governing load case, as it would be for a vault built of stone. One example of that is the shaping of the great court British museum roof, shown in Figure 2.39, which is partially driven by a need to push the horizontal thrust towards the corners of the roof where tension cables could carry it [195]. Therefore, the combination of a load case and boundary conditions drives the shape. The design work with the roof for the Mexico City airport, as described in [182], is another example of a challenging form-finding situation where the governing load case is seismic. In contrast, the form-finding load case is a scaled version of the self-weight. However, the undulating form achieved with form-finding created a bending-stiff surface, and the shape of the columns was carefully controlled in response to the seismic load [182].

Dynamic equilibrium methods can be used to find the shape of such a structure. In this case, the governing load case is applied to the initial geometry, and the static form is found by solving a dynamic problem where the oscillations are eventually damped with some form of artificial damping.

2.4.2 Topology optimisation

The optimisation of geometry and topology of a structure has, according to [20], led to a major improvement in structural efficiency in the automotive and aerospace industry. Topology optimisation (TO) was introduced by Bendsoe in 1988 in [21] and addressed the problems in shape optimisation with the boundary variation method regarding re-meshing and stability. The original TO method was based on a finite element analysis where the domain is divided into a grid of cells where mechanical properties are calculated based on numerical homogenisation.

An alternative soon replaced the homogenisation approach called the Solid Isotropic Material Penalization (SIMP) method, where the density distribution in the design domain is represented by a scalar field where $\rho = 1$ is solid and $\rho = 0$ is void. Regardless of the density value, the material is assumed to be isotropic and homogeneous and material properties such as Young's modulus are related to the density number through a power law interpolation [199]. The scaling of Young's modulus with the SIMP approach could for example, look like,

$$E = E_0 + \rho^p(E_1 - E_0), \quad (2.38)$$

where the penalisation factor p determines the contribution of elements in areas of intermediate density and is typically set between [1, 3], E_0, E_1 represents the lower and upper bound for Young's modulus. Other TO methods include the level set method and evolutionary procedures as described in [199]. Topology optimisation has recently been applied in the concept stage of a design process since the resulting geometry is typically challenging to manufacture. The results have been interpreted indicatively, and the design has been adapted to constraints from manufacturing. However, the advancement of additive manufacturing has resulted in a resurgent interest in topology optimisation in the last few years [199]. An attempt to print a topology optimised space frame node in steel using powder bed laser fusion can be seen in figure 2.20. The printing was aborted half way through the printing process due to deformations in one of the cantilevering parts, potentially due to overheating.

2.4.3 Emergence

The term emergence is a debated concept in sciences, systems theory, philosophy and art. Emergence can be understood as the appearance of new properties achieved by mixing, adding, and interacting parts that do not possess this new property. The new property, or for that matter, the new behaviour, can be said to have emerged from the lower level constituent parts but to put it simply, the whole is greater than the parts [65]. Emergence can also be described as the failure of reduction. Whereas the reductionist may argue that molecules, as higher level entities than the more fundamental subatomic particles which are governed by the laws of quantum mechanics, would make chemistry reducible to quantum mechanics. The emergentist on the other hand, may point to the lack of explanatory capacity with the lower level phenomena in relation to the emerged properties or behaviour on the higher level. In that case, the challenge for the emergence supporter would be to explain what is added as we climb up the complexity levels in the emergence tree [65].

Emergence has inspired architects, engineers and artists in the process of making and is often found in relation to bio-mimicry, where the inspiration for the material organisation is taken from nature. Helen Castle situates emergence in the architectural context in an article for the Architectural association, 2004 , [34] stating that:

Rather than regarding buildings as unchanging, isolated tectonic objects, the goal of emergence when applied to architecture is to construct structures that have evolved through a process of morphogenesis (a never-ending series of exchanges between system and environment), in which form or structure is elaborated to the point of attaining an ecology of performance.

The popularity of emergence in architecture came around a time of rapid development of parametric and computation design tools. The concept is seemingly vague in this context as it seems to act as a wrapper for many simulation-based computational design-related ideas, such as morphogenesis, evolutionary algorithms, parametric design, bio-mimicry, etc. Nevertheless, in the architectural application of emergence, the idea revolves around the design of processes that are generative rather than the design of objects in the classical sense. This approach is explored in the work of Oxman in [141], by Hensel, Menges and Weinstock, in [112] and [113].

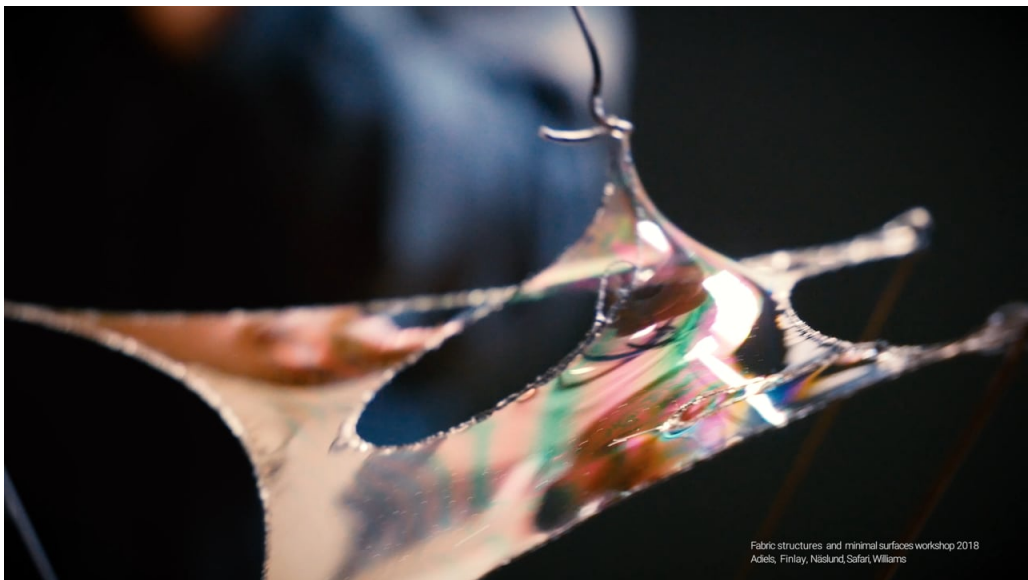


Figure 2.38: *Minimal surface shaped using a soap bubble and thread from a workshop at Chalmers. See attribution in figure credits list.*



Figure 2.39: *The great court roof structure at the British museum deigned by Chris Williams. The shape is defined such that the horizontal thrust is concentrated to the corners. The project was an important reference for the work with the Mexico City Airport project. See attribution in figure credits list.*

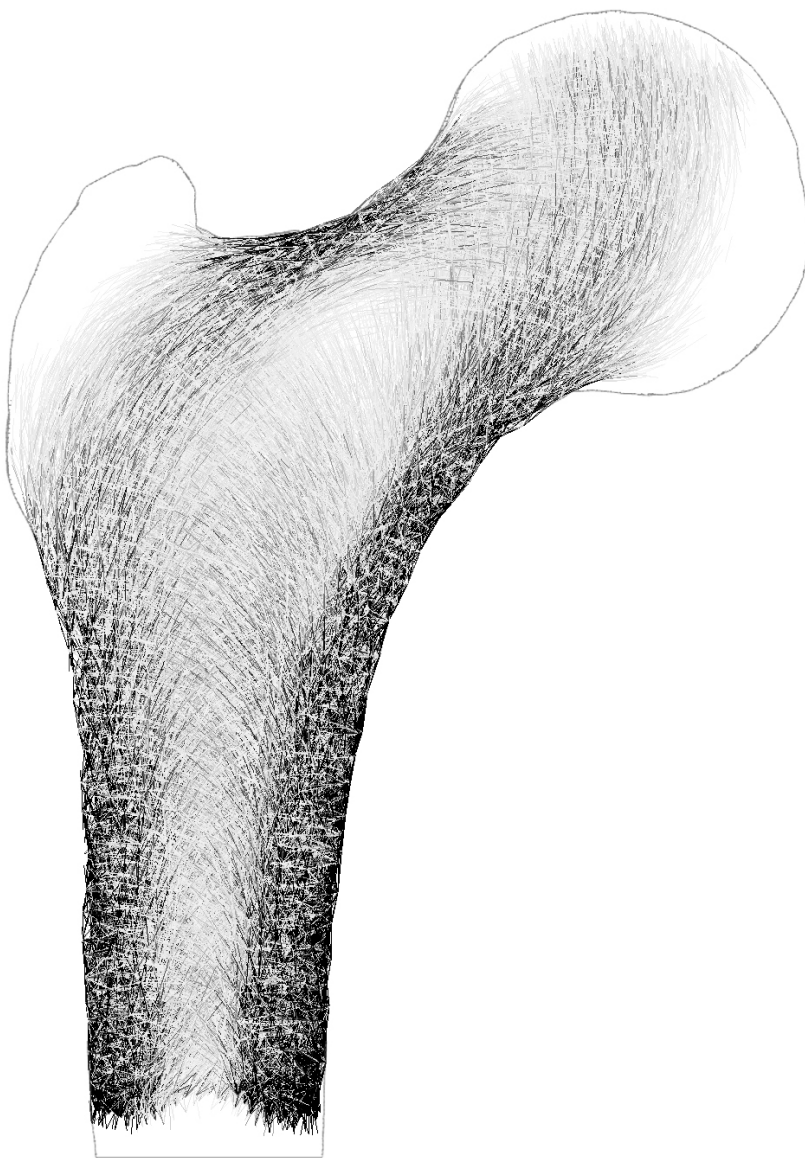


Figure 2.40: Section through a 3D femur from paper C. The arm stiffness is scaled based on the strain over average strain using a third order polynomial function. Black arms have a stiffness scaling of 25 while the white arms have a stiffness scaling of 0.01. The emergent pattern has many similarities with cross sections of real bones and the thin outline indicate the section cut through the initial domain.

3 Methodology

This chapter presents a brief overview of the methods used in this research project, followed by a methodological description of the work behind the contextualisation and each of the five publications. The theory development and results reside in the papers. For example, the derivation of the Force flux peridynamics theory is found in paper D, and the background is presented in section 2.3.

3.1 Methods

Research through design

The relationship between research and design has become a debated topic. A range of different terms have been used to formalise design as a research method or as a research approach, including *research by research*, *practice based research*, *artistic research* etc. However, design research is still evolving and seems to resist reduction to a specific methodology. Rather the many different approaches may present a collection of strategies for knowledge production through design work. Research in this vain of thinking may involve the production of prototypes and artefacts, and knowledge could be of a process character or embodied in the artefact itself.

Lawson compares traditional and design-driven research and notes that the former is mainly descriptive, whereas the latter tends to be largely prescriptive [102]. In other words, the design research endeavour is less focused on how the world is and more on how it could be.

Among other attempts to define the research production by architects and designers, Frayling distinguishes between three approaches. Research into/about, for and through art and design [59]. Research through design according to Frayling can be exemplified by *materials research*, *development work* and *action research*. *Materials research* includes the processing of materials to explore form, texture and finish. *Development work* includes, for example, the reconfiguration of a piece of technology to do something no one had thought of before. *Action research* deals with the procedural documentation of experimental methodology and achieved results.

Numerical experiments

Experimental research is sometimes referred to as the standard to which all other research strategies should be judged and becomes a bridge between theory or hypothesis and reality [69]. This thesis project is focused on digital tools; therefore, the use of experiments is limited to the application of numerical experiments. A further distinction is made between two different types of numerical experiments. These are defined as *narrow* and *speculative*.

The *narrow* numerical experiment is typically applied in theory development, aiming to reduce the complexity of a problem such that the correlation between parameters can be established. These experiments are often used in science and engineering and aim to prove or disprove theories and hypotheses that make claims of the type - *how things*

are. The *speculative* numerical experiments, on the other hand, are applied in the case of design exploration. These types of experiments are aimed to spark imagination and contribute with examples that broaden the horizon of possibilities of the topic at hand. This approach can be understood as related to the concept of research by design which aims to address questions of the type - *how things could be*.

3.2 Research methodology

Thesis contextualisation

The contextualisation in chapter 2 is organised based on the following reasoning. The introduction to the context, which concerns the design process and related tools, is motivated as a background for the work but is not specifically a research subject. The choice of references reflects the author's experience-based perspective on the design process and the use of digital tools in that context.

The first part of the contextualisation concerns a note on the use of geometry in a digital design context. The two techniques which have dominating the development of 3D form representation – mesh in a discrete setting and NURBS as a continuous representation – are introduced, followed by an account of point cloud representation. Some practical strategies for modelling with point clouds are discussed, including volume mesh point inclusion, particle-zone numbering and particle shaking. These strategies are found in discussion threads in the stack-overflow technology development forum. In the section that follows, the three standard materials for building structures, steel, concrete and wood, are introduced. The choice is based on their important place in the modern building industry. Where reinforced concrete is the most commonly used material, steel is very capable, reliable and possible to recycle, and wood is a renewable material gaining popularity for structures on a larger scale. The literature review for this section is focused on publications related to history of construction and mechanical engineering properties for materials.

The following section concerns numerical methods and describes specifically the family of meshless methods, including the two dominant techniques SPH and peridynamics. The literature review for this section is based on articles and books as per the references. These references are found to a large degree in the Scopus database. The same applies to the last part of the contextualisation, where a range of digital shape-finding strategies is introduced.

Paper A

The first paper in the thesis concerns the documentation of how the roof geometry of the Mexico City airport was created, including the re-adaption of a new mesh smoothing technique into a design context. It is a highly complex project from a structural and geometrical perspective with multiple interdependent and conflicting constraints. The project development was furthermore driven by a great collaboration effort within the office at Foster + Partners, with the Mexican collaborator FREE architects and a range of consultants. Such a process is far too complex to describe fairly in a paper, so the

paper's aim was to record and document some of the reasoning and results of the roof design in an *action research* type of spirit. The purpose of the documentation is to share the knowledge gained in the process.

Paper B

The second paper [5] concerns the digital shaping of structural components using form finding and topology optimisation. In each case, the goal was to generate structurally sound and material-efficient components. However, the evaluation was not strictly focused on just material savings but on the design possibilities that each approach provides.

The method that has been applied is based on research through design, and a *speculative* numerical experiments are used to test each approach. The first step in the paper is to define a structural context for the node, and a tetrahedral space frame was chosen as a continuation of the work presented in paper A. Finite element analysis was carried out for a scaled version of the space frame self-weight, and the node on the inner layer at the top of the structure was chosen as the object for further study. The choice was motivated by the fact that symmetrical loading may simplify the validation of the topology optimisation, which can be expected to produce symmetric results. The nodal form finding was carried out using Rhinoceros and Kangaroo with simple spring elements and bending spline elements as defined in [3]. Once the implementation was done for one node, it could be extended to all the other nodes with relative ease. The topology optimisation approach was explored using the Altair Optistruct engine inside Solid thinking inspire. The nodes in each of the two cases were given form through simulations, but a comparative quantitative evaluation of material efficiency was not performed.

Paper C

The work behind paper C was carried out based on the curiosity to explore the potential of Meshless methods to produce porous structures with inspiration from Bone Re-modelling, and the seminal work of Wolff from 1892 [197]. The purpose was to develop a generative process that could be used for the initial phases of a design situation to evaluate relative quantities for comparative studies. Thus the goal is not to simulate the real strength of bone trabeculae. Since the paper was produced after paper E, the C++ programming implementation of FFPD and the visualisation engine could be used as a starting point.

The development of the numerical strategy was first carried out on simple geometrical shapes in 2D such that convergence and good results were obtained. These shapes could be hard-coded using domain limits in the x and y directions. Results were compared with other optimisation strategies based on qualitative judgement on bench-making problems such as a cantilever.

In order to enable the analysis of free-form geometry, export and import functions were developed to get geometry from Rhinoceros to this stand-alone C++ environment. A polyline import for 2D and a volume mesh import for 3D were developed. Point inclusion algorithms needed to be implemented both for the 2D and the 3D case to enable the imported geometry as 'containers' for point clouds in the setting up of the meshless model.

Since the point-in-polygon problem is rather well explored in the computer graphics context, various approaches are available. In the 2D case, a line intersection strategy

based on the even-odd rule algorithm has been used to calculate point inclusion. In the 3D case the inclusion is determined by calculating the Barycentric coordinates for a given point in a given set of the volume mesh element, see section 2.1.2. A zoning strategy was also implemented to enable the use of large models with many 3D mesh elements for the point inclusion problem.

The work with this paper follows a rather speculative approach, and the method builds on the production of digital artefacts. The numerical experiments that are used are both *narrow* followed by qualitative evaluation and *speculative* in character.

Paper D

The work behind paper D started with an implementation of the bond-based and ordinary state-based Peridynamics written in C# as a general-purpose analysis plugin to Rhinoceros with the ambition to explore the possibilities with this method for analysis of nodal connections. Limitations found in the present formulation regarding the ability to varying particle sizes lead to the formulation of a hypothesis; that the SPH theory may provide means by which the Peridynamic formulation could be simplified for the case of variable density particle distributions and irregular particle arrangement. The background to the SPH formulation and the bond-based peridynamics can be found in 2.3. The hypothesis was developed and formulated in the mathematical language using the introduction of the force flux concept, see [138]. The new mathematical theory was implemented in computer code as a re-wised version of the C# plugin to Rhinoceros.

A numerical experiment of the *narrow* sort was then formulated based on the analytical function of an elliptical coordinate system. By discretising the analytical expression of the coordinate system, an elliptical disk with a predefined crack was generated based on the chosen crack width parameter c and the domain bounds in ξ and η coordinates. The parameters were chosen such that the predefined crack should be small compared to the overall size of the disk.

$$x = c \cosh(\xi) \cos(\eta), \quad (3.1)$$

$$y = c \sinh(\xi) \sin(\eta). \quad (3.2)$$

The elliptical disk was populated with a random distribution of particles that are connected with arms to their neighbouring particles within their horizon size. The particles and arms were given steel material properties as specified in [138] table 1. The numerical model was set up for plain strain analysis meaning no strain perpendicular to the disk. Multiple simulations were run for a fixed particle arrangement, fixed yield stress σ_y , and a fixed crack width c but with different values of the plastic elongation limit δ , which controls the brittleness of the material. By recording the failure stress σ_f a linear relationship between σ_f/σ_y and $\sqrt{\delta/c}$ could be shown, which indicates agreement with Griffith's prediction since for fracture as described in [138].

Paper E

The ideas behind paper E build on the intuition that a numerical concept which enables spontaneously forming cracks may be suitable for the simulation of concrete, where the mechanical properties are largely determined by crack formation when the material is pushed beyond the elastic range. Instead of trying to recreate the actual constituents of the concrete, the aim was to create a macro model that mimics the concrete behaviour without the need to model the microscopic scale. A macro model was regarded as more suitable for a design situation, which motivated the choice of approach. A *narrow* type of numerical experiment was deemed appropriate, and the chosen strategy was to recreate the standardised physical testing procedures for concrete following the American Society of Testing and Material science (ASTM) routines. The previous 2D implementation of FFPD as a Rhinoceros plugin developed for paper D had somewhat limited capabilities for geometry visualisation and was deemed insufficient for the task of 3D simulations. So the numerical implementation was therefore rewritten as a 3D implementation in C++ with a custom-made visualisation environment based on OpenGL, enabling real-time visualisation of simulation progress with millions of arms.

The numerical model of the compression cylinder was set up by filling the containing geometry with a regular grid of particles. In order to deal with large amounts of geometric data, the zoning strategy presented in 2.1.2 was used. The particles were then shaken to introduce noise using a Monte Carlo simulation before each particle was connected to its neighbours within the distance of the horizon.

A parameter sensitivity study was performed on the compression cylinder to better understand the consequence that the plastic elongation limit δ , the yield strain ϵ_y , the random seed and the horizon size have on the model performance. A set of parameters were then chosen with the ambition to recreate a high-strength concrete with 60 MPa in compression strength.

Two additional numerical testing procedures, the split cylinder and the modulus of rupture test were introduced to estimate the tension strength the model could produce. Since the results indicated a tension strength far higher than expected, a 'direct tension' test was added as a third test.

In each test case, the load was added in small increments. Numerical testing was performed to ensure that the loading rate did not impact the failure stress. The failure stress for each test case was calculated in the same way that the failure stress is calculated in the physical testing.

4 Summary of papers

4.1 Paper A

The computational challenges of a mega space frame

The first paper discusses modelling the envelope and space frame for the new Mexico City Airport, including the development of methods, tools and processes to deal with the complexity and scale of the project. The structural logic was conditioned by the construction principles enabled by a steel space frame. The shape was defined using form finding, leading to an all-encompassing lightweight shell with internal spans reaching 170 m. The paper presents how a wide range of computational techniques was merged into the design process driven by visions of lightness, smoothness and grid-line continuity while simultaneously complying with stringent spatial and programmatic constraints and structural performance criteria. The paper includes a first-time (to the author's knowledge) application of Optimal Delaney triangulation smoothing in a design context. The paper thus exemplifies how computational techniques can be integrated into a design context characterised by iterations of analysis and synthesis.

The project was an effort by a large team of architects, engineers and specialist airport planners. The author's involvement was first and foremost regarding the geometry definition, form finding and smoothing of the roof, which is also reflected in the written contribution to the paper.

4.2 Paper B

Form Finding Nodal Connections in Grid Structures

The second paper applies minimal surface form finding to the shaping of a structural nodal connection under conditions of steel 3D printing. The hypothesis is that form findings may present an alternative to topology optimisation where the designer has more control over the outcome since the object's topology remains unchanged. A spline-based bending element was used to control the shape and oppose the form-finding simulation's "will" when needed. The shape of the node was also derived using topology optimisation to enable a comparison.

This paper was the product of introductory discussions on the possibilities of additive manufacturing for steel in an architectural engineering context. The setup of the tetrahedral space frame was inspired by paper A. The author carried out the modelling and analysis using the finite element analysis toolbox CALFEM in Matlab for the global structure. The nodal form finding was carried out using bending spline elements with Kangaroo, and the topology optimisation was done with OptiStruct. The paper is written by the author with support from the co-authors.

4.3 Paper C

Adaptive bone re-modelling for optimization of porous structural components

The third paper presents a speculative approach where adaptive bone re-modelling has been used to generate lightweight structural nodal connections with an internally porous structure. The porous structures were generated using an emergent process described in 2.4.3. The generative method was developed through mathematical derivations that mimic the densification and resorption in bone tissue found in the literature. The aim was to produce a generative process that can be used to explore relative quantities of stiffness and force. The implementation was evaluated through qualitative inspection based on visualisations of force and stiffness distribution.

The idea behind the paper came from William's implementation of a trabeculae simulation from [193]. The author wrote the new implementation as a C++ program to enable such optimisation for generic objects in 2D and 3D. The objects are defined using a polyline boundary in 2D and a volume mesh in 3D. The new implementation represents the resorption and densification distribution by mapping the arm stain over average arm strain to a polynomial function. This approach makes it easy and intuitive to modify the growth and de-growth behaviour by changing the degree of the polynomial function. The paper is written by the author with support from the two co-authors.

4.4 Paper D

The Use of Peridynamic Virtual Fibres to Simulate Yielding and Brittle Fracture

The fourth paper presents a modification of peridynamics presented in section 2.3.1 to enable irregular particle distribution and variable particle sizes to analyse yielding and brittle fracture. The hypothesis was that some aspects of SPH would enable such a reformulation while simplifying the overall theory. The reformulation was made possible by introducing a concept called *force flux density*, and the resulting theory has a strong resemblance with SPH, which was discussed in section 2.3.1. The theory is developed through mathematical derivation and evaluated using numerical experiments. The results from the experiments demonstrate that the fracture stress is inversely proportional to the square root of the crack length, as predicted by Griffith's theory of fracture.

The derivation of the theory in this paper was done in collaboration with Chris J.K. Williams, and the implementation of the computer code and the numerical experiments were carried out by the author. This implementation involved modifying the theory to produce an algorithm that generated stable and consistent results. The background and the section on numerical experiments are written by the author.

4.5 Paper E

The numerical simulation of standard concrete tests and steel reinforcement using force flux peridynamics

The fifth paper presents an implementation of Force flux Peridynamics in 3D for concrete and steel reinforcement analysis. The hypothesis was that the FFPD model might be appropriate in this situation because it can model spontaneous fracture, which is assumed to have a significant impact on the mechanical behaviour of concrete. Numerical models are used to recreate the material testing procedure typically used in a physical lab. A parameter sensitivity study was performed for the parameters that determine the brittleness of the concrete. The resulting stress-strain curves indicate a reasonable ability to recreate different types of concrete mixes. The fracture stress from the simulations was compared with the fracture stress from physical testing found in the literature. It was concluded that the tension strength obtained in the simulation is approximately 3-4 times larger than expected from physical experiments. This discrepancy could be explained by the lack of initial imperfections in the numerical model.

The application of the theory from paper C, including an extension to 3D, is done by the author. The program that was developed for the work with paper E was rewritten by the author in C++ with a visualisation engine based on OpenGL to enable the visualisation of millions of objects at reasonable frame rates. The code was also written to be compiled on Linux to utilise a computational cluster with 60 parallel computers used in the parameter sensitivity study for steel. The paper is written by the author with support from the two co-authors.

5 Conclusions and discussion

This chapter starts with a section where the research questions that were formulated in the introduction are presented again, together with a reflection on the achieved results. The following section contains a broader reflection on the work and some concluding thoughts.

5.1 Research questions and achieved results

...

Question i: *How can form finding as a strategy usually applied to shape the global geometry of structures be applied in the shaping of structural components, and what may be the pros and cons of such an approach compared to topology optimisation?*

The application of form finding to the shaping of a global structure is discussed in paper A, and the re-adaption of such a strategy for the shaping of a nodal connection is addressed in paper B, while simultaneously comparing the process with the shaping enabled through topology optimisation.

The form-finding approach was found to benefit from the way the topology of the object is left unchanged. That enables the designer to control the overall expression, and a wide range of similar but locally adapted nodes could be created, see figure 5.1. Setting up the initial geometry requires an understanding of the form-finding process where the loading should mirror the expected structural action of the component in service. That works well under the assumption of pure axial loads but would be more challenging in loading conditions that involve bending moments. The shell-like node needs to undergo sizing for appropriate load cases and real constraints. The topology optimisation approach was found to be relatively flexible since the initial configuration is very simple (in this case, a partial sphere), and quite convincing results could be achieved. The setting up of the model is however a little more involved since rigid body motions need to be avoided for the numerical solver while simultaneously avoiding the attraction of mass in the optimisation procedure at locked degrees of freedom. The approach enabled shape finding for a more extensive range of load cases and load combinations, including bending moments. However, each load case also results in a unique set up for boundary condition to achieve equilibrium without attraction of unwanted mass in the optimisation and a method to automate that would have to be developed. The results can be used as indicative for further design development or interpreted quite literally as a non-negotiable shape-defining process (assuming appropriate loading and use of safety factors).

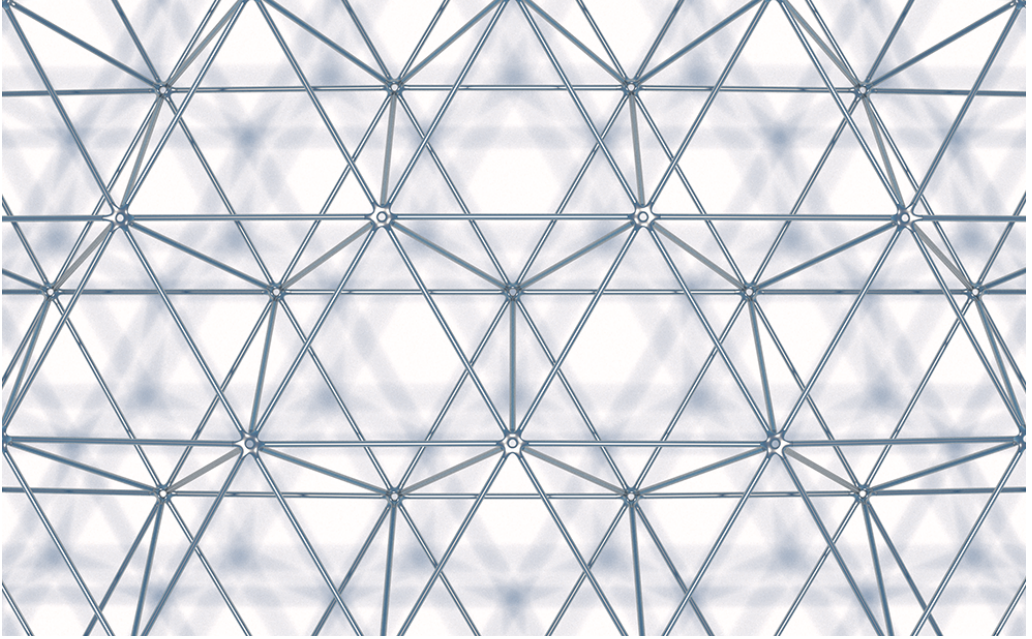


Figure 5.1: *Top view render of the space frame from paper B where the form found nodes are adapted individually to each unique situation while maintaining their common topology.*

...

Question ii: *How can meshless methods be used to generate light weight structural components with an internal porous structure?*

A simple form of a meshless model is presented in paper C based on a domain discretisation in 2D and 3D. By introducing a scaling of the arm stiffness based on the arm strain over the average arm strain and mapping that to a third-order polynomial, resorption and densification behaviour is achieved, which is similar to the theory of bone growth postulated by Wolf. This is similar to the power law relationship between the density ρ and Young's modulus in SIMP topology optimisation. Strained areas of the component become gradually stiffer, and less strained areas are gradually weakened during the simulation.

The numerical implementation of the theory applied to the femur in 2D and 3D produce the expected results where the stiffness distribution, shown in figures 5 and 8 in paper C, follows the moment diagram. The distribution of compression and tension for the arms and strain for the particles shown in figures 4 and 7 respectively reflect the same expected behaviour. The same goes for the distribution of force, strain and stiffness for the 2D frame as shown in figures 10 and 11 in paper C. While the numerical experiments indicate a type of porosity distribution as a result of the stiffness scaling, the translation from a digital to a physical artefact is not dealt with in this paper and points out a direction for future work.

...

Question iii: *The ability to vary particle density is essential to vary precision in the analysis of structural components where yielding and fracture may occur. How can the Peridynamic formulation be modified to enable variable particle density and irregular particle distribution?*

The extension of peridynamics with FFPD through integrating the SPH kernel and reformulating the arm force allows for varying particle size in an overall simpler formulation than the original theory. The variable size ability is an essential feature in a design situation where a varying precision might be necessary to capture a phenomenon such as stress concentrations which are closely linked to the prediction of fracture.

A numerical experiment with an elliptical disk with a predefined crack is used to test the fracture prediction capabilities. By comparing the failure stress over the yield stress with the square root of the elongation limit over the crack width, a linear relationship for a large range of elongation limit settings is shown, which indicates a correlation with Griffith's theory. The expected linear proportionality can be written as

$$\frac{\sigma_{\text{failure}}}{\sigma_{\text{yield tension}}} \propto \sqrt{\frac{\delta}{c}}. \quad (5.1)$$

where $\sigma_{\text{failure}}, \sigma_{\text{yield tension}}$ is the failure and yield stress respectively, δ is the plastic elongation limit and c is the crack width as elaborated in paper D. The results from the numerical experiments can be seen in figure 5.2. These results indicate that the fracture prediction for FFPD corresponds with Griffith's theory. The focus has been concentrated specifically on fracture prediction because it seemed like the most challenging validation.

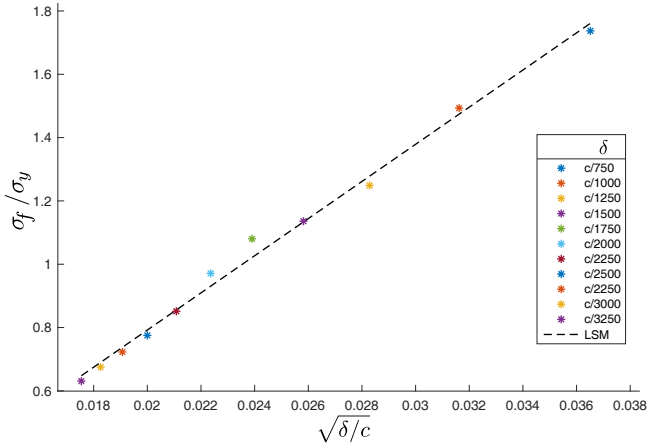


Figure 5.2: *Showing the relationship between LHS and RHS in Eq. (5.1) that was achieved in the numerical experiments. The dashed line is a least mean square approximation of the data and a linear relation is expected for correlation with Griffith's theory.*

Question iv: *Force flux peridynamics enables modelling of brittle materials. What is an appropriate strategy to tune such a meshless method for analysis of materials in general and concrete specifically?*

The tuning of the FFPD model for concrete and steel is carried out by recreating the numerical setup from physical testing such that the numerical model can be compared with the results from physical testing. Such a strategy could also be used for other materials with their specific testing procedures. For concrete and steel, this was done by recreating the physical testing procedure by the ASTM as described in paper D. The scope of paper D was limited to the study of four parameters which are varied in a sensitivity study. That includes the horizon size, the plastic elongation limit, the yield strain and the random seed for particle shaking. In the parameter sensitivity study, it was concluded that the plastic elongation limit parameter has the most impact on the material's brittleness for both concrete and steel and that the yield strain parameter has the dominant influence on the strength of each of the two materials. The FFPD concrete model is evaluated based on its ability to predict compression and tension strength. The results indicate that the FFPD model overestimates the tension strength of concrete by a factor of 3-4. These findings seem reasonable due to the inherent difficulty for a macro model to capture micro-cracks and initial small-scale imperfections, which are likely to weaken the material in the actual case.

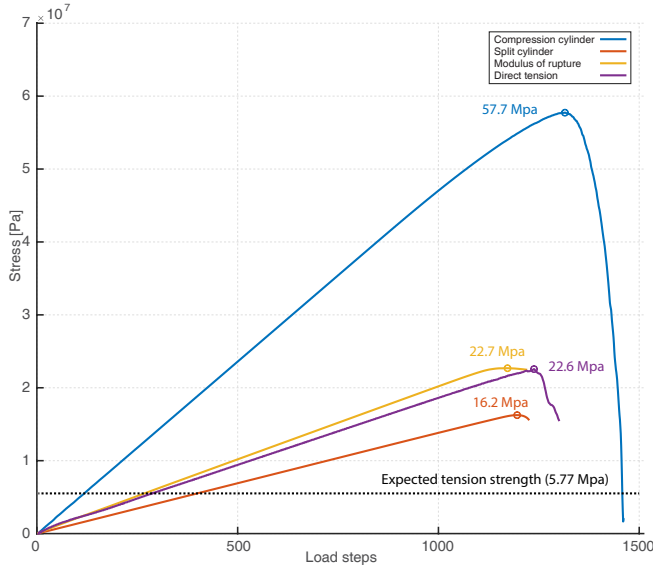


Figure 5.3: *Compression and tension strength from the simulation of concrete with FFPD from paper E. The expected tension strength is approximately 10% of the compression strength.*

The numerical experiments with the steel tension test indicate the possibility of simulating a range of different steel qualities. However, the randomised particle discretisation was shown to have an undesired impact on yielding compared to the regular particle distribution. The irregular particle distribution introduces a random distribution of the mechanical properties that are better for concrete than steel, which is a more homogeneous material.

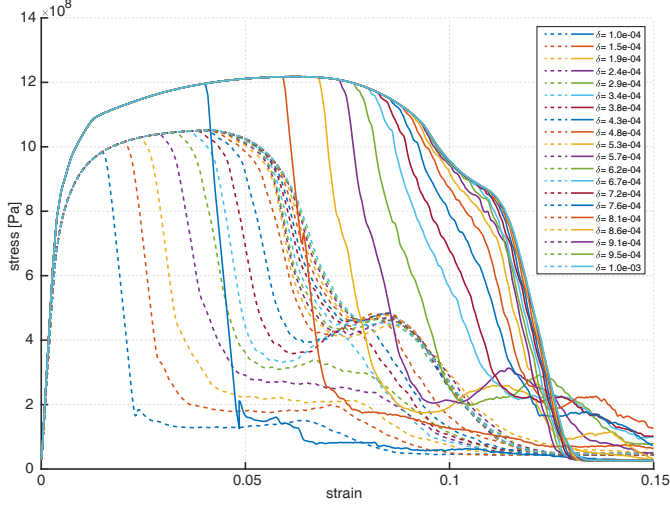


Figure 5.4: Stress strain curves for a direct tension test of a digital steel specimen from paper E simulated with FFPD where the plastic elongation limit δ is varied. The continuous and dashed lines represent regular and irregular particle distributions respectively.

...

5.2 Conclusions

The thesis develops and explores the use of meshless methods for application in a design context. These methods are associated with the design of nodal connections by addressing four themes; digital form representation, conditions from materials and production, shape finding, and numerical analysis. Thus, the thesis touches upon a broad range of topics which are assumed to be relevant for the digital shaping of structural connections. While materials are discussed from a production point of view in section 2.2, the main focus has been concentrated on methods for the simulation of mechanical properties. Partly because of the vast amount of shaping constraints that different production techniques impose on the design process and partly because of the challenge to map such constraints to a digital context in a comprehensive way. For example, the design space enabled with 3D printed steel relies on the use of support material which holds the printed piece in place. However, the support also provides heat diffusion during the printing process making support placement challenging to estimate. The printed object is furthermore conditioned by the method for support removal, should that be through robotic milling or by other means.

The findings in the papers are not packaged comprehensively into a tool such that the implications on a design situation can be studied. However, some groundwork for creating such tools based on the meshless methods has been addressed. That includes a derivation of a new meshless method called Force flux peridynamics for analysis of brittle fracture, with an ability to deal with small material scales for prediction of failure. The work also suggests how to tune such a method for a specific material through the recreation of physical tests using numerical analysis. Other suggestions include how to work with containing geometry such as polylines and volume meshes to create 2D and 3D models ready for meshless analysis. The work furthermore explores a way to generate lightweight porous components based on a meshless model. However, the translation from a digital porous component to a physical object calls for future work.

The point cloud representation was found to be relatively easy to implement and provides an opportunity to introduce material properties into digital design rather comprehensively. The domain of an object is defined using a bounding geometry, and the point-in-polygon evaluation is the only tie between the particle distribution and the bounding geometry. A designer using meshless analysis could be levitated from the task of mesh discretisation and could work relatively unconstrained in the process of digital shaping. However, the choice of particle arrangement in the analysis should reflect the material characteristics. Paper E indicated that the irregular distribution significantly impacted the possibility of modelling the yielding of steel as the tension test is pushed to the limits.

Force flux peridynamics offers a simple way to set up complex analyses such as brittle fracture. It could therefore be an appropriate method for analysis of complex materials such as concrete and timber. The method could also be used to assess existing structures, such as the study of cracks in concrete bridges. However, future work would have to address the overestimate of tensile strength in the concrete. A wide range of work is still needed to map the implications of various setup configurations for modelling different materials. From a design tool perspective, there seem to be interesting possibilities with

meshless methods to shift between different levels of accuracy, which could fit the different stages of design development. From simple models in the study of relative quantities as exemplified in paper C to detailed analysis including fracture in paper D and E. The shift from a coarse to a detailed analysis only requires a different distribution of particles and a different function for calculating the arm force and is, therefore, relatively straightforward. The explicit node-wise iterative method provides geometrical and material non-linearity without extra computational cost. However, that also means that this method might not be the right choice for linear elastic analysis, where it will be very slow compared to the finite element method.

6 Future work

In order to gain confidence in the analysis results with Force flux peridynamics, additional studies for arrangement and density of particles for different materials need to be performed. In order to study prescribed imperfections, particle distribution strategies need to be developed to enable gradual densification of particles towards areas of weakness or stress concentration. The discretisation could also be linked to the characteristic length scale of the material in question.

Future work may also include addressing the problems with an overestimated tension strength for concrete modelling. The FFPD model could also be tuned for timber analysis by recreating the physical tests of timber, similarly to the tuning of concrete in paper E. In that case, there could be interesting opportunities to link the setup of the model with scanning of real timber elements to be able to capture the real imperfections in the material.

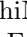
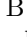
Other interesting possibilities involve developing a 2D version of the theory to model surface structures more efficiently by integrating bending using rotational degrees of freedom. That would reduce computational time for thin-walled structures.




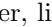
The possibility for particles to move and reconnect with new neighbours with the meshless methods could present opportunities for new forms of shape finding. One could imagine a situation where the particles are attracted to areas of high stress as a strategy to guide material placement.

In the same vain of thinking, one could also use meshless methods to simulate materials that shift between a solid and a fluid state. The state shifting could be explored from a design point of view where modification of a shape takes place in the fluid state while the solid state enables material mechanical simulations. One could also use the fluid state to, for example, simulate the 3D printing process, including the melting and hardening of metal powder in the production of an object. That would shift the focus towards solving heat equations and could include modelling inner stress resulting from temperature changes in the material.

The analysis would also be suitable for parallelisation, for example, with GPU acceleration which would speed up convergence for all sorts of implementations.

FIGURE CREDITS

1.1	Render by courtesy of Foster and Partners, © Foster + Partners.	2
1.2	Render by courtesy of Foster and Partners, © Foster + Partners.	3
1.3	Photo by courtesy of Fondazione Renzo Piano. Author Richard Ringoletti, copyright owner Fondazione Renzo Piano, Rogers Stirk Harbour + Partners. Project: Centre Georges Pompidou, Paris, France, built 1971 - 1977. Client: Ministry of Cultural Affairs, Ministry of National Education. Architects: Studio Piano & Rogers, architects.	12
1.4	Photo by courtesy of Fondazione Renzo Piano. Author Bernard Vincent, copyright owner Fondazione Renzo Piano, Rogers Stirk Harbour + Partners. Project: Centre Georges Pompidou, Paris, France, built 1971 - 1977. Client: Ministry of Cultural Affairs, Ministry of National Education. Architects: Studio Piano & Rogers, architects.	12
1.5	Photo by courtesy of Fondazione Renzo Piano. Author Bernard Vincent, copyright owner Fondazione Renzo Piano, Rogers Stirk Harbour + Partners. Project: Centre Georges Pompidou, Paris, France, built 1971 - 1977. Client: Ministry of Cultural Affairs, Ministry of National Education. Architects: Studio Piano & Rogers, architects.	13
1.6	Photo by courtesy of Fondazione Renzo Piano. Author Bernard Vincent, copyright owner Fondazione Renzo Piano, Rogers Stirk Harbour + Partners. Project: Centre Georges Pompidou, Paris, France, built 1971 - 1977. Client: Ministry of Cultural Affairs, Ministry of National Education. Architects: Studio Piano & Rogers, architects.	13
1.7	Photo of drawing licensed under the Public domain PD-art, https://www.loc.gov/resource/hhh.ny2019.sheet/?sp=13 . The image has been cropped.	14
1.8	Photos taken by Balthazar Korab, licensed under the Public domain PD-art, https://www.loc.gov/resource/krb.00623 . The image has been cropped.	14
1.9	Photos taken by Balthazar Korab, licensed under the Public domain PD-art, https://www.loc.gov/resource/krb.00574/	15
1.11	Photo by Forgemind ArchiMedia, licensed under (CC BY 2.0) ©  https://flic.kr/p/mpewDW . Edited by making the image black and white. . .	16
2.11	Diagram drawn by the author inspired by from the graphs by the dep. of Engineering at university of Cambridge http://www-materials.eng.cam.ac.uk/mpsite/	32
2.12	Figure created by the author but inspired by [85].	34
2.14	Diagram drawn by the author inspired by from the graphs by the dep. of Engineering at university of Cambridge http://www-materials.eng.cam.ac.uk/mpsite/	36
2.15	Diagram drawn by the author inspired by Rswarbrick's diagram found at https://commons.wikimedia.org/wiki/File:Yield_surfaces.svg . .	37
2.16	Licensed under ©  CC BY-SA 4.0, photo by Uncle Silver,	39
2.18	Photo taken by Lewis Hine, licensed under the Publid domain PD-art, https://en.wikipedia.org/wiki/File:Old_timer_structural_worker2.jpg .	40

2.19	Photo taken by Piergiorgio Rossi, licensed under the Publid domain, https://commons.wikimedia.org/wiki/File:Dettaglio_del_British_Museum_(Londra_2005).jpg	40
2.21	Diagram drawn by the author inspired by from the graphs by the dep. of Engineering at university of Cambridge http://www-materials.eng.cam.ac.uk/mpsite/	43
2.23	Reinforcement drawing for Pont du Naou-Hount by Alexandre Sarrasin, In Bulletin technique de la Suisse romande 59 (1933), Nr. 26, Planche Nr. 5. Licensed under the Public domain , https://www.e-periodica.ch/digbib/view?pid=bts-002:1933:59::286#1376	46
2.24	Photos taken by Balthazar Korab, licensed under the Public domain PD-art, https://www.loc.gov/resource/krb.00623	47
2.25	Photo by courtesy of Aectual 	47
2.26	Diagram drawn by the author inspired by from the graphs by the dep. of Engineering at university of Cambridge http://www-materials.eng.cam.ac.uk/mpsite/	48
2.28	Photo licensed under the public domain, from Charles Daniels Photo Collection album called <i>British Aircraft</i> . SOURCE INSTITUTION: San Diego Air and Space Museum Archive. http://www.sandiegoairandspace.org/library/stillimages.html	51
2.29	Copyright Centre Pompidou, Bibliothèque Kandinsky.	51
2.30	Photo by Trevor Ryan Patt, licensed under (CC BY-NC-SA 2.0)  https://flic.kr/p/zhFQbR . Edited through cropping, brightness and colour adjustments.	52
2.31	Photo by courtesy of Milo Keller. http://milokeller.com	53
2.32	Photo by courtesy of Milo Keller. http://milokeller.com	53
2.34	Photo from the Final report from the board of investigation [46].	56
2.36	Illustration create by the author, inspired by [90].	61
2.38	Photo by courtesy of Emil Adiels 	67
2.39	Photo by C. R. K. Lander, licensed under the  3.0, https://commons.wikimedia.org/wiki/File:British_Musem_Great_Court_CRKL.JPG . . .	68

References

- [1] B. Addis. *Building: 3000 years of design engineering and construction*. London, New York: Phaidon, 2007.
- [2] E. Adiels et al. “The use of virtual work for the formfinding of fabric, shell and gridshell structures”. *Proceedings of the Advances in Architectural Geometry conference*. 2018.
- [3] S. M. L. Adriaenssens. “Stressed spline structures”. PhD thesis. University of Bath, 2000.
- [4] H.-K. Ahn et al. Separating an object from its cast. *Computer aided design* 34 (2002), 547–559.
- [5] F. Aish et al. “Form Finding Nodal Connections in Grid Structures”. *Conference proceedings: IASS Boston 2018*. 2018.
- [6] F. Aish et al. The use of a particle method for the modelling of isotropic membrane stress for the form finding of shell structures. *Computer-Aided Design* 61 (Apr. 2015), 24–31. DOI: 10.1016/j.cad.2014.01.014. URL: <https://doi.org/10.1016/j.cad.2014.01.014>.
- [7] R. Aish. “DesignScript: Scalable Tools for Design Computation”. *Computation and Performance – Proceedings of the 31st eCAADe Conference*. Ed. by S. Rudi and S. Sevil. Vol. 2. eCAADe Conference. 2013, pp. 87–95.
- [8] R. Aish and S. Hanna. Comparative evaluation of parametric design systems for teaching design computation. *Design Studies* 52 (2017). Parametric Design Thinking, 144–172. ISSN: 0142-694X. DOI: <https://doi.org/10.1016/j.destud.2017.05.002>. URL: <https://www.sciencedirect.com/science/article/pii/S0142694X17300327>.
- [9] S. Akboy-Ilk. The nature of drawing in the changing cultur of architectural documentation. *Journal of Architectural and Planing Research* 33.1 (2016), 29–44.
- [10] W. Z. Albert E. Green. *Theoretical Elasticity (Dover Civil and Mechanical Engineering)*. Dover Publications, 2012.
- [11] V. Alic and K. Persson. “NURBS based form finding of efficient shapes for shells”. *Proceedings of 29th Nordic Seminar on Computational Mechanics – NSCM29*. 2016.
- [12] M. Ander et al. “A building of unlimited height”. *Conference proceedings - IASS Annual Symposium*. 2019.
- [13] K. F. Arisya and R. Suryantini. Modularity in Design for Disassembly (DfD): Exploring the Strategy for a Better Sustainable Architecture. *IOP Conference Series: Earth and Environmental Science* 738.1 (Apr. 2021), 012024. DOI: 10.1088/1755-1315/738/1/012024. URL: <https://doi.org/10.1088/1755-1315/738/1/012024>.
- [14] A. Z. Aydemir and S. Jacoby. Architectural design research: Drivers of practice. *The Design Journal* 25.4 (2022), 657–674. DOI: 10.1080/14606925.2022.2081303. eprint: <https://doi.org/10.1080/14606925.2022.2081303>. URL: <https://doi.org/10.1080/14606925.2022.2081303>.
- [15] P. Ball. *A short history of steel*. 2016. URL: <http://www.theheritageportal.co.za/%20article/short-history-steel> (visited on 05/12/2020).

- [16] M. Y. H. Bangash. *Concrete and concrete structures: numerical modelling and applications*. Elsevier applied Science, 1999.
- [17] K. Barry. An Engineer Imagined. *The Irish Review (Cork)* 51 (2015), 87–94.
- [18] R. Baumann. *Die bisherigen Ergebnisse der Holzprüfungen in der Materialprüfungsanstalt an der Technischen Hochschule Stuttgart*. Springer, 1922.
- [19] A. Beim. *Tectonic Visions*. Kunstakademiets Arkitektskoles Forlag, 2004.
- [20] M. P. Bendsoe. *Optimization of Structural Topology, Shape, and Material*. Springer Berlin Heidelberg, 1995. DOI: 10.1007/978-3-662-03115-5.
- [21] M. P. Bendsoe and N. Kikuchi. Generating optimal topologies in structural design using a homogenization method. *Computer Methods in Applied Mechanics and Engineering* 71 (1988), 197–224.
- [22] B. Bergdoll. *European Architecture 1750-1890*. Oxford University Press, 2000.
- [23] S. Berthier. Timber in the buildings of Jean Prouvé: an industrial material. *Construction History* 30.2 (2015), 87–106. ISSN: 02677768. (Visited on 04/10/2022).
- [24] P. Block. “Thrust Network Analysis: Exploring Three-dimensional Equilibrium”. PhD dissertation. PhD thesis. Cambridge, MA, USA: Massachusetts Institute of Technology, May 2009.
- [25] A. Borrelli and J. Wellmann. Computer Simulations Then and Now: an Introduction and Historical Reassessment. *NTM Zeitschrift für Geschichte der Wissenschaften, Technik und Medizin* 27.4 (Nov. 2019), 407–417. DOI: 10.1007/s00048-019-00227-6. URL: <https://doi.org/10.1007/s00048-019-00227-6>.
- [26] J. M. BROWN. W. B. Wilkinson (1819-1902) and his place in the History of Reinforced Concrete. *Transactions of the Newcomen Society* 39.1 (Jan. 1966), 129–142. DOI: 10.1179/tns.1966.009.
- [27] R. Brown and T. Porter. The Methodology of Mathematics. *The Mathematical Gazette* 79.485 (1995), 321–334. ISSN: 00255572. URL: <http://www.jstor.org/stable/3618304> (visited on 06/28/2022).
- [28] E. Bueno. Algorithmic Form Generation of a Radiolarian Pavilion. *International Journal of Architectural Computing* 7.4 (Dec. 2009), 677–688. DOI: 10.1260/1478-0771.7.4.677. URL: <https://doi.org/10.1260/1478-0771.7.4.677>.
- [29] C. Bundgaard. “Tectonics of montage. Architectural positions for a tectonic sustainable building practice”. *Structures and Architecture*. Taylor & Francis group, 2013.
- [30] H. Buri and Y. Weinand. *Building with Timber – Paths into the Future*. Pretzel, 2011. Chap. The Tectonics of Timber Architecture in the Digital Age, pp. 56–63.
- [31] L. Butler. Patronage and the Building Arts in Tokugawa Japan. *Early Modern Japan: An Interdisciplinary Journal* 12.2 (2004), 39–52.
- [32] C. Caldenby and E. Nygaard. *Arkitekturteoriernas historia*. Stockholm: Formas, 2011. ISBN: 9789154060412.
- [33] M. Carpo. *The Second Digital Turn: Design Beyond Intelligence*. MIT Press, 2017. URL: <http://www.jstor.org/stable/j.ctt1w0db6f>.
- [34] H. Castel. Emergence in Architecture. *AA Files* (2004), 50–61.
- [35] R. Castelo-Branco, I. Caetano, and A. Leitão. Digital representation methods: The case of algorithmic design. *Frontiers of Architectural Research* (Jan. 2022). DOI:

- 10.1016/j.foar.2021.12.008. URL: <https://doi.org/10.1016/j.foar.2021.12.008>.
- [36] D. Chakrabarty. The Climate of History: Four Theses. *Critical Inquiry* **35.2** (2009), 197–222. ISSN: 00931896, 15397858. URL: <https://www.jstor.org/stable/10.1086/596640>.
 - [37] H. Chen, Y. Hu, and B. W. Spencer. “Peridynamics Using Irregular Domain Discretization With MOOSE-Based Implementation”. *Volume 9: Mechanics of Solids, Structures and Fluids; Structural Health Monitoring and Prognosis*. American Society of Mechanical Engineers, Nov. 2017. DOI: 10.1115/imece2017-71527. URL: <https://doi.org/10.1115/imece2017-71527>.
 - [38] J.-S. Chen, M. Hillman, and S.-W. Chi. Meshfree Methods: Progress Made after 20 Years. *Journal of Engineering Mechanics* **143.4** (Apr. 2017), 04017001. DOI: 10.1061/(asce)em.1943-7889.0001176.
 - [39] R. W. Clough and J. Penzien. *Dynamics Of Structures*. third. Computers & Structures, Inc., 1995.
 - [40] E. Cornell. *Byggnadstekniken : Metoder och Idéer Genom Tiderna*. Byggeförlag, 1970.
 - [41] K. Crane. *Discrete differential geometry: An applied introduction*. Tech. rep. Carnegie Mellon University, 2019.
 - [42] *Creative Commons License, Attribution Share Alike*. Version 2.0. Creative Commons. URL: <https://creativecommons.org/>.
 - [43] D.Veenendaal and P.Block. An overview and comparison of structural form finding methods for general networks. *International Journal of Solids and Structures* **49** (26 2012).
 - [44] R. Das and P. W. Cleary. Evaluation of Accuracy and Stability of the Classical SPH Method Under Uniaxial Compression. *Journal of Scientific Computing* **64.3** (Dec. 2014), 858–897. DOI: 10.1007/s10915-014-9948-4. URL: <https://doi.org/10.1007/s10915-014-9948-4>.
 - [45] M. Dawod and S. Hanna. BIM-assisted object recognition for the on-site autonomous robotic assembly of discrete structures. *Construction Robotics* **3** (2019), 69–81.
 - [46] U. S. B. of investigation to inquire into the design and methods of construction of welded steel merchant vessels. *Final Report of a Board of Investigation: Convened by Order of the Secretary of the Navy, to Inquire Into the Design and Methods of Construction of Welded Steel Merchant Vessels*. Tech. rep. 1946.
 - [47] dictionary.com. URL: <https://www.dictionary.com/browse/simulation> (visited on 06/28/2022).
 - [48] P. Diehl, S. Prudhomme, and M. Lévesque. A Review of Benchmark Experiments for the Validation of Peridynamics Models. *Journal of Peridynamics and Nonlocal Modeling* **1.1** (Feb. 2019), 14–35. DOI: 10.1007/s42102-018-0004-x. URL: <https://doi.org/10.1007/s42102-018-0004-x>.
 - [49] D. Dipasquale et al. Dependence of crack paths on the orientation of regular 2D peridynamic grids. *Engineering Fracture Mechanics* **160** (July 2016), 248–263. DOI: 10.1016/j.engfractmech.2016.03.022. URL: <https://doi.org/10.1016/j.engfractmech.2016.03.022>.

- [50] D. C. DRUCKER and W. PRAGER. SOIL MECHANICS AND PLASTIC ANALYSIS OR LIMIT DESIGN. *Quarterly of Applied Mathematics* **10.2** (1952), 157–165. ISSN: 0033569X, 15524485. (Visited on 09/21/2022).
- [51] C. Dyka and R. Ingel. An approach for tension instability in smoothed particle hydrodynamics (SPH). *Computers & Structures* **57.4** (Nov. 1995), 573–580. DOI: 10.1016/0045-7949(95)00059-p. URL: [https://doi.org/10.1016/0045-7949\(95\)00059-p](https://doi.org/10.1016/0045-7949(95)00059-p).
- [52] G. Edefors and D. Jonsson. “Interactive Design Using Peridynamics”. MSc thesis. Chalmers university of technology, 2021.
- [53] T. editors. Drawing Futures - leader. *Architectural Research Quarterly* **9.3/4** (2005), 179.
- [54] U. Environment and I. E. Agency. *UN Environment Global Status Report 2017 Towards a zero-emission, efficient, and resilient buildings and construction sector*. 2017.
- [55] F. A. Fathelbab. “The effect of joints on the stability of shallow single layer lattice domes”. PhD thesis. University of Cambridge, 1987.
- [56] J. W. Fisher and L. S. Beedle. *Bibliography on bolted and riveted structural joints*. Tech. rep. 48. ASCE Manual. Lehigh University, 1966.
- [57] M. Frascari. “The Tell-the-Tale Detail”. *Semiotics 1981*. Springer US, 1983, pp. 325–336. DOI: 10.1007/978-1-4615-9328-7_32. URL: https://doi.org/10.1007/978-1-4615-9328-7_32.
- [58] M. Fraser. *Design research in architecture : an overview*. Routledge, 2013.
- [59] C. Frayling. Research in art and design. *Royal Collage of Art Research Papers* (1993).
- [60] J. Frazer. Parametric Computation: History and Future. *Architectural Design* **86.2** (Mar. 2016), 18–23. DOI: 10.1002/ad.2019. URL: <https://doi.org/10.1002/ad.2019>.
- [61] W. E. Frazier. Metal additive manufacturing: A review. English. *Journal of Materials Engineering and Performance* **23.6** (2014). Cited By :2046, 1917–1928.
- [62] G. C. Ganzenmüller, S. Hiermaier, and M. May. On the similarity of meshless discretizations of Peridynamics and Smooth-Particle Hydrodynamics. *Computers & Structures* **150** (Apr. 2015), 71–78. DOI: 10.1016/j.compstruc.2014.12.011. URL: <https://doi.org/10.1016/j.compstruc.2014.12.011>.
- [63] T. C. GERMANN and K. KADAU. TRILLION-ATOM MOLECULAR DYNAMICS BECOMES A REALITY. *International Journal of Modern Physics C* **19.09** (Sept. 2008), 1315–1319. DOI: 10.1142/s0129183108012911.
- [64] C. Geuzaine and J.-F. Remacle. Gmsh: A 3-D finite element mesh generator with built-in pre- and post-processing facilities. *International Journal for Numerical Methods in Engineering* **79.11** (2009), 1309–1331. DOI: 10.1002/nme.2579.
- [65] S. Gibb, R. F. Hendry, and T. Lancaster, eds. *The Routledge Handbook of Emergence*. Routledge Taylor and Francis group, 2019. ISBN: 9780367783884.
- [66] R. A. Gingold and J. J. Monaghan. Smoothed particle hydrodynamics: theory and application to non-spherical stars. *Monthly Notices of the Royal Astronomical Society* **181.3** (Dec. 1977), 375–389. DOI: 10.1093/mnras/181.3.375. URL: <https://doi.org/10.1093/mnras/181.3.375>.

- [67] J. Glucklich. “Proceedings of the international conference on structure of concrete and its behaviour under load”. *Strength and failure of concrete*. Sept. 1965, pp. 176–189.
- [68] J. Gray, J. Monaghan, and R. Swift. SPH elastic dynamics. *Computer Methods in Applied Mechanics and Engineering* **190**.49-50 (Oct. 2001), 6641–6662. DOI: 10.1016/s0045-7825(01)00254-7. URL: [https://doi.org/10.1016/s0045-7825\(01\)00254-7](https://doi.org/10.1016/s0045-7825(01)00254-7).
- [69] L. Groat and D. Wang. *Architectural Research Methods*. Wiley, 2013.
- [70] N. Gromicko and K. Shepard. *The History of Concrete*. URL: <https://www.nachi.org/history-of-concrete.htm> (visited on 05/13/2020).
- [71] M. D. Gross. The Electronic Cocktail Napkin—a computational environment for working with design diagrams. *Design Studies* **17**.1 (1996), 53–69. ISSN: 0142-694X. DOI: [https://doi.org/10.1016/0142-694X\(95\)00006-D](https://doi.org/10.1016/0142-694X(95)00006-D). URL: <http://www.sciencedirect.com/science/article/pii/0142694X9500006D>.
- [72] X. Gu, E. Madenci, and Q. Zhang. Revisit of non-ordinary state-based peridynamics. *Engineering Fracture Mechanics* **190** (2018), 31–52. ISSN: 0013-7944. DOI: <https://doi.org/10.1016/j.engfracmech.2017.11.039>. URL: <https://www.sciencedirect.com/science/article/pii/S0013794417309104>.
- [73] M. Hambach and D. Volkmer. Properties of 3D-printed fiber-reinforced Portland cement paste. *Cement and Concrete Composites* **79** (May 2017), 62–70. DOI: 10.1016/j.cemconcomp.2017.02.001.
- [74] B. Hamzeian. “The evolution of the cast node of the Pompidou Centre: From the ‘friction collar’ to the ‘gerberette’”. *Building Knowledge, Constructing Histories*. CRC Press, Sept. 2018, pp. 715–723. DOI: 10.1201/9780429506208-91. URL: <https://doi.org/10.1201/9780429506208-91>.
- [75] S. Hanna. “Data in Design Practice”. *Design Transactions: Rethinking Information Modelling for a New Material Age*. UCL Press, 2020, pp. 138–141. ISBN: 9781787354890. URL: <http://www.jstor.org/stable/j.ctv13xprf6.28> (visited on 07/15/2022).
- [76] R. Harik, H. Gong, and A. Bernard. 5-Axis flank milling: A state-of-the-art review. *Computer Aided Design* **45**.3 (Jan. 2012).
- [77] L. Harzheim and G. Graf. A review of optimization of cast parts using topology optimization. *Structural and Multidisciplinary optimization* **31**.5 (May 2006), 388–399.
- [78] S. F. Henke and S. Shanbhag. Mesh sensitivity in peridynamic simulations. *Computer Physics Communications* **185**.1 (Jan. 2014), 181–193. DOI: 10.1016/j.cpc.2013.09.010. URL: <https://doi.org/10.1016/j.cpc.2013.09.010>.
- [79] J. Hilmersson. “Isogeometric analysis and form finding”. 2019.
- [80] J. Hilmersson et al. “Isogeometric analysis and form finding for thin elastic shells”. *Conference proceedings: IASS Barcelona 2019*. 2019.
- [81] D. Hockney. *Secret Knowledge: Rediscovering the Lost Techniques of the Old Masters*. Viking Studio, 2006.
- [82] I. Horváth. “On some Crucial Issues of Computer Support of Conceptual Design”. *Product Engineering*. Kluwer Academic Publishers, 2004, pp. 123–142. DOI: 10.1007/1-4020-2933-0_9. URL: https://doi.org/10.1007/1-4020-2933-0_9.

- [83] X. Huang et al. Finite element method of bond-based peridynamics and its ABAQUS implementation. *Engineering Fracture Mechanics* **206** (Feb. 2019), 408–426. DOI: 10.1016/j.engfracmech.2018.11.048. URL: <https://doi.org/10.1016/j.engfracmech.2018.11.048>.
- [84] K. J. Hwang. “Advanced Investigations of Grid Spatial Structures Considering Various Connection Systems”. PhD thesis. University of Stuttgart, 2010.
- [85] J. M. Illstone, ed. *Construction Materials: Their nature and behaviour*. Second Edition. CRC Press, 1993.
- [86] E. B. Inc. *Revolution And The Growth Of Industrial Society, 1789–1914*. 2020. URL: <https://www.britannica.com/topic/history-of-Europe/The-Industrial-Revolution> (visited on 11/10/2020).
- [87] M. Ivanyi and C. C. Baniotopoulos. *Semi-Rigid Joints in Structural Steelwork*. Springer, 2000.
- [88] J. Cottrell, T. Hughes, and Y. Bazilevs. *Isogeometric analysis - Toward integration of CAD and FEA*. Wiley, 2009.
- [89] M. Jarzombek. Architecture Against Architecture: Disengaging the Metaphysical Alliance. *Thresholds* **29** (Jan. 2005), 67–70. DOI: 10.1162/thld_a_00307. URL: https://doi.org/10.1162/thld_a_00307.
- [90] A. Javili et al. Peridynamics review. *Mathematics and Mechanics of Solids* (Oct. 2018), 108128651880341. DOI: 10.1177/1081286518803411. URL: <https://doi.org/10.1177/1081286518803411>.
- [91] J. T. Kajiya. “The rendering equation”. *Proceedings of the 13th annual conference on Computer graphics and interactive techniques - SIGGRAPH 86*. ACM Press, 1986. DOI: 10.1145/15922.15902. URL: <https://doi.org/10.1145/15922.15902>.
- [92] S. Karl. “Particle Animation and Rendering Using Data Parallel Computation”. *Proceedings of the 17th Annual Conference on Computer Graphics and Interactive Techniques*. SIGGRAPH ’90. Dallas, TX, USA: Association for Computing Machinery, 1990, pp. 405–413. ISBN: 0897913442. DOI: 10.1145/97879.97923. URL: <https://doi.org/10.1145/97879.97923>.
- [93] A. Kefal et al. Topology optimization of cracked structures using peridynamics. *Continuum Mechanics and Thermodynamics* **31.6** (Oct. 2019), 1645–1672. DOI: 10.1007/s00161-019-00830-x. URL: <https://doi.org/10.1007/s00161-019-00830-x>.
- [94] *Keynote Lecture Norman Foster and Francis Aish*. Viemo. 2016. URL: <https://vimeo.com/195500916> (visited on 04/27/2020).
- [95] J. Kiendl et al. Isogeometric shell analysis with Kirchhoff-Love elements. *Computer Methods in Applied Mechanics and Engineering* **September** (2009).
- [96] J. M. Kiendl. “Isogeometric analysis and shape optimal design of shells structures”. PhD thesis. The Technical University of Munich, 2011.
- [97] B. Kilic and E. Madenci. An adaptive dynamic relaxation method for quasi-static simulations using the peridynamic theory. *Theoretical and Applied Fracture Mechanics* **53.3** (June 2010), 194–204. DOI: 10.1016/j.tafmec.2010.08.001. URL: <https://doi.org/10.1016/j.tafmec.2010.08.001>.

- [98] J. Krupinska. *Att skapa det tänkta : en bok för arkitekturintresserade*. Studentlitteratur AB, 2016.
- [99] H. Kupfer, H. K. Hilsdorf, and H. Rusch. Behavior of Concrete Under Biaxial Stresses. *ACI Journal Proceedings* **66** (1969).
- [100] Lawson. *How Designers Think*. Routledge, Aug. 2006. DOI: 10.4324/9780080454979. URL: <https://doi.org/10.4324/9780080454979>.
- [101] B. Lawson. Oracles, draughtsmen, and agents: the nature of knowledge and creativity in design and the role of IT. *Automation in Construction* **14.3** (June 2005), 383–391.
- [102] B. Lawson. The subject that won’t go away But perhaps we are ahead of the game. Design as research. *Architectural Research Quarterly* **6.2** (June 2002), 109–114. DOI: 10.1017/s1359135502001574. URL: <https://doi.org/10.1017/s1359135502001574>.
- [103] F. K. Lester and D. R. Kerr. Some Ideas about Research Methodologies in Mathematics Education. *Journal for Research in Mathematics Education* **10.3** (May 1979), 228. DOI: 10.2307/748813. URL: <https://doi.org/10.2307/748813>.
- [104] S. L. Lewis and M. A. Maslin. Defining the Anthropocene. *Nature* **519**.7542 (Mar. 2015), 171–180. DOI: 10.1038/nature14258. URL: <https://doi.org/10.1038/nature14258>.
- [105] H. Li and S. S. Mulay. *Meshless Methods and Their Numerical Properties*. CRC Press, 2013. DOI: <https://doi.org/10.1201/b14492>.
- [106] Q. Li et al. Topology optimization design of cast parts based on virtual temperature method. *Computer Aided Design* **94** (Jan. 2018), 28–40. DOI: <https://doi.org/10.1016/j.cad.2017.08.002>.
- [107] T. M. Lillehoff. “Building Images: Toward a Non-Dualistic Architecture”. *Proceedings: 91st ACSA International conference*. July 2003, pp. 131–136.
- [108] D. J. Littlewood. *Roadmap for Peridynamics Implementation*. Tech. rep. Sandia National Laboratories, Oct. 2015.
- [109] W. Liu and J.-W. Hong. Discretized peridynamics for brittle and ductile solids. *International Journal for Numerical Methods in Engineering* **89.8** (Oct. 2011), 1028–1046. DOI: 10.1002/nme.3278. URL: <https://doi.org/10.1002/nme.3278>.
- [110] S. LLC. *A Brief History of Steel Construction*. 2022. URL: <https://www.steelincga.com/a-brief-history-of-steel-construction/> (visited on 04/09/2022).
- [111] C. Lowney. Rethinking the Machine Metaphor Since Descartes: On the Irreducibility of Bodies, Minds, and Meanings. *Bulletin of Science, Technology & Society* **31.3** (May 2011), 179–192. DOI: 10.1177/0270467611406514. URL: <https://doi.org/10.1177/0270467611406514>.
- [112] M. W. M. Hensel A. Menges. Emergence – Morphogenetic Design Strategies. *Architectural Design* **74.3** (July 2004).
- [113] M. W. M. Hensel A. Menges. *Emergent Technologies and Design - Towards a Biological Paradigm for Architecture*. Routledge Oxford, Jan. 2010.
- [114] R. W. Macek and S. A. Silling. Peridynamics via finite element analysis. *Finite Elements in Analysis and Design* **43.15** (Nov. 2007), 1169–1178. DOI: 10.1016/j.finel.2007.08.012. URL: <https://doi.org/10.1016/j.finel.2007.08.012>.

- [115] E. Madenci and E. Oterkus. *Peridynamic Theory and Its Applications*. Springer, 2014.
- [116] T. Mann. Review: Secret Knowledge: Rediscovering the Techniques of the Old Masters. *Archives of American Art Journal* **42**.1/2 (Jan. 2002), 34–37. DOI: 10.1086/aaa.42.1_2.1557850. URL: https://doi.org/10.1086/aaa.42.1_2.1557850.
- [117] M. Marmor. BACK TO THE DRAWING BOARD: THE ARCHITECTURAL MANUAL OF SEBASTIANO SERLIO (1475-1554). *The Yale University Library Gazette* **70**.3/4 (1996), 115–125. ISSN: 00440175. URL: <http://www.jstor.org/stable/40859730> (visited on 07/13/2022).
- [118] A. Mårtensson and H. Carlsson. *The Development of the Finite Element Method*. Tech. rep. Lund Institute of technology, 1987.
- [119] A. McRobie. *The Seduction of Curves: The Lines of Beauty That Connect Mathematics, Art, and the Nude*. Princeton University Press, 2017.
- [120] U. Meyer. *Tamedia Office Building Commercial*. URL: <https://dac.dk/en/knowledgebase/architecture/tamedia-office-building/> (visited on 09/27/2022).
- [121] D. Miranda, C. Williams, and J. Orr. *Dataset for An Explicit Method for Simulation of Cracking Structures Based on Peridynamic Theory*. 2016. URL: <https://researchdata.bath.ac.uk/194/>.
- [122] H. D. Miranda, J. Orr, and C. Williams. Fast interaction functions for bond-based peridynamics. *European Journal of Computational Mechanics* **27**.3 (May 2018), 247–276. DOI: 10.1080/17797179.2018.1547356. URL: <https://doi.org/10.1080/17797179.2018.1547356>.
- [123] W. J. Mitchell and M. McCullough. *Digital Design Media*. Van Nostrand Reinhold, 1997.
- [124] J. J. Monaghan. Smoothed Particle Hydrodynamics. *Annual Review of Astronomy and Astrophysics* **30**.1 (Sept. 1992), 543–574. DOI: 10.1146/annurev.aa.30.090192.002551. URL: <https://doi.org/10.1146/annurev.aa.30.090192.002551>.
- [125] J. Monaghan. SPH without a Tensile Instability. *Journal of Computational Physics* **159**.2 (Apr. 2000), 290–311. DOI: 10.1006/jcph.2000.6439. URL: <https://doi.org/10.1006/jcph.2000.6439>.
- [126] M. Moussard, P. Garibaldi, and M. Curbach. “The Invention of Reinforced Concrete (1848 – 1906)”. *High Tech Concrete: Where Technology and Engineering Meet*. Springer International Publishing, Aug. 2017, pp. 2785–2794. DOI: 10.1007/978-3-319-59471-2_316.
- [127] C. Murray. *Engineering Disasters: SS Schenectady, a Lesson in Brittle Fracture*. 2015. URL: <https://www.designnews.com/materials-assembly/engineering-disasters-ss-schenectady-lesson-brittle-fracture/173702193545746> (visited on 04/28/2020).
- [128] *MX3D Bridge*. 2020. URL: <https://mx3d.com/projects/mx3d-bridge/> (visited on 10/27/2020).

- [129] naturally:wood. *Complex Structures: Solutions in Wood, interview with Martin Antemann*. URL: <https://www.youtube.com/watch?v=WvbZ6hniWVc> (visited on 06/17/2022).
- [130] P. F. Y. Neil Leach. *Computational Design*. Tongji University Press, 2018.
- [131] V. N. Nerella, H. Ogura, and V. Mechtcherine. “Incorporating reinforcement into digital concrete construction”. The annual Symposium of the IASS. 2018.
- [132] D. Norell. Geometries with agency: mathematics of form revisited. *Architectural Research Quarterly* **25.3** (Sept. 2021), 255–265. DOI: 10.1017/s1359135521000324. URL: <https://doi.org/10.1017/s1359135521000324>.
- [133] NVIDIA. *GPU Technology Conference 2014: TITAN Z Rendering Demos (part 6) GTC*. 2014. URL: <https://www.youtube.com/watch?v=XISqvBVyASo> (visited on 05/14/2020).
- [134] J. Ockman. Review: Complexity and Contradiction in Architecture by Robert Venturi: Complexity and Contradiction in Architecture. *Journal of the Society of Architectural Historians* **75.4** (Dec. 2016), 490–492. ISSN: 0037-9808. DOI: 10.1525/jсах.2016.75.4.490.
- [135] J. Olsson. “In conversation with simulation: The application of numerical simulation to the design of structural nodal connections”. Licentiate Thesis. Chalmers University of Technology, 2021.
- [136] J. Olsson, M. Ander, and C. J. K. Williams. “Adaptive bone re-modelling for optimization of porous structural components”. *Conference proceedings: IASS Beijing 2022*. 2022.
- [137] J. Olsson, M. Ander, and C. J. K. Williams. The numerical simulation of standard concrete tests and steel reinforcement using force flux peridynamics. *Structural Concrete* (Aug. 2022).
- [138] J. Olsson, M. Ander, and C. J. K. Williams. The Use of Peridynamic Virtual Fibres to Simulate Yielding and Brittle Fracture. *Journal of Peridynamics and Nonlocal Modeling* **3.4** (Apr. 2021), 348–382.
- [139] J. Olsson et al. “Sculptural form finding with bending action”. *Conference proceedings: IASS Hamburg 2017*. 2017.
- [140] J. Orr and A. Darby. Flexible formwork for visual concrete (2012). DOI: 10.17863/CAM.17617. URL: <https://www.repository.cam.ac.uk/handle/1810/270675>.
- [141] N. Oxman. “Material-based Design Computation”. PhD thesis. Massachusetts Institute of Technology, 2010.
- [142] J. Pallasmaa. *The Eyes of The Skin*. Chichester, 1996.
- [143] J. Pallasmaa. “The Routledge Companion for Architecture Design and Practice Established and Emerging Trends”. Ed. by M. Kanaani and D. Kopec. Routledge, 2015. Chap. Spatial Choreography and Geometry of Movement as the Genesis of Form - The material and immaterial in architecture, pp. 35–44.
- [144] J. Pallasmaa. *The Thinking Hand – Existential and Embodied Wisdom in Architecture*. John Wiley Sons Inc, 2009.
- [145] A. Paolini, S. Kollmannsberger, and E. Rank. Additive manufacturing in construction: A review on processes, applications, and digital planning methods. *Additive Manufacturing* **30** (Dec. 2019), 100894. DOI: 10.1016/j.addma.2019.100894. URL: <https://doi.org/10.1016/j.addma.2019.100894>.

- [146] M. Peck. *Concrete: Design, Construction, Examples*. Birkhäuser; In Kooperation Mit DETAIL, 2006.
- [147] A. Penn and J. S. Turner. Can we identify general architectural principles that impact the collective behaviour of both human and animal systems? *Philosophical Transactions of the Royal Society B: Biological Sciences* **373**.1753 (July 2018), 20180253. DOI: 10.1098/rstb.2018.0253. URL: <https://doi.org/10.1098/rstb.2018.0253>.
- [148] A. Pérez-Gómez and L. Pelletier. Architectural Representation beyond Perspectivism. *Perspecta* **27** (1992), 20–39. URL: <https://www.jstor.org/stable/1567174>.
- [149] L. Piegl and W. Tiller. *The NURBS Book*. second. New York, NY, USA: Springer-Verlag, 1996.
- [150] P. Poinet and A. Fisher. “Computational Extensibility and Mass Participation in Design”. *Design Transactions: Rethinking Information Modelling for a New Material Age*. UCL Press, 2020, pp. 56–61. ISBN: 9781787354890. URL: <http://www.jstor.org/stable/j.ctv13xprf6.9> (visited on 07/15/2022).
- [151] M. Polanyi. *The tacit dimension*. Ed. by 1. Doubleday & company inc., 1966.
- [152] M. Popescu et al. Structural design, digital fabrication and construction of the cable-net and knitted formwork of the KnitCandela concrete shell. English. *Structures* (2020).
- [153] H. Pottman et al. *Architectural Geometry*. Bently Institute Press, 2007.
- [154] N. Prakash and R. J. Stewart. A Multi-threaded Method to Assemble a Sparse Stiffness Matrix for Quasi-static Solutions of Linearized Bond-Based Peridynamics. *Journal of Peridynamics and Nonlocal Modeling* **3.2** (Sept. 2020), 113–147. DOI: 10.1007/s42102-020-00041-y. URL: <https://doi.org/10.1007/s42102-020-00041-y>.
- [155] A. Pressley. *Elementary Differential Geometry*. Springer London, 2010. DOI: 10.1007/978-1-84882-891-9. URL: <https://doi.org/10.1007/978-1-84882-891-9>.
- [156] H. Ren et al. Dual-horizon peridynamics. *International Journal for Numerical Methods in Engineering* **108**.12 (July 2016), 1451–1476. DOI: 10.1002/nme.5257. URL: <https://doi.org/10.1002/nme.5257>.
- [157] P. Rice. *An engineer imagines*. Batsford, 2017.
- [158] C. Robeller. Integral Mechanical Attachment for Timber Folded Plate Structures. en (2015). DOI: 10.5075/EPFL-THESIS-6564.
- [159] K. Runesson and R. Larsson. “Constitutive Modeling of Engineering Materials - Theory and Computation”. Lecture Notes, Department of Industrial and Materials Science, Chalmers University of Technology, Göteborg. 2018.
- [160] N. Saabye Ottosen and H. Petersson. *Introduction to the finite element method*. New York: Prentice Hall, 1992. ISBN: 0134738772.
- [161] E. Saarinen. *Eero Saarinen on his work*. Ed. by A. B. Saarinen. Yale University Press, 1962.
- [162] R. Sawhney and K. Crane. Monte Carlo Geometry Processing: A Grid-Free Approach to PDE-Based Methods on Volumetric Domains. *ACM Transactions on Graphics* **38.4** ().

- [163] M. H. Sawyer. World's First Iron Bridge. *Civil Engineering—ASCE* **49.12** (1979), 46–49.
- [164] D. Schon. *The reflective practitioner. How professionals think in action*. London: Temple Smith, 1983.
- [165] SciArc. *Shigeru Ban Keynote at SciArc 2022 April 13*. URL: <https://channel.sciarc.edu/browse/shigeru-ban-april-13-2022> (visited on 06/16/2022).
- [166] S. A. Silling. Reformulation of elasticity theory for discontinuities and long-range forces. *Journal of the Mechanics and Physics of Solids* **48.1** (Jan. 2000). Introduction of Peridynamics, 175–209. DOI: [https://doi.org/10.1016/S0022-5096\(99\)00029-0](https://doi.org/10.1016/S0022-5096(99)00029-0).
- [167] S. A. Silling and E. Askari. A meshfree method based on the peridynamic model of solid mechanics. *Computers & Structures* **83.17-18** (June 2005), 1526–1535. DOI: [10.1016/j.compstruc.2004.11.026](https://doi.org/10.1016/j.compstruc.2004.11.026). URL: <https://doi.org/10.1016/j.compstruc.2004.11.026>.
- [168] S. Silling et al. Peridynamic states and constitutive modeling. *Journal of Elasticity* **88.2** (2007). cited By 647, 151–184. DOI: [10.1007/s10659-007-9125-1](https://doi.org/10.1007/s10659-007-9125-1).
- [169] K. Sims. Particle Animation and Rendering Using Data Parallel Computation. *SIGGRAPH Comput. Graph.* **24.4** (Sept. 1990), 405–413. ISSN: 0097-8930. DOI: [10.1145/97880.97923](https://doi.org/10.1145/97880.97923). URL: <https://doi.org/10.1145/97880.97923>.
- [170] P. Sjömar. *Byggnadsteknik och Timmermanskonst*. Chalmers tekniska högskola, 1988.
- [171] D. Slater et al. The anatomy and grain pattern in forks of hazel (*Corylus avellana* L.) and other tree species. *Trees* **28.5** (July 2014), 1437–1448. DOI: [10.1007/s00468-014-1047-5](https://doi.org/10.1007/s00468-014-1047-5).
- [172] R. J. Smith. *Engineering*. 2020. URL: <https://www.britannica.com/technology/engineering> (visited on 04/24/2020).
- [173] R. J. Smith and M. R. Willford. The damped outrigger concept for tall buildings. *The Structural Design of Tall and Special Buildings* **16.4** (2007), 501–517. DOI: [10.1002/tal.413](https://doi.org/10.1002/tal.413).
- [174] I. Soroka. *Portland Cement Paste and Concrete*. The Macmillan Press LTD, 1979.
- [175] Statista. *Volume of data/information created, captured, copied, and consumed worldwide from 2010 to 2020, with forecasts from 2021 to 2025*. URL: <https://www.statista.com/statistics/871513/worldwide-data-created/> (visited on 10/02/2022).
- [176] O. Stein, E. Grinspun, and K. Crane. Developability of triangle meshes. *ACM Transactions on Graphics* **37.4** (July 2018), 1–14. DOI: [10.1145/3197517.3201303](https://doi.org/10.1145/3197517.3201303). URL: <https://doi.org/10.1145/3197517.3201303>.
- [177] D. J. Struik. *Lectures on Classical Differential Geometry*. Dover Publications Inc, 1988.
- [178] J. Sutherland. Revival of structural timber in Britain after 1945. *Construction History* **25** (2010), 101–113.
- [179] J. Swegle, D. Hicks, and S. Attaway. Smoothed Particle Hydrodynamics Stability Analysis. *Journal of Computational Physics* **116.1** (Jan. 1995), 123–134. DOI: [10.1006/jcph.1995.1010](https://doi.org/10.1006/jcph.1995.1010). URL: <https://doi.org/10.1006/jcph.1995.1010>.

- [180] G. Tang. An Overview of Historical and Contemporary Concrete Shells, Their Construction and Factors in Their General Disappearance. *International Journal of Space Structures* **30.1** (Mar. 2015), 1–12. DOI: 10.1260/0266–3511.30.1.1. URL: <https://doi.org/10.1260/0266–3511.30.1.1>.
- [181] K. Thorsager and M. Udén. “3D Strut-and-Tie Modelling - Interactive Design Using Peridynamics”. MSc thesis. Chalmers university of technology, 2022.
- [182] M. Tsigkari et al. “The computational challenges of a mega space frame”. *ACADIA Conference proceedings*. Association for Computer Aided Design in Architecture (ACADIA). 2017.
- [183] L. Tupenaite et al. Sustainability Assessment of Modern High-Rise Timber Buildings. *Sustainability* **13.16** (2021). ISSN: 2071-1050. DOI: 10.3390/su13168719. URL: <https://www.mdpi.com/2071-1050/13/16/8719>.
- [184] d. o. E. University of Cambridge. *Material selection chart*. 2020. URL: http://www-materials.eng.cam.ac.uk/mpsite/interactive_charts/default.html (visited on 11/25/2020).
- [185] S. L. Vatanabe et al. Topology optimization with manufacturing constraints: A unified projection-based approach. *Advances in Engineering Software* **100** (2016), 97–112.
- [186] D. Veenendaal, M. West, and P. Block. History and overview of fabric formwork: using fabrics for concrete casting. *Structural Concrete* **12.3** (Sept. 2011), 164–177. DOI: 10.1002/suco.201100014. URL: <https://doi.org/10.1002/suco.201100014>.
- [187] L. V. Vela, J. Reynolds-Barredo, and R. Sánchez. A positioning algorithm for SPH ghost particles in smoothly curved geometries. *Journal of Computational and Applied Mathematics* **353** (June 2019), 140–153. DOI: 10.1016/j.cam.2018.12.021.
- [188] G. Vrachliotis et al. *Frei Otto: Thinking by Modeling*. Spector Books, 2017.
- [189] M. Vriesendorp et al. “Drawing Futures, Speculations in Contemporary Drawing for Art and Architecture”. Ed. by L. Allen and L. C. Pearson. UCL Press, 2016. Chap. Augmentations, pp. 7–68. URL: <https://www.jstor.org/stable/j.ctt1ht4ws4.5>.
- [190] E. Walker. Renzo Piano & Richard Rogers in conversation with Enrique Walker. *AA Files* 70 (2015), 46–59.
- [191] M. Whelton and A. Macilwraith. Timber/steel composite members in multi-storey buildings under fire test loadings. *Journal of Structural Integrity and Maintenance* **2.3** (July 2017), 152–167. DOI: 10.1080/24705314.2017.1354153. URL: <https://doi.org/10.1080/24705314.2017.1354153>.
- [192] R. Whitehead. “Formative experiences: Saarinen’s shells and the evolutionary impact of construction challenges”. *5th International congress on construction history*. 2015.
- [193] C. J. Williams. *structure-geometry*. URL: <http://structure-geometry.eu/> (visited on 04/17/2022).
- [194] C. Williams. Air supported structures: the state if the art. *Institution of Structural Engineers* (1980), 99–120.

- [195] C. J. Williams. “The Analytics and Numerical Definition of the Geometry of the British Museum Great Court Roof”. *Mathematics & design*. 2001.
- [196] C. D. Wolf. “Low Carbon Pathways for Structural Design: Embodied Life Cycle Impacts of Building Structures”. PhD thesis. Massachusetts Institute of Technology, 2017. DOI: 10.13140/rg.2.2.31570.96960. URL: <http://rgdoi.net/10.13140/rg.2.2.31570.96960>.
- [197] J. Wolff. *The Law of Bone Remodelling*. Springer Berlin Heidelberg, 1986. DOI: 10.1007/978-3-642-71031-5. URL: <https://doi.org/10.1007/978-3-642-71031-5>.
- [198] P. Wriggers. *Computational Contact Mechanics*. Springer Berlin Heidelberg, 2006. DOI: 10.1007/978-3-540-32609-0. URL: <https://doi.org/10.1007/978-3-540-32609-0>.
- [199] J. Wu, O. Sigmund, and J. P. Groen. Topology optimization of multi-scale structures: a review. *Structural and Multidisciplinary Optimization* **63** (2021), 1455–1480.
- [200] Q. Xia et al. Simultaneous optimization of cast part and parting direction using level set method. *Structural and multidiciplinary optimization* **44.6** (Dec. 2011), 751–759.
- [201] G. Yazici. Embodied cognition and critique of cartesian dualism in design learning. *IJEAD International Journal of Education in Architecture and Design* **1.1** (Mar. 2020), 55–65.
- [202] M. A. Zboinska. Influence of a hybrid digital toolset on the creative behaviors of designers in early-stage design. *Journal of Computational Design and Engineering* **6.4** (Dec. 2018), 675–692.